

UC Irvine

UC Irvine Previously Published Works

Title

Continuous flow biocatalysis

Permalink

<https://escholarship.org/uc/item/40v4g21t>

Journal

Chemical Society Reviews, 47(15)

ISSN

0306-0012

Authors

Britton, Joshua

Majumdar, Sudipta

Weiss, Gregory A

Publication Date

2018-07-30

DOI

10.1039/c7cs00906b

Peer reviewed



Published in final edited form as:

Chem Soc Rev. 2018 July 30; 47(15): 5891–5918. doi:10.1039/c7cs00906b.

Continuous Flow Biocatalysis

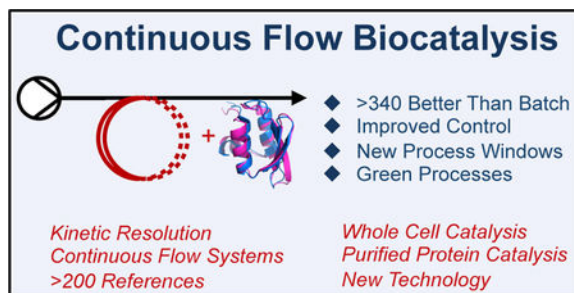
Joshua Britton^a, Sudipta Majumdar, and Gregory A. Weiss^a

^aDepartments of Chemistry, Molecular Biology, and Biochemistry, University of California, Irvine, CA 92697-2025, USA

Abstract

The continuous flow synthesis of active pharmaceutical ingredients, value-added chemicals, and materials has grown tremendously over the past ten years. This revolution in chemical manufacturing has resulted from innovations in both new methodology and technology. This field, however, has been predominantly focused on synthetic organic chemistry, and the use of biocatalysts in continuous flow systems is only now becoming popular. Although immobilized enzymes and whole cells in batch systems are common, their continuous flow counterparts have grown rapidly over the past two years. With continuous flow systems offering improved mixing, mass transfer, thermal control, pressurized processing, decreased variation, automation, process analytical technology, and in-line purification, the combination of biocatalysis and flow chemistry opens powerful new process windows. This Review explores continuous flow biocatalysts with emphasis on new technology, enzymes, whole cells, co-factor recycling, and immobilization methods for the synthesis of pharmaceuticals, value-added chemicals, and materials.

Graphical Abstract



Continuous Flow Biocatalysis: Merging the power of proteins and continuous flow for improved chemical synthesis.

Introduction

Continuous flow processing has been used extensively in industry since the early 20th century. While manufacturing of bulk chemicals including hydrocarbons, fertilizers,

Conflict of interest

The authors declare the following competing financial interest: JB and GAW are co-founders of Synthase Inc., which is developing products related to the research described here. The terms of this arrangement have been reviewed and approved by the University of California, Irvine in accordance with its conflict of interest policies.

synthetic fibers, paper, wastewater, steel, methane, and iron ore can be dated back to 1771, continuous flow manufacturing of fine chemicals is relatively new. In this respect, recent research has advanced continuous flow synthesis of active pharmaceutical ingredients (APIs),^{1–5} value-added chemicals,^{6–9} modern agrochemicals,^{10–17} and materials for hydrogen capture, storage, and electronics.^{18–21}

The concept of flow chemistry is simple. A fluid containing starting material is pumped through a reactor in a continuous manner to yield a stream of product (Figure 1). A pump (or series of pumps) injects the solution(s) into the reactor, and these can be grouped into semi-continuous and continuous pumps. Semi-continuous pumps (e.g., syringe pumps) require refilling the syringe, while continuous pumps do not require refilling, and can theoretically process solutions indefinitely (Figure 2).

Continuous flow reactors are typically constructed from metals, glass, and plastic, with the most common material being PFA (perfluoroalkoxy) tubing. While plastic reactors are the most common, metal reactors can withstand higher temperatures and pressures, and can be constructed from catalytic metals such as copper.^{22–24} The types of continuous flow reactors include *i*) reactor coils, *ii*) micro or mesofluidic chips, *iii*) packed bed reactors, *iv*) cartridges containing immobilized reagents, or *v*) tube-in-tube reactors for reactions involving gases (Figure 2).^{25–28}

Pumping solutions through continuous reactors allows rapid heating or cooling with temperature ranges being dependent on the reactor capabilities, typically -78°C to $+300^{\circ}\text{C}$.^{29–31} Additionally, specific reactor tubing can be effectively irradiated with light to accelerate photo-catalyzed reactions,^{32–35} and solid precipitation can be handled by sonicating reactor coils or other methods.^{36, 37} Finally, semi-permeable Teflon AF-2400 tubing allows gases such as CO_2 , H_2 , N_2 , and O_2 to diffuse through the reactor tubing; the approach is useful for reactions requiring slow diffusion of gases in or out of solution.^{38–41}

The final piece of a basic continuous flow system is the backpressure regulator that pressurizes the system (Figure 3). If a backpressure regulator has an internal pressure of 200 psig, then the fluid in the continuous flow system must achieve a pressure of 200 psig to exit the backpressure regulator. The backpressure regulator has several advantages. First, solvents can be heated above their atmospheric boiling points without evaporation, opening novel process windows. Second, even if the continuous flow system is operating at atmospheric temperature, the backpressure regulator ensures even fluid flow through the reactor (Figure 3). While several backpressure regulators are available, including regulators that can be tuned to the exact pressure required. Additionally, these backpressure regulators can handle solids to a certain extent.

Continuous flow systems have the potential to improve a large number of chemical processes (~50%).⁴² The first research area to capture the interest of flow chemistry was API (active pharmaceutical ingredient) synthesis. For example, the continuous flow synthesis, purification, and formulation of several APIs was achieved in a manually reconfigurable system.⁴³ More recently, scientists at Pfizer demonstrated continuous automated screening of >1500 Suzuki reaction conditions per day.⁴⁴ While these systems are complex, expensive,

and require significant expertise, the examples highlight potential solutions to real world problems. However, in reality, most researchers have access to only several pumps, basic reactors, and maybe a backpressure regulator and separator. This limitation, however, is not due to reluctance for technology adoption, but the high price of equipment (Figure 3).

The rapid growth and adoption of continuous flow synthesis was driven by the arrival of commercially available technology, methodology, and industrial interest.^{7, 45–50} Likewise, continuous flow biocatalysis is currently undergoing its own revolution, generating a number of publications over the past three years including an general overview of the area (Figure 4).⁵¹ There has also been an increase in continuous flow knowledge in both academia and industry that did not previously exist; it is now common for researchers to have continuous flow experience, and thus it has expanded into new laboratories.

Before exploring continuous flow biocatalysis, an understanding of the differences between whole cell and purified protein biocatalysis is required. Whole cell catalysis uses the whole organism such as *Escherichia coli* (*E. coli*) for the transformation.^{52–54} It should also be noted that the field of continuous flow biocatalysis builds on seminal work in biocatalysis from the laboratories of Stan Roberts, Alexander Klivanov, George Whitesides, Bryan Jones, and their co-workers.^{55–61}

In whole cell biocatalysis, unless the protein is excreted from the organism, or displayed on the surface of the organism,^{62–65} the substrate must enter into the cell for it to be transformed, and the product must also exit the organism after the reaction. Two branches of whole cell catalysis exist – fermentation⁶⁶ and biocatalysis. This Review focuses on biocatalysis only. The advantages of whole cell biocatalysis include *a*) it's less expensive than using purified proteins, *b*) the reaction doesn't need to be supplemented with expensive co-factors, which are contained within the cell, and *c*) the reaction is performed in its native environment avoiding problems associated with *in vitro* biosynthesis.^{67, 68}

The disadvantages of whole cell biocatalysis include *a*) the cell membrane limits penetration of the substrate and product making the reaction slower compared to purified protein,^{69, 70} *b*) the cell can have undesirable metabolic pathways creating toxic byproducts or unwanted chemicals, *c*) the process is more complicated, so research & development can take longer, and *d*) from a process standpoint, the reaction chamber is fouled from cellular debris and residual product, and this can hinder downstream processing. For detailed examples, additional Reviews exist.^{67, 71, 72}

Purified protein is typically obtained *via* bacterial expression in *E. coli* (but can also include yeast or mammalian cell lines).⁷³ In this process^{74–76}, a host cell (such as BL21 DE3 *E. coli*^{77, 78}) is transformed with a plasmid encoding the gene for the required protein. When the cells are grown, the protein of interest is expressed using native cellular machinery. After protein expression, cells are exposed to high-energy sonication to break open the cells and release the protein into solution. After centrifugation of the solution, the protein, if correctly folded, resides in the supernatant. The protein can then be purified through chromatography or precipitation.

Purified enzymes have the advantage of being incredibly specific. This property reduces byproduct formation, but also makes enzymes typically quite specific for substrates. Notably, lipases, are used ubiquitously in biocatalysis, and are promiscuous in their substrate preferences.^{79–84} Additionally, the substrate is only required to diffuse into the active site of the protein, and not through the cell membrane. Finally, the concentration of the desired enzyme is higher compared to the same mass of whole cells. Purified proteins also have several disadvantages, including *a*) the purification process can be expensive, *b*) sometimes overexpressed proteins are not correctly folded, *c*) proteins often require cellular environments or additional co-factors for high activity, and finally *d*) proteins can be unstable outside of the cell.

Though enzymes are used in continuous systems without immobilization, attaching proteins to solid supports offers advantages. Most importantly, some enzymes are only available in small quantities; attaching the enzyme to the reactor decreases quantities required for processing. Additionally, enzyme immobilization simplifies product purification, through retention of the enzyme. Enzymes have shown increased stability, selectivity, and improved reaction rates after immobilization.⁸⁵ Many immobilization techniques exist, and have been reviewed previously.^{86–94}

In general, immobilization supports should offer the following properties: large surface area, sufficient functional groups for attachment, hydrophilic character, water insolubility, chemical and thermal stability, mechanical strength, high rigidity, resistance to microbial degradation, and ease of regeneration. Ideally, resins will also be non-toxic, and have a low price.⁹⁵ In reality, many immobilization supports have several of these qualities, but not all.

Adsorption

Adsorption of biocatalysts onto solid supports (or carriers) relies on hydrophobic, salt bridge, van der Waals, and hydrogen bonding interactions between the protein or cell, and the immobilization support.⁹⁶ Solid supports include coconut fibers,^{97, 98} cellulose,⁹⁹ kaolin,^{100, 101} and micro and mesoporous materials.^{102, 103} Additionally, biocatalysts have been immobilized onto molecular sieves,^{104, 105} polypropylene based hydrophobic granules,¹⁰⁶ agarose gel,¹⁰⁷ poly (3-hydroxybutyrate-co-hydroxyvalerate) and APTES surfaces (Figure 5).¹⁰⁸ Adsorption is easier to perform, and can avoid enzyme denaturation through minimal distortion to the protein. However, immobilization lifetimes and efficiencies can be lower than comparable covalent immobilization.¹⁰⁸

Covalent immobilization

Covalent immobilization creates chemical attachment(s) from surface-exposed amino acids on the protein or cell to a solid support. Surface-exposed functional groups include guanidines, carboxylic acids, imidazoles, indoles, phenols, hydroxyl groups, and thiols.⁹⁵ Immobilization surfaces used for covalent immobilization include peptide-modified surfaces for high specific activity and controlled protein orientation,^{109, 110} cyanogen bromine-infused agarose and Sepharose,¹¹¹ gluteraldehyde-modified glass surfaces,¹⁰⁸ silica,^{112, 113} chitosan,^{114–116} epoxides,^{117–121} and nanowires amongst others (Figure 6).^{122, 123} The major benefit of covalent immobilization is the potential for improved catalyst lifetime due

to decreased leaching, however, it should be noted that not all proteins are suitable for immobilization and this should be experimentally tested.¹⁰⁸

Affinity immobilization

Affinity immobilization revolves around enzymes having different affinities for immobilization supports under different conditions. For example, during recombinant protein expression a polyhistidine affinity tag (His_n-tag) is often encoded at a protein terminus. This His_n-tag allows protein purification on nickel-nitrilotriacetic acid (Ni-NTA) resin, as the His_n-tag has an affinity for the resin under fairly neutral buffer conditions (pH 8.0). The protein of interest will complex to the Ni-NTA resin allowing selective protein removal from bulk solution. Once the protein of interest is isolated, adding 250 mM imidazole, or lowering the pH of the solution, will leach the protein from the resin.^{124, 125} Affinity immobilization supports can be categorized into two groups. First, the matrix is pre-coupled to an affinity ligand (such as the NTA ligand mentioned above), or second, the enzyme is pre-bound to an affinity ligand that gets incorporated into a matrix. Examples of affinity supports include chitosan-coated porous silica beads¹²⁶ and agarose-linked with concanavalin protein (Figure 7).¹²⁷

Entrapment immobilization

Entrapment immobilization is achieved by trapping the biocatalysts into a caged network *via* covalent or non-covalent interactions with an immobilization support (Figure 8). Examples of immobilization entrapment supports include alginate-gelatin hybrids,¹²⁸ nano-materials such as nanowires,^{129, 130} chitosan,¹³¹ mesoporous silica,¹³² calix[n]arene polymers,¹³³ and κ -carrageenan.¹³⁴

With the basics of continuous flow, equipment, whole cell, and purified biocatalysts covered, this Review now addresses whole cell biocatalysis, specialty transformations, lipases, enzymatic resolution, co-factor regeneration, and new technological approaches. The examples in each section are presented in chronological order to demonstrate the advancements in each field.

Whole Cell Biocatalysis

In 1990, an immobilized whole cell process containing nitrile hydratase was translated to continuous flow using two packed bed reactors cooled to 4 °C. Under optimal conditions, a feed of 6% (v:v) acrylonitrile was pumped into the first reactor at 1.1 mL/min before meeting a second stream of pure acrylamide at 35 μ L/min (to ensure 6% (v:v) acrylonitrile was present at all times, Figure 9).¹³⁵ Using a system comprised on two packed beds, the space-time yield increased almost two-fold to 93.2 g/(L.h) The system showed impressive stability over 240 h with no loss in biocatalytic activity at 4 °C. However, at 30 °C, more than 60% of biocatalytic activity was lost in 40 h.

In 2003, a continuous system for producing non-reducing maltodextrins was developed.¹³⁶ Trehalosyl-dextrin-forming enzyme was found in the thermoacidophilic archaeon *Sulfolobus solfataricus*, but could be easily expressed in *E. coli*. Here, *E. coli* were permeabilized before immobilization onto supports including polyacrylamide, egg white, chitosan, and calcium-

alginate. The *E. coli* entrapped into calcium-alginate gel were found to be thermally stable at 75 °C, and were used in a glass packed bed reactor. Maltodextrin trehalosylmaltotetraose was produced at 106.5 mg ml⁻¹ h⁻¹ when using a 30% (w/v) solution of maltohexaose substrate (Figure 10). Importantly, the immobilization efficiency vs. activity is discussed. This raises an important concern in continuous flow biocatalysis: is a larger quantity of immobilized cells with lower activity preferred, or vice versa? In this case, only 24% of cells were immobilized into calcium-alginate beads, but 100% activity was retained. In contrast, the polyacrylamide support retained 81% of the cells, but after <5 h of processing, activity was reduced to ~20%. In our opinion, a smaller quantity of highly active immobilized material allows increased performance compared to a reactor containing the same mass.

Continuous flow whole cell biocatalysis has been used for the asymmetric reduction of cyclohexanone analogs using super critical CO₂.¹³⁷ Here, *Geotrichum candidum* cells were immobilized onto water-absorbing polymer beads (BL-100) and the substrate added semi-continuously. The continuous system was operated under 10 MPa at 35 °C and cyclohexanone was reduced to cyclohexanol in 36% conversion. The authors also demonstrated the enantioselective reduction of *o*-fluoroacetophenone (>99.9%) using the same system (Figure 11). Impressively, this continuous system out-performed the batch approach at almost twice the product formation rate (0.24 μmol min⁻¹ vs. 0.13 μmol min⁻¹).

Immobilized whole cells have extensive use in food manufacturing. For example, immobilized and permeabilized *Kluyveromyces lactis* cells expressing β-galactosidase are used to hydrolyze lactose in milk.¹³⁸ Whole cells were immobilized onto the surface of stainless steel sheets *via* gelation with manganese alginate before being placed into a vertical reactor. Milk is flowed through this reactor at 45 °C. This continuous system had lower hydrolysis rates than a continuous stirred tank reactor (CSTR). However, this is not surprising as the residence time in the CSTR was greater (600 min vs. 125 min); notably, CSTRs can also handle solid precipitation, and are commonly used in API synthesis.^{139–141} A residence time of 125 min in the continuous flow system yielded ~40% lactose hydrolysis while the CSTR yielded near quantitative hydrolysis in 600 min. Additionally, the CSTR demonstrated accelerated reactivity compared to the continuous flow system. Finally, the stability of the whole cells was best when stored in milk at 4 °C; no decrease in activity was observed over seven weeks of storage. This contrasts with many storage methods requiring ~50% glycerol at decreased temperatures.¹³⁸

The synthesis of enantiopure (5*R*)-hydroxyhexane-2-one was achieved with immobilized *Lactobacillus kefir*.¹⁴² In this continuous system, whole cells were immobilized with sodium cellulose sulfate at 40% efficiency, and although the immobilization reduced activity, switching from batch to continuous flow (0.8 h residence time) improved performance by an average of 19-fold. The continuous system reduced (2,5)-hexanedione to (2*R*,5*R*)-hexanediol at 64 g L⁻¹ day⁻¹ with >99% ee (Figure 13). In this system, inexpensive glucose was added to regenerate the co-factors. The continuous system was run for six days and the immobilization method retained 68% of residual activity. This example highlights the benefits of continuous flow biocatalysis.

Generating enantiopure alcohols for both the agrochemical and pharmaceutical industry is vitally important. To this aid, the continuous flow synthesis of (*S*)-1-phenylethanol was achieved by immobilizing *Rhodotorula glutinis* on calcium alginate beads for use in a packed bed reactor (Figure 14).¹⁴³ The substrate was flowed through the reactor at room temperature using a peristaltic pump, and interestingly, the fluid exited through an overflow channel at the opposite side of the reactor. Under optimal conditions, (*S*)-1-phenylethanol was afforded at 75% yield (>99% purity). The continuous flow system was operated for 30 days to produce 10.8 mL of product.

In this example, considerations for future experiments arise. First, limited to no active mixing is present in the traveling fluid. Could process efficiency be increased with active mixing disrupting concentration gradients of product and substrate? Second, was dispersion of the immobilized biocatalyst equal throughout the whole reactor? Could process efficiency be improved by confining the substrate solutions to a smaller reaction chamber with increased surface area?

Biodiesel synthesis is a continually growing field for new technology and methodology.^{144–146} In one approach, whole cells of *Aspergillus niger* were immobilized onto polyurethane biomass particles for the transesterification of palm oil.¹⁴⁶ Here, a flow rate of 250 mL min⁻¹ through the packed bed reactor yielded 90% fatty acid methyl ester. To note, this is the first example in this Review where the reaction mixture recycled through the reactor to achieve higher yields. Interestingly, higher flow rates improved mixing, leading to improved yields. The possibility for acceleration from high flow rates should always be tested.

While an entire section below is dedicated to biocatalytic kinetic resolution, we introduce it here with whole cells. Here, the non-steroidal anti-inflammatory drug (NSAID) (*R,S*)-flurbiprofen is resolved by enantioselective esterification using dry mycelium of *Aspergillus oryzae*.¹⁴⁷ In this example, a two-step catch-and-release protocol esterifies the (*R*)-enantiomer, and the second reactor traps the undesirable carboxylic acid on the polymer-supported (PS) base Amberlyst. After several steps, the non-desirable mixture can be re-subjected to resolution. In this system, the commercially available R2+/R4 flow reactor from Vapourtec was fitted with an Omnifit glass column containing 180 mg of cells, and 180 mg of molecular sieves to drive the reaction (Figure 16). This is also the first example in this Review of commercial continuous flow equipment - both the reactor and backpressure regulator. Optimal conditions for this resolution required heating the reactor at 60 °C with a flow rate of 116 $\mu\text{L min}^{-1}$ (6.5 min residence time). Under these conditions the desired product was produced at 2.64 $\mu\text{L min}^{-1} \text{ g}^{-1}$ in 90% ee.

Finally, in 2014, Souza *et. al.* demonstrated a bioreduction of fluorinated acetophenone analogues with several varieties of whole cells.¹⁴⁸ After vigorous experimentation, *Geotrichum candidum* was immobilized onto calcium alginate for the reduction of 2,2,2-trifluoroacetophenone and 4'-Br-2,2,2-trifluoroacetophenone. Immobilized whole cells were packed into an Omnifit column, and the commercially available Asia flow reactor from Syrris was used. Under optimized conditions, the substrate was flowed through at 30 $\mu\text{L min}^{-1}$ (90 min residence time) to achieve >99% conversion (>99% ee) with a space-time yield

of 5.87 kg/ (L. d). This space-time yield describes the quantity of product produced per litre of solution per hour.

Lipases

While the previous section focused on whole cell catalysis, many examples in the following section focus on cell free transformations and often require co-factors and enzyme purification processes prior to processing.

Lipases constitute an enormous proportion of continuous flow biocatalysis achievements, most likely due to their commercial availability,^{149, 150} promiscuity,^{79–84} usage in industry and academia, and ability to operate under a wide variety of conditions such as organic solvents.^{151–154}

In 2000, the enantioselective esterification of (*rac*)-trans-2-phenyl-1-cyclohexanol with an immobilized lipase adsorbed onto EP100 polypropylene powder was achieved (Figure 18).¹⁵⁵ Two different continuous systems were examined. First, a plug flow reactor achieved 30% conversion in 228 min, while the second reactor, a CSTR, required 355 min. The stainless steel packed bed reactor housing 4.1 g of lipase was operated for 220 h at a flow rate of 28 $\mu\text{L min}^{-1}$ (302 min residence time) to yield 32% conversion, 47% ee, and 1.38 g of (*1R,2S*) trans-2-phenyl-1-cyclohexanol propionate. Interestingly, the water generated from the esterification (8.0 $\mu\text{g min}^{-1}$) was not a problem in this system; the water capacity of the co-solvent isooctane (8.5 $\mu\text{g min}^{-1}$ at 42°C) was sufficient. This method of co-solvent water absorption would benefit system scale up, but could the esterification be enhanced with active water removal?

Novozyme 435 (lipase B from *Candida antartica*) is a common lipase due to its commercial availability and advanced properties. This lipase is immobilized onto a hydrophobic acrylic resin that gives the lipase stability in a wide range of physiological conditions such as operating between 20–110 °C, good recyclability up to 5–10 times, and activity of 10000 PLU/g. Additionally, this immobilized enzyme can be purchased from many commercial suppliers (~\$13/g). In 2008, Novozyme 435 was used for the synthesis of alkyl esters in a continuous flow packed-bed system (Figure 19).¹⁵⁷ Here, a 0.2 M solution of 1:1 acid/ alcohol in hexane was flowed through a packed bed of Novozyme 435 (~100 mg, 23 °C) at 1 $\mu\text{L min}^{-1}$ to yield alkyl esters at close to 100% conversion over two hours. Over 7.5 h, a steady 97% conversion yield was achieved to demonstrate good lifetime and stability. A batch vs. flow comparison found that the continuous flow system rapidly accelerated ester formation compared to the batch reaction; this example again provides evidence for the benefits of continuous flow. Notably, it is vital to always compare batch vs. continuous flow experiments.

Novozyme 435 has also been used for the oxidation of alkenes under continuous flow conditions.¹⁵⁸ Here, a packed bed reactor performed chemo-enzymatic oxidation of alkenes in high purity and yield. For this transformation, peracetic acid (a peroxy substrate) was used as a cost effective oxygen donor (~\$5/mL). In this reaction, the peracetic acid transforms the alkene into the epoxide, and the lipase regenerates the peracetic acid from the resulting

acetic acid and hydrogen peroxide (Figure 20). This system performed the oxidation of five substrates in excellent yields (97–99%). The importance of testing reaction mixture solubility prior to continuous flow experiments is emphasized in this work. In this reaction set up, the substrate solution was loaded into a gas tight syringe and passed through the packed bed reactor. If the solubility of the substrate solution changes over time, then the solution is not at a steady state, which will adversely affect system performance. Before performing reactions in continuous flow, examining the solubility of solutions, either qualitatively or quantitatively can save a lot of time. Finally, notice the correct use of a backpressure regulator in this system (Figure 20). The system was tested at temperatures up to 70 °C; without the backpressure regulator maintaining 100 psig, uncontrollable flow rates and substrate vaporization would have resulted.

An interesting application of Novozyme 435 was the ring opening polymerization of ϵ -caprolactone to polycaprolactone in a microfluidic device (Figure 21).¹⁵⁹ Here, microfluidic channels are filled with the immobilized lipase, and the substrate is pumped through the channels. As expected, faster polymerization and higher molecular mass of product polymer was observed compared to the same reaction in batch. Typically, during propagation the reaction mixture becomes increasingly viscous with higher molecular mass, limiting the diffusion of the growing polymer. This problem was overcome in continuous flow allowing higher mass polymers to be formed; presumably micromixing and increased surface area drove this beneficial quality. Finally, the degree of enzyme leaching was lower in continuous flow compared to the same experiment in batch (<1% leaching).

A chemoenzymatic synthesis of chiral enantiopure 2-(1*H*-imidazol-yl)cycloalkanols requiring ring opening followed by a chiral resolution with Novozyme 435 was achieved (Figure 22).¹⁶⁰ While ring opening under continuous conditions afforded the same conversion as the microwave-assisted variant, chiral resolution in continuous flow was superior compared to the batch reaction. For this substrate, Novozyme 435 acylated the (*R,R*)-trans product, and left the (*S,S*)-trans product unaltered. Continuous flow resolution provided easy product separation, enzyme recycling, reduced system downtime, and increased productivity of the biocatalytic step, as instant enzyme/substrate ratios can be achieved. Finally, the continuous stream passing over the enzymes can remove product build up, allowing the reaction to be driven forward by Le Chatelier's principle - an opportunity not so easily available in large batch style reactors.

Additionally, this example illustrates the size and cost of continuous flow equipment. This set-up would be expensive by most standards. It is worth noting that the first reactor coil could possibly be placed in an oil bath to save on microwave costs; but this would need to be tested. Additionally, there are publications available to build your own continuous flow equipment, but, pumps are still the most expensive assets.¹⁶¹ This is one of the reasons why large sequences cannot be readily created – equipment costs can get very large.

A lipase isolated from *Rhizomucor miehei* and immobilized onto macroporous weak anionic-exchange resin (commercially available from Novozymes) was used to synthesize nonionic surfactants with applications in the food and pharmaceutical industry (Figure 23).¹⁶² Here, a packed bed reactor containing the immobilized lipase was subjected to a

substrate solution of (\pm)-1,2-isopropylidene and stearic acid. In a 40 second residence time, 95% conversion was achieved (Figure 23). In this example, response surface methodology (RSM) was used to elucidate optimal best reaction conditions; the approach offers a computationally guided optimization method. This biocatalytic process allowed an environmentally benign esterification moving away from alkaline catalysis.

The technical aspects of this continuous system are interesting. The H-cube (a commercially available continuous flow system from ThalesNano) operating a Knauer pump was used. Thus pump has a lower flow rate of 0.1 mL/min, hence this was the lowest flow rate tested. The benefit of this system is that cartridges full of immobilized catalyst (bio and metals) can be connected to the system for immediate testing. The downside to this commercial system is that the pumping unit does not go to low enough flow rates for long reaction times, but on the upside, the solution can be recycled if necessary, and the flow rates are more suitable for industrial translation.

While biodiesel synthesis *via* transesterification of fats and oils using lipase is common, Maugard *et al.*, demonstrated chemoenzymatic esterification of 3-amino-1,2-propanediol using Novozyme 435 to afford pseudo-ceramides (Figure 24).¹⁶³ Ceramides are active compounds in pharmaceuticals and cosmetics typically synthesized through batch processes. In this two step continuous process, 3-amino-1,2-propanediol is first amidated with stearic acid in 92% yield, before one of the remaining hydroxyl groups is esterified with myristic acid in 54% yield. Impressively, the system operated for three weeks without loss of yield in the first step. With Novozyme 435 having this greater stability, this process could be considered economically attractive despite the cost of Novozyme 435 (~\$1360/ kg).

Few multi-step continuous biocatalytic approaches exist, however, Ley *et al.* developed a beautiful three step synthesis of chiral *O*-acetylcyanohydrins (Figure 25).¹⁶⁴ This continuous flow procedure has two biocatalytic, and one organic transformation in sequence. The first transformation uses Novozyme 435 to create HCN *in situ* from cyanofornate. This reaction is performed in a 10 cm packed bed reactor under five bar of backpressure at a flow rate of 40 $\mu\text{L min}^{-1}$ yielding HCN in 97% conversion in 17.5 min. The second transformation uses the HCN as a substrate for (*R*)-selective hydroxynitrile lyase from *Arabidopsis thaliana*. After first optimizing the second reaction in batch, the authors coupled the first and second step into a multi-step process with no purification to afford (*R*)-mandelonitrile in 85% conversion (96% *ee*).

The largest challenge in this process was the purification of large quantities of overexpressed (*R*)-selective hydroxynitrile lyase. To overcome this, lyophilized *E. coli* BL21 (DE3) cells expressing (*R*)-selective hydroxynitrile lyase were used as the whole cell variant in the packed bed reactor. This two-step system afforded 99% conversion and 95% *ee*. Finally, as cyanohydrins have poor aqueous stability in alkaline pH, the authors incorporated an acylation reaction at the end of the process to afford protected chiral cyanohydrins in 75–99% yield (40–98% *ee*). In our opinion, this system is very impressive, and sets the bar for future work.

On a different note, refineries increasingly use edible oils for fuel sources, which also increases the amounts of edible oil found in waste streams. To combat this environmental hazard, lipases have been immobilized onto nanoporous activated carbon from rice husks.¹⁶⁵ Here, activated carbon was treated with glutaraldehyde and ethylenediamine for Schiff-base immobilization, before reduction with sodium borohydride. Under continuous flow operation in a 20 cm packed bed reactor containing 15 g of immobilized lipase, the hydrolysis of edible oils in wastewater was found to be optimal at pH of 7 at a flow rate of 1 mL min⁻¹ (4 h residence time). Under these conditions, up to 99% of the oils in the wastewater were hydrolyzed (Figure 26).

Finally, caffeic acid phenylethyl ester (CAPE) is a natural flavonoid-like compound with anticancer, antiviral, and antioxidant activity. While industrial batch syntheses using ionic liquids and enzymes exist, using Novozyme 435 in a packed bed reactor demonstrated the benefits of continuous flow (Figure 27).¹⁶⁶ Here, alkyl caffeates are transesterified with phenylethanol using ionic liquid ([Bmim][Tf₂N]) as the solvent. Under optimal conditions, CAPE was synthesized in 93% yield at 2 μL min⁻¹ (2.5 h residence time), and the enzyme used for nine days with no observable decrease in activity. The increase in yield using a continuous flow system was attributed to the increased surface area of the catalyst and the smaller volume of the microfluidic reactor to decrease diffusion paths.

In concluding this section on lipases, several important points have been demonstrated. First, Novozyme 435 is readily available, promiscuous, thermally stable, and demonstrates limited enzyme leaching over long time periods. These properties contrast with expressing a specialty protein in-house, which is typically an expensive and time consuming process. Second, immobilized lipases can handle toxic and unusual chemicals. Here, lipases handled HCN and ionic liquids; such capabilities will surely open novel process windows. Third, many continuous flow examples showed improved yields compared to batch reactions. This important feature is due to increased surface area of the catalyst, micromixing, removal of product concentrations from the protein active site to drive the reaction and avoid product inhibition, and finally the system can decrease distances required for substrate diffusion.

Specialty Transformations

This section examines the synthesis of pharmaceutical motifs and high-value molecules. One of literature's earliest examples uses an purified invertase, and a glucose-fructose oxidoreductase in *Zymomonas mobilis* for synthesizing sorbitol (Figure 28).¹⁶⁷ Here, a co-immobilized system comprising of invertase on chitin transforms sucrose into fructose and glucose, before *Zymomonas mobilis* on calcium alginate beads transforms fructose into sorbitol. Here, the second reaction requires the co-factor NADP(H); using whole cells provides both the co-factor. This system operates as a recycling packed bed reactor where the solution is passed back through the reactor during the reaction. The system was operationally stable for 250 h at 20 mL min⁻¹, producing sorbitol at 5.20 g/ (L. h). Interestingly, this system had a pH titrator using 5 M NaOH solution for maintaining pH 6.0 during reaction recycling. This system provided an alternative approach to sorbitol synthesis removing Ni²⁺-catalyzed hydrogenation under 40–50 atm at 140–150 °C.

In 2005, Mulchandani *et al.*, developed a continuous system for detoxifying organophosphate agents using immobilized whole cells of *E. coli* expressing organophosphorous hydrolase with a cellulose binding domain on the protein terminus (Figure 29).¹⁶⁸ Here, *E. coli* cells were immobilized onto cellulose fibers before placement into a packed bed reactor. Paraoxon (an acetylcholine esterase inhibitor) was then flowed through the system and degraded into *p*-nitrophenol. Conveniently, *p*-nitrophenol absorbs visible light at 412 nm making it possible to monitor degradation spectroscopically. Under optimal conditions, paraoxon was degraded at 5,220 $\mu\text{mol}/(\text{h. L})$.

Pentaerythritol tetranitrate reductase is a NADP(H) dependent enzyme used in the degradation of explosives, nitroaromatics, nitroesters, cyclic triazines, and α,β -unsaturated activated alkenes. In a study by Fielden *et al.*, a two-phase microfluidic chip under anaerobic conditions reduced α,β -unsaturated activated alkenes including enals, enones, enamides and nitro-olefins (Figure 30).¹⁶⁹ Here, the enzyme was not immobilized, but was dissolved in the aqueous phase with NADP(H) and glucose-6-phosphate dehydrogenase (to recycle the NADP⁺), while the substrate was dissolved in isooctane. The two phases meet in the microfluidic chip and form a bi-phasic continuous system with increased surface area and shorter diffusion distances. As a result, the reaction in continuous flow generated higher yields compared to the batch reaction. Notably, this example illustrates in-line monitoring. Passing the reactant streams through UV detectors monitored the concentration of substrate and NAD(P)H.

Peroxidase enzymes can catalyze phenol oxidation into phenolic polymers, and copolymers from *p*-cresol and *p*-phenylphenol. In particular, horseradish peroxidase was immobilized on micro- and nano-lithographic gold surfaces to oxidize phenol into polymers. Here, the gold provided a surface to either physically adsorb horseradish peroxidase, or to form a horseradish peroxidase monolayer. This simple microfluidic system converted 35% of phenol in solution, as well as several other phenol-like motifs in 4–7% conversion (Figure 31).¹⁷⁰ Although low conversions were observed, this research created a useful method to immobilize enzymes into a specific pattern that could be used for multi-step reactions.

Acid phosphatase was immobilized onto polymethacrylate beads through an epoxy-based attachment for alcohol phosphorylation (Figure 32).¹⁷¹ Here, the immobilized enzyme was placed into a packed bed reactor and alcohols flowed through with inorganic phosphate. The reactor showed good stability for 12 days at a flow rate of 30 $\mu\text{L min}^{-1}$ and produced 32 g of material (78% isolated yield). However, the fed batch reactor also showed similar conversion. Compared to current chemical methods of alcohol phosphorylation, this offers an inexpensive route for producing multi-gram quantities of material. Since the fed batch reactor gave the same conversion, the reaction was likely not diffusion-limited, or the residence time was not short enough to see a difference in reaction rates. Although conversion was the same in the fed batch process and continuous flow processes, sampling a shorter timescale may reveal a different trend; it is possible for continuous flow reactors to reach equilibrium in shorter times.

A fed-batch reactor allows substrates to be delivered in low concentrations to avoid substrate inhibition and protein denaturation. Until 2013, this was not possible in continuous flow

systems.¹⁷² However, Szita *et al.*, developed a multi-input reactor for transketolase biosynthesis. Here, a solution of wild-type transketolase forms a new C-C bond between lithium hydroxypyruvate and glycoaldehyde to yield (*L*)-erythrulose at 15 mg h⁻¹ (Figure 33). Transketolases are particularly sensitive to high substrate concentrations, limiting throughput. This reactor increased substrate concentrations delivered to the reaction and afforded a 4.5-fold increase in output concentration, and a 5-fold increase in throughput. This is a particular exciting advancement as many enzymes suffer from substrate inhibition at the high concentrations preferred for industrial applications.

Tube-in-tube reactors allow gas diffusion in-and-out of liquid reactions contained within a reactor. The reactor set up is simple; one gas permeable tube lies within another, non-permeable tube. To demonstrate how this reactor can benefit continuous flow biocatalysis, the hydroxylation of 2-hydroxybiphenyl to 3-phenylcatechol was explored (Figure 34).¹⁷³ Here, a biphasic reaction mixture is passed through a reactor comprised of Teflon AF-2400 tubing where O₂ can diffuse in, and CO₂ out. The Teflon AF-2400 tubing is contained within larger diameter tubing that is significantly less permeable to gases (PFA tubing for example). In this reaction, 2-hydroxybiphenyl-3-monooxygenase, sodium formate, NAD⁺, formate dehydrogenase (to recycle the NAD⁺), and Tween 20 (for increased enzyme stability) are contained in the aqueous phase, and 2-hydroxybiphenyl in *n*-decanol. During the reaction, the substrate diffuses from the organic phase into the aqueous phase, along with O₂. Once the enzymatic reaction is complete, the product diffuses back into the organic phase, and the CO₂ byproduct diffuses out through the Teflon AF-2400 tubing, helping maintain the correct pH. Using this set-up, the product was achieved at 17.7 g/(L. h).

Many natural products contain optically pure amines. Although enantiopure amines can be obtained *via* chemical synthesis, it could be more attractive to use biocatalysis. As a proof of concept, *E. coli* overexpressing ω-transaminase were immobilized onto methacrylate polymer resin.¹⁷⁴ The cells used isopropylamine (IsoPA) as the amine donor for transforming non-natural ketones into their respective amines. Using two streams, one containing IsoPA, and the other the ketone, the solutions were fed into a packed bed reactor housing immobilized cells for a residence time of 30–60 min at 20–50 °C. Under a backpressure of 75 psi (and with methyl tert butyl ether as the solvent), enatiopure amines were synthesized in high ee (>99%). Additionally, the system was stable for five days of processing, and this is a good example of whole cell use. Although the co-factor PLP is expensive, it was created *in situ* for immediate use. Furthermore, to isolate the amine product, the continuous stream was passed through a silica cartridge to ‘catch’ the product. After the reaction completion, the silica was rinsed with methanol to ‘release’ the product – ‘known as a catch and release method’.

Multi-step (or cascade) biocatalysis is becoming popular as improved attachment methodology emerges. While many enzyme immobilization methods exist, Niemeyer and co-workers used a streptavidin affinity peptide on the biocatalyst to bind with high affinity to streptavidin immobilized on magnetic beads. In their microfluidic system, three different proteins reduced 5-nitrononane-2,8-dione to a range of products.¹⁷⁵ The microfluidic chip was placed in heating block at 30 °C, and magnets under the chip kept the magnetic beads in place during processing. Here, two different enzymes could reduce the substrate twice

(either (*S*)- or (*R*)-selective), and the third enzyme (glucose 1-dehydrogenase) regenerated NADP(H). Controlling which enzymes the substrate is exposed (and in which order) allowed control over which product is formed. Under optimal conditions, the meso-diol (3c in Figure 36) was generated in excellent conversion and diastereoselectivity (>95% conv., d.r >99:1, Figure 36).

Our laboratory used a thin film of substrate and immobilization metal affinity chromatography resin for multi-step biocatalysis (Figure 37).¹²⁴ Our system addressed several key issues including: *a*) IMAC resin allows for simultaneous protein purification and immobilization in ten minutes and in near quantitative attachment yields, *b*) using a thin film flow system allows cell lysate to be used that would block a microfluidic device, *c*) high flow rates could be used (>13.3 mL/min), and *d*) there was no need to dialyze the purified protein into a reaction solvent, saving days. These advances allowed proteins to be painted onto the reactor in a variety of styles and patterns for multi-step biocatalytic reactions.

Additionally, regulating enzyme concentrations in each zone allowed equal k_{cat}/K_M values for different enzymes. This enzyme balancing meant that for reactions requiring 1:1 reaction stoichiometry, a higher level of control was possible. The system ran for five days with only 0.34% protein leaching. Compared to our previous work using borosilicate reactors,¹⁰⁸ this methodology opened several exciting avenues, including protein purification and multi-step pathways within a single flow system.

Many enzymatic transformations require co-factors. While a whole section below is dedicated to co-factor regeneration, one example uses a system where co-factor and enzyme are co-immobilized to yield a self-sufficient system. Here, a ketoreductase and NADP(H) are co-immobilized onto porous agarose beads with tertiary amine groups, and placed into a packed bed reactor for the stereoselective reduction of an aryl ketone (Figure 38).¹⁷⁶ Here, 280 mg of the co-immobilized system was used, and the substrate flowed through at 50 $\mu\text{L min}^{-1}$. Isopropyl alcohol (IPA) is also present in the substrate mixture to recycle the co-factor upon oxidation to acetone. Under optimal conditions, the ketone was selectively reduced in 80% yield with a space-time-yield of 104 g/(L. day). Additionally, this self-sufficient system operated for 120 h with no loss in enzyme or co-factor activity. To note, a similar example in the context of co-factors is described in Figure 57 below.

Paradisi *et. al.*, demonstrated amine production using transaminase from *Halomonas elongate* immobilized onto cobalt-derivatized epoxy-resin (Figure 39).¹⁷⁷ After 24 h, 30% of the enzyme was immobilized onto the support, and the enzyme became more tolerant to several organic solvents. The immobilized enzyme was used in a packed bed reactor to convert a handful of aldehyde substrates to their respective amines in good to excellent yield (50–99% yield). Additionally, in-line separation isolated the amine in ethyl acetate by adjusting the pH to 11 with 1 M NaOH. The authors also use polymer-supported (PS) benzylamine to capture any unreacted aldehyde (<1%) from the reaction for substrate recycling. This capture of unreacted substrate is a great feature; though uncommon in continuous flow biocatalysis, such on-line purification appears often in continuous flow organic synthesis.

The authors also examined continuous flow *vs.* batch, and in all situations the continuous flow system was more efficient. For example, aminating cinnamaldehyde required two-minutes in continuous flow and afforded 90% conversion; the equivalent reaction required 24 h in batch. Also, aminating vanillin took two minutes in continuous flow and yielded an 18% conversion; the same conversion took 24 h in batch. Although improved productivity in continuous flow is often reported, authors should always ask the following questions: is comparing a 24 h reaction in batch to a rapid continuous flow reaction fair? For accurate examination, the reaction in batch should be tested after two minutes. Additionally, initial rates of reaction are more interesting in continuous flow due to increased mass transfer and shorter diffusion distances.

The same style of continuous system was also used to transform amines to aldehydes, operating the enzyme in reverse with pyruvate as the amine acceptor (Figure 40).¹⁷⁸ Here, 16 amines were converted in 3–15 min residence times; conversions between 90–99% were observed. The comparison to a batch process was also made, and the authors concluded the continuous flow system offers rate acceleration. Interestingly, they found that aldehydes became immobilized in the packed bed reactor. Cleverly, incorporating a toluene stream before the packed bed reactor allowed products to be carried through to the aqueous separation. Opposite to the previous system, the product stream was treated with 1 M HCl to purify the reactant stream by forcing the amine into the aqueous waste stream.

Phenylalanine ammonia lyases produce valuable aromatic amino acids by amination of *trans*-acrylic acid. Pohl and co-workers immobilized phenylalanine ammonia lyase from *Arabidopsis thaliana* onto Avicel (carbohydrate resin, \$118 kg⁻¹) through expressing a carbohydrate binding module on the C-terminus of the protein (Figure 41).¹⁷⁹ This method allowed rapid immobilization and purification at a flow rate of 0.2 mL min⁻¹ to create a protein cartridge of exceptional purity. Once immobilized, the substrate was pumped through at 5–15 mL h⁻¹ to yield (*S*)-phenylalanine in >85% conversion and >99% ee. The system was operated for 70 h to afford 2.9 g of material. Additionally, operating this biocatalytic transformation in continuous flow *vs.* batch afford rates 28–66 fold higher.

Inositol moieties are ubiquitous in several biologically active species, and play important roles cellular signaling and pathogen virulence. While several syntheses exist, Smith *et al.* demonstrated a continuous flow biocatalytic synthesis of (*L*)-*myo*-inositol 1-phosphate (~\$200 mg⁻¹, Figure 42).¹⁸⁰ Here, (*L*)-*myo*-inositol 1-phosphate synthase from *Trypanosoma brucei* was immobilized using Ni²⁺ IMAC resin and placed into a packed bed reactor. Under batch conditions, a 0.4–10 mg scale reaction yielded >95% conversion, but scaling up to 100 mg scale afforded only 76% in six days; NAD⁺ degraded in the basic reaction media. To overcome this scaling problem, the reaction was transferred to a continuous flow system with a 5 mL packed bed reactor with a flow rate of 41.6 μL min⁻¹ to yield 81% conversion. After 36 h of processing, ~420 mg of the product was obtained, and could be further chemically modified to create high value compounds such as inositol pentaacetate for the synthesis of natural product mycothiol.

In 2017, Szita *et al.* reported sequential use of a transketolase and transaminase to convert hydroxypyruvate and glycoaldehyde into the chiral amino alcohol (2*S*, 3*R*)-amino-1,3,4-

butanetriol (ABT), a common building block in protease inhibitors, detoxifying agents, and pharmaceuticals (Figure 43).¹⁸¹ This environmentally friendly approach allows an efficient synthesis through enzyme compartmentalization. Here, the transketolase fully converts hydroxypyruvate and glycoaldehyde in ten minutes at pH 7, to provide the vital C-C bond formation. The intermediate is then transformed over two hours into ABT using transaminase and co-factor (*S*)- α -methylbenzylamine at pH 9. Unlike most continuous flow biocatalytic systems, the enzymes were not immobilized, but were recovered through in-line filtration devices. This style of processing has several benefits including *a*) avoiding enzyme activity loss upon immobilization, *b*) larger, more sensitive proteins could be amenable to recycling instead of immobilization, and *c*) providing a known concentration of biocatalyst could aid process reproducibility; in contrast, immobilized enzymes can decrease in concentration over time, which could be problematic.

Captopril is a widely used API used in the treatment of anti-hypertension. While many routes for the synthesis of captopril have been reported, Tamborini and co-workers developed a chemoenzymatic route starting from low cost prochiral 2-methyl-1,3-propandiol (Figure 44).¹⁸² Here, a stereoselective oxidation is performed *via* whole cells of *Acetobacter aceti* MIM 2000/28 immobilized onto alginate. Immobilized cells were loaded into a packed bed reactor, and a segmented flow regime (acetate buffer at pH 6, and air), transformed the substrate in 95% conversion, and <97% ee in ten minutes. A 'catch and release' system was used for purification, as a liquid-liquid extraction was not possible given the highly polar nature of the carboxylic acid. Additionally, no co-factor was required given the use of whole cells, and correctly, a backpressure regulator is used to ensure smooth fluid flow. The system was stable for ten hours at 60 $\mu\text{L min}^{-1}$, and an additional series of impressive continuous flow organic transformations yielded Captopril.

Terpene cyclases have long interested the chemical community for their ability to synthesize highly complex carbon backbones found in natural products. Typically, these enzymes suffer from low stability, low reaction rates, and low expression levels. While expression levels can be optimized through protein expression protocols, Wirth *et al.* used continuous flow to drive terpene biosynthesis (Figure 45).¹⁸³ To obtain good yields, a segmented continuous flow stream comprised of alternating segments of aristolochene synthase and farnesyl diphosphate in the aqueous phase, and pentane as the organic phase generated enhanced surface-liquid volumetric ratio. Performing the reaction biphasically allowed continuous product removal to drive higher reaction rates. Additionally, a design of experiment (DOE) model explored the influences of internal reactor diameter, volumetric ratio of aqueous: organic components, and residence time. With a 90 min residence time, 0.5 mm internal diameter tubing and a 1:1 organic: aqueous (v:v), a 96% GCMS yield of the terpene was obtained. This research could open many avenues for improved API and natural product synthesis.

Our final example in this section uses alcohol dehydrogenase immobilized onto HaloLink resin for ketone asymmetric reduction (Figure 46).¹⁸³ Here, alcohol dehydrogenase is expressed with a C-terminal fusion of a halogenase. The halogenase domain covalently bioconjugates the fusion protein to the resin through an ester bond. However, HaloLink resin is expensive (10 mL = ~\$350), and co-expressing a protein weighing 27 Kda may affect protein folding. After protein immobilization, only ~35% residual activity was obtained,

which is not uncommon. Brilliantly, in-line UV spectroscopy (at 282 nm) allowed real-time monitoring of the immobilization process. This technique allows accurate determination of immobilization efficiency, while decreasing column-to-column variation. Using an optimized system allowed for the reduction of 14 different ketones in 19 min in 23–99% yield (>99% ee). Additionally, chemical reaction of the product with 1 M NaOH in a glass microfluidic chip afforded the epoxide in 98% yield (98% ee) in 16 min.

Methodology and Technology

This section covers recent advances in novel methodology for continuous flow biocatalysis. Such advances will include new technology, reactors, and approaches, and some of the problems and solutions of transferring from batch to continuous flow.

Archer *et al.*, conducted an elegant examination of two continuous flow reactors *vs.* a batch reactor.¹⁸⁴ Here, a Coflore agitated cell reactor (Coflore ACR), and a Coflore agitated tube reactor (Coflore ATR) were compared to a batch reactor for chiral resolution of racemic amino acids using non-immobilized whole cells with (*D*)-amino acid oxidase (Figure 47A). The Coflore ACR is a dynamically mixed plug flow reactor that uses moving agitators to promote mixing (Figure 47B), while the Coflore ATR is a tube-shaped reactor using lateral movement (like twisting a spring in a horizontal direction) for improved mass transfer in two-phase reactions (Figure 47C). Given that oxygen is required for this biocatalytic process, it was an ideal system to test the effects of scaling on reactor performance. As expected, increasing the batch reactor size from 250 mL to 4 L decreased the reaction rate; four hours were required to reach ~50% conversion in a 250 mL reactor *vs.* 25 h in a 4 L reactor. Additionally, both continuous flow reactors improved the reaction rates due to improved mass transfer; in the ACR, ~75% conversion was achieved in two hours compared to only ~50%. For the 1 L ATR continuous flow reactor, five hours afforded 65% conversion compared to ~22% in a 1 L batch reactor. This example illustrates the benefits of continuous flow systems for biocatalysis compared to batch, while also demonstrating the correct way to achieve an accurate comparison. In this work, the authors track the conversion at equal times for both the batch and continuous flow reactions, and also use the same volume reactor for the comparison.

Next, processing parameters of a segmented flow micro-reactor were examined to yield a high performing system.¹⁸⁵ Unlike most examples, many parameters were examined such as *a)* which biocatalytic transformations benefit from continuous flow, *b)* optimal ratios of aqueous and organic solvents, *c)* reactor tubing diameter, and *d)* flow velocity. This research examined a wide range of considerations that are often overlooked. First, only biocatalytic reactions with a high mass transfer co-efficient will likely benefit from segmented flow biocatalysis. Thus, a reaction limited by substrate or product diffusion could be improved by continuous flow. Second, reducing heptaldehyde to heptanol using thermophilic alcohol dehydrogenase was optimal in smaller diameter tubing. This is due to an increase in mass transfer and flow velocity. An increase in flow velocity (increasing the flow rate through the same reactor length) improved the transformation until the flow became too powerful and denatured the enzyme. Although this observation seems counter intuitive, increasing flow velocity improves mixing; thus, this parameter could allow the same conversion at higher

flow rates and decreased residency times. For example, a residence time of 10 min (1.86 cm s^{-1}) afforded high space-time yields, while increasing the residence time to 20 or 30 min (0.91 cm s^{-1} and 0.61 cm s^{-1} respectively) decreased space-time yields. Third, in segmented flow reactors, the ratio of organic to aqueous solvents will determine the size of the respective plug moving through the system. In this particular example, a 1:1 ratio of organic to aqueous solvents was optimal. This is important to test in order to aid downstream separation processes for industrial applications.

The authors also provided a novel method for improved reactor performance based on substrate concentration. In this enzymatic system, lower substrate concentrations were transformed more effectively in smaller diameter tubing, and vice versa. To aid this finding, a reactor with three different reactor-tubing diameters was constructed. The initial reaction with a high substrate concentration of 300 mM was mediated in 2.15 mm diameter tubing for improved reactivity. As the substrate concentration decreased, the reaction mixture was flowed into smaller diameter reactor tubing (1.0 and 0.5 mm) to improve reaction rates at lower concentrations (Figure 48). This reactor design could be highly useful for many reactions that are both substrate- and product-inhibited.

Nidetzky *et al.*, reported a immobilization approach for a 87 μL volume microfluidic reactor using silica nanosprings as the support (Figure 49).¹⁸⁶ Here, sucrose phosphorylase is expressed with a silica-binding domain (SBD, known as $Z_{\text{basic}2}$) for rapid immobilization onto the silica nanosprings. Without the SBD, 87% of protein is lost in the immobilization process, making it inefficient. Simply fusing a SBD onto the N-terminus of the protein allows rapid immobilization in two hours by filling the microfluidic cell with an enzyme solution. Using silica nanosprings with a high surface area of $\sim 300 \text{ m}^2 \text{ g}^{-1}$ allowed a 4.5-fold average increase in activity. Additionally, further modifying the nanosprings with sulfonate groups increased this improvement to 10-fold. This solution inspires new microstructure-supported biocatalysts. For mesoscale continuous flow reactors, it would be beneficial to create a packed bed from these materials and see the benefit of such an immobilization strategy still persists at higher flow rates.

3D printing has been used in continuous flow synthesis to create customizable reactors known as 'reactionware'. While common for continuous flow synthesis, the first 3D-printed continuous flow biocatalytic reactor didn't appear until 2017.¹⁸⁷ Here, a 0.5 mL reactor was manufactured from Nylon Taulman 618 (Figure 50). Using Nylon Taulman 618 avoided the common problems of reactor leaking and warping. The reactor channels were then activated with HCl and glutaraldehyde to immobilize (*R*)-selective ω -transaminase (ATA117). Testing the reactor for the kinetic resolution of (*rac*)-methylbenzylamine yielded 49% of the (*S*)-amine in >99% *ee* for a 50 min residence time. Importantly, reactor stability was tested, and little to no effect on performance was observed over 48 h storage.

A carbon nanotube packed bed reactor has been used to provide the necessary conditions for electron transfer between two cascading enzymes (Figure 51).¹⁸⁸ This system avoids sacrificial reductants by regenerating NADH in a cascade process involving three enzymes. First, a hydrogenase converts H_2 to 2H^+ and e^- , then NAD^+ reductase converts NAD^+ back to NADH. The final enzyme (alcohol dehydrogenase) uses the NADH to reduce

acetophenone enantiospecifically. For this process, three enzymes were immobilized onto surface of the carbon nanotube reactor to facilitate electron transfer between the hydrogenase and NAD⁺ reductase. Thus, in this system, H₂ behaves as an indirect reductant under biocatalytic conditions. Under optimal conditions, acetophenone was reduced to (*S*)-1-phenylethanol in 30% conversion, noting that NAD⁺ is reduced to NADH in 67% conversion. This methodology paves the way for multi-step biocatalysis with electron transport, and illustrates co-factor recycling, the topic of the next section.

Co-Factor Recycling

Co-factor recycling is critical for efficient biocatalysis; however, this process can be difficult to engineer in continuous flow. Chemicals typically move in a mono-directional flow with limited reverse diffusion back down the reactor. Thus, once a sacrificial reductant such as a hydride transfer reagent is used, it can only be regenerated via interaction with chemicals in that individual flow segment or the surface of the continuous flow reactor. In contrast, sacrificial reductants or hydride transfer reagents in batch reactors can be regenerated easily as there is multi-directional diffusion. This next section examines current state-of-the-art continuous flow co-factor regeneration methods.

Co-factors are low molecular weight organic or inorganic compounds required for enzyme function (Figure 52). Metal co-factors include iron, magnesium, and zinc, which can play both structural and catalytic roles. The most popular co-factor examined in this Review is nicotinamide adenine dinucleotide (NAD), which can exist either in an oxidized or reduced state, NAD⁺ and NADH respectively. Enzymes use co-factors as reagents and co-catalysts during complex chemical transformations. For example, NADH can provide a hydride source during bioreduction. The versatile co-factor PLP plays roles in diverse reactions involving amino acids including transamination, decarboxylation, deamination, and racemization. Co-factors are often essential for biocatalytic activity, and their requirements must always be considered.

Co-factors require regeneration for multiple rounds of biocatalysis. For example, NAD⁺, must be re-oxidized after conversion to the NADH to yield a catalytic system. Additionally, co-factors are expensive for industrial processes (NADH=\$260 g⁻¹). Thus, for biocatalysis to be economically attractive, co-factors should be regenerated. Furthermore, co-factor regeneration can drive reactions to completion, simplify product isolation, and prevent by-product formation.¹⁸⁹ However, co-factor recycling is a hurdle to enzyme implementation at industrial scales.

Extensive research has produced new chemical, enzymatic and electrochemical methods for the regeneration of co-factors.^{190–192} The regeneration method must match several specifications. First, enzymes, reagents, and equipment should be readily available, inexpensive, easily controlled and robust. Second, the energetics of regeneration should be both kinetically and thermodynamically favourable. Third, reagents or by-products of regeneration should not interfere with the reaction or the isolation of the product. Finally, while co-factors can be regenerated using enzyme and whole-cell based methods,¹⁹³

electrochemical methods are of particular interest due to their effortless product isolation.^{194–196} In this next section, continuous flow co-factor regeneration is described.

Electrochemical regeneration of NAD^+ was achieved using a plug flow reactor constructed from graphite (Figure 53).¹⁹⁷ Here, NADH is produced from NAD^+ via glucose dehydrogenase activity using glucose as a substrate. For the system to be catalytic, NADH must be oxidized back to NAD^+ . This oxidation was achieved using graphite as an electrode with a low voltage of 0.35 V versus SCE, and NADH concentration was determined by absorbance at 340 nm. Optimal conditions provided NADH oxidation with >99.95% yields.

Next, NADH was regenerated in a microfluidic set-up using multi-stream laminar flow (Figure 54).¹⁹⁸ Here, NAD^+ results from using NADH in an enzyme-catalyzed reaction. To regenerate the required NADH, the molecule FADH_2 acts as a hydrogen donor to afford FAD and NADH. However, the FAD then also needs to be regenerated. For this to occur, an electron is transported from the cathode to formate dehydrogenase, which then regenerates FADH_2 . Under multi-stream laminar flow conditions, reactants close to the electrode promote reversal of the unfavourable reaction equilibrium present in co-factor regeneration. The authors first test the regeneration efficacy using only NAD^+ , FAD and formate dehydrogenase; a regeneration efficiency of 31% was achieved. This methodology was then extended to converting a chiral pyruvate into chiral (*L*)-lactate with a yield of 41%.

A major challenge for scaling electrochemical regeneration is limited diffusion, which can impair the rate of electro-enzymatic reactions. This problem was overcome by using a three-dimensional electrode system with an improved electrode surface area of 24 m^2 (Figure 55). The three-dimensional cell consisted of a packed bed graphite anode, and two cathodes positioned on both sides of a cell.¹⁹⁹ A feeder electrode connects the packed bed to the electrical circuit, and each of the cathode chambers was filled with 5 mL of buffer solution. Indirect electrochemical oxidation of NADH was achieved with 2,2-azino-bis-(3-ethylbenzo-thiazoline-6-sulfonic acid, ABTS). Here, ABTS exhibited the highest catalytic performance of 1200 turnovers h^{-1} compared to other mediators such as Azure B, methylene green, PMSF, and caffeic acid. A maximum space-time yield of $1.4 \text{ g}/(\text{L} \cdot \text{h})$ was found, corresponding to a 8-fold improvement compared to a two-dimensional cell.

For scaling electro-enzymatic reactions, an electrochemical plate with six frame filter press cells were assembled into a continuous flow system (Figure 56).²⁰⁰ The reactor provided high regeneration rates by using porous, three-dimensional reticulated vitreous carbon electrodes. The three-dimensional electrodes afforded an exceptionally large surface area up to $19,685 \text{ m}^2\text{m}^{-3}$.²⁰¹ The optimized system afforded improved mass transfer rates with flavin adenine dinucleotide (FAD) being reduced at 93 mM h^{-1} , resulting in the generation of styrene oxide at 1.3 mM h^{-1} . This new continuous setup provides efficient FAD regeneration for broad impact on flavin dependent enzymes in biocatalysis.

Immobilizing co-factors incurs several limitations. First, enzymatic activity using immobilized co-factors is typically low. Second, the re-usability of both the enzymes and the co-factor is limited.^{202–206} Third, the turnover number of the immobilized co-factors is poor.²⁰⁴ Finally, the fabrication of these systems is not currently scalable.²⁰⁷ To aid in the

scalability of this process, enzymes were co-immobilized with co-factors on a solid support.²⁰⁸ Here, alcohol dehydrogenase and formate dehydrogenase were immobilized on activated and modified agarose microbeads (Figure 57). After immobilization, NAD⁺ was ionically adsorbed onto the agarose microbeads to afford a system where both the enzymes and co-factor were immobilized. This continuous system mediated asymmetric reduction of ketones with >79% conversion for 107 h.

Enzymatic Resolution

This section examines continuous flow biocatalytic kinetic resolution. Although batch reactors are used for resolution, key advancements have driven enzymatic resolution into continuous flow.

Super critical CO₂ (sc-CO₂) was used for the continuous kinetic resolution of (*R,S*)-1-phenylethanol using immobilized lipase B.²⁰⁹ The continuous esterification was studied in a 17-cm long reactor with an internal volume of 2.7 mL containing 300 mg of cells expressing lipase B. Here, the lipase is extremely selective for esterifying the (*R*)-isomer, and total conversion was achieved using a 10% molar excess of vinyl laurate. A series of separators are used to remove the vinyl alcohol from the desired product, and (*S*)-PhEtOH can be recovered with a purity of 86% (Figure 58).

Immobilised lipase B has been used for the continuous synthesis of flurbiprofen.²¹⁰ Flurbiprofen is a non-steroidal anti-inflammatory and anti-cancer drug typically synthesized as an (*R,S*) mixture (Figure 59). Here, (*R,S*)-flurbiprofen in toluene containing three equivalent of n-BuOH was flowed through a glass column (10 mm × 100 mm length) loaded with 250 mg of lipase B and 250 mg of molecular sieves. The optimized continuous flow reaction yielded 8.40 μmol/(min. g), a 10-fold increase in productivity compared to batch (0.84 μmol/(min. g)). The process was scaled to 80 mM and high performance was observed for several hours. Furthermore, a “catch and release” system using a column containing polymer supported base Amberlyst A21 caught the unreacted carboxylic acid. This additional step allowed easy separation and recovery of both (*S*)-flurbiprofen and (*R*)-flurbiprofen butyl ester with an *ee* 90% (purity >98%). Notably, this system is similar to one described in the whole cell section of this review.

Ionic liquids (ILs) are simple salts with low melting points (<100 °C), low vapour pressures, excellent thermal stability, and excellent abilities to dissolve organic and inorganic compounds. We previously mentioned using sc-CO₂ and ionic liquids as an alternative to organic solvents, but in some cases, detrimental enzyme effects are observed in sc-CO₂.^{211, 212} To overcome this, coating or suspending a biocatalyst in an IL has protected enzymes against the adverse effects of sc-CO₂. Therefore, a “biphasic system”, of super critical liquid and IL can lead to greener and highly efficient biocatalytic processes.

This style of biphasic system was studied by non-covalently immobilizing Novozyme 435 onto a solid ionic liquid like phase (SILLP).²¹³ SILLP are solid nanostructured materials with microenvironments of tuneable polarity.²¹⁴ Here, different lipase B–SILLPs were tested for the continuous resolution of (*R,S*)-PhEtOH, as previously described (Figure 60). The

desired polymers were synthesized by grafting butyl imidazole onto the commercial bead-type Merrifield resin.^{215–217} Two fractions of the immobilized derivative, and one fraction of acid zeolite coated with [Btma][NTf₂] were packed into three separated columns (Figure 60A). The three columns were arranged into the order 1) immobilized lipase, 2) acid catalyst, and 3) immobilized lipase. The process was operated in a continuous sc-CO₂ flow for four-hour cycles. The resolution was achieved by pumping (*R,S*)-1-PhEtOH and vinyl propionate at 21.2 μmol min⁻¹ using a HPLC pump.²¹³ The column assembly worked for more than three weeks without a reduction in performance. In addition, excellent yield (92%) and enantioselectivity (>99.9%) were observed using a one-column reactor containing a mixture of the enzyme and zeolite coated [Btma][NTf₂] (Figure 60B).

Most examples using lipase use commercially available *Candida antarctica B* (Novozyme 435). However, with new developments in enzyme immobilization, lipases from different organisms can be utilized.²¹⁸ Sol-gel immobilized lipase from *Burkholderia cepacia* has been used for the kinetic resolution of 1,5-dihydroxy-1,2,3,4-tetrahydronaphthalene by trans-esterification (Figure 61). The lyophilized lipase (120 mg mL⁻¹) was dissolved and mixed with [Omim][BF₄]. Optimal conditions were obtained in batch and then translated into continuous flow using a packed-bed reactor. The column reactor was filled with 1.45 g of lipase immobilized by sol-gel entrapment. Additional testing showed that vinyl acetate was the most efficient acyl donor with 43% THF as a co-solvent to increase substrate solubility. The immobilized lipase demonstrated excellent operational stability for four-days, preserving a productivity above 180 μmol h⁻¹ per gram of catalyst. It should be noted, that this example translated conditions directly from batch, and although this is likely suitable, we recommend additional optimization to account for continuous flow benefits.

Different lipases from *Candida antarctica B* and *Pseudomonas fluorescens* were immobilized into a sol-gel matrix to improve their thermal and operational stability (Figure 62).²¹⁹ Various silane precursors for the sol-gel matrix such as methyl vinyl, octyl, phenyl-trimethoxysilane, and tetra-methoxysilane were tested for kinetic resolution of chiral heteroaromatic secondary alcohols with benzofuran, benzothiophen, phenothiazine, and 2-phenylthiazol moieties. Lipases were immobilized in the sol-gel entrapment with NaF for simultaneous hydrolysis and polycondensation,²²⁰ or using HCl for pre-forming a polymer.²²¹ Continuous flow experiments were performed in a thermo-regulated stainless steel column filled with immobilized lipase attached to a HPLC pump. The substrate solution comprised of racemic alcohols and vinyl acetate (3 equiv) in n-hexane was pumped through reactor for chiral resolution. After optimizing the best reaction conditions in batch, resolution of the racemic benzofuranylethanol with lipase from *C. antarctica B* and *P. fluorescens* were studied in continuous flow; reaction rates were 2–4 fold higher.

Translating into continuous flow and immobilizing proteins can increase their stability. A report by Yu, Xu and co-workers describes using a mutant enzyme based upon an esterase from *Pseudomonas putida*.²²² Here, the enzyme was covalently linked to a solid support for long processing times in continuous flow. A number of resins were compared, and epoxide-based and hydrophobic resins were less effective at enzyme stabilization than amine-functionalized and hydrophilic resins; in the later example, the enzyme was bioconjugated using glutaraldehyde cross-linking, and this conjugation to a solid support lead to a dramatic

increase in protein stability; protein lifetime increased from 50 h to 1440 h at 30 °C. Using the immobilized enzyme, the resolution of 2-acetoxy-2-(2-chlorophenyl)acetate provides the (*R*)-enantiomer, a key intermediate for API clopidogrel (Figure 63). This continuous flow process operated for 42 days with approximately 50% conversion (maximum conversion for racemate resolution) and >99% ee. Additionally, the space-time-yield for this transformation was 3.34 kg / (L. day) at 0.5 mL min⁻¹ (12 min residence time) using a packed bed reactor.

Using a protease for its ligation capabilities, a N-Boc-phenylalanine ethyl thioester was resolved through amidation with benzylamine.²²³ For direct comparison of batch vs. continuous flow, the authors compared “tea bags” of enzymes immersed in flasks with a packed bed reactor; continuous flow suppressed the undesirable, non-stereoselective, direct reaction between benzylamine and the racemic starting material allowing the desired reaction. Notably, the authors tested a large number of different immobilization methods and resins to find that cross-linked enzyme crystals (CLECs), or as cross-linked enzyme aggregates were prone to clogging for continuous flow applications. Furthermore, rather than losing the unreacted (*S*)-amino acid derivative, a dynamic kinetic chemoresolution was employed. Here, the output of the enzymatic continuous flow reactor was passed into a packed bed reactor containing ethyl-grafted silica gel. In the presence of DBU, this reactor racemized the (*S*)-enantiomer, and the output was connected to a third continuous flow reactor to run the subtilisin-catalyzed amidation reaction for another round of kinetic resolution (Figure 64). This clever system yielded the desired (*R*)-amide in good yield (71%) with excellent volumetric productivity 8.17 g / (L. h) and 98% ee.

The use of enzymes wrapped in inert gauze “tea bags” allowed direct comparison of enzyme-based kinetic resolution in batch vs. continuous flow.²²⁴ In this example, Turner and co-workers demonstrated a significant reduction in reaction times for the continuous flow lipase-catalyzed resolution of a cyclopropanecarboxylate ester. A 5.5 min residence time in a packed bed reactor housing *Thermomyces lanuginosus* lipase compared favourably to the batch reaction after 23 h. The authors cite a 64-fold improvement in space-time yield from 0.4 mmol / (L. h) in batch to 28.2 mmol / (L. h) in continuous flow. Additionally, enantioselectivity was improved in continuous flow, and the authors report using a co-solvent system of heptane and glycine buffer to avoid substrate inhibition through accumulation around the resin (Figure 65).

As we noted several times, lipases are excellent at chiral resolution via selective hydrolysis or esterification. In this final system, translating this enzyme into continuous flow decreased reaction times and lowered the catalyst loading. Friere, de Souza, and co-workers described the stereoselective acetylation of (±)-1,3,6-tri-O-benzyl-myo-inositol with vinyl acetate using Novozyme 435. Their continuous process displayed remarkable consistency with maximum yields of 50% obtained during nine cycles with a three min residence time per run at 50 °C using TBME as the solvent (Figure 66).²²⁵ Another use of this methodology allowed ethyl acetate as the acyl donor to resolve (±)-1-phenylethylamine, however, using ethyl acetate resulted in unacceptable levels of non-specific, non-enzyme-catalyzed acylation.²²⁶

Conclusions

Continuous flow biocatalysis is a powerful tool in chemical synthesis. Although continuous flow organic synthesis has enjoyed significant popularity, continuous flow biocatalysis is not far behind. What started as an industrial area focused on bulk chemical generation has grown into a thriving R&D arena for fine chemical generation. Many examples detail the range of enhancements continuous flow can bring to enzyme-mediated transformations. These include improved reaction rates, in-line product removal and purification, better mixing, improved control, use of process analytical technology, and improved enzyme stability and lifetime. It is remarkable that improved performances of up to 351-fold were observed in continuous flow, and that is without any directed evolution of the enzyme; it is worth considering the improvements possible by combining directed evolution and continuous flow.

Upon reflection, there are areas that need to be improved. First, immobilization efficiencies are often low, and once immobilized, many enzymes lose considerable activity. For continuous flow biocatalysis to become even more beneficial, general solutions to improve immobilization and residual activity are required. Second, comparisons between batch and continuous flow need to be carefully monitored. The reaction in batch should be performed under conditions that closely emulate the contrasting continuous flow conditions. Here, enzyme loading, concentration, temperature, pressure and time should be kept constant, otherwise comparisons are hard to believe. Third, continuous flow conditions need to be reported accurately so that systems can be transferred from lab-to-lab without additional optimization. Finally, continuous flow process lifetime is not always explored. For continuous flow biocatalysis to be considered on industrial routes, the process lifetime and efficiency needs to be explored. If authors are trying to demonstrate the benefit of the enzyme-driven process over the chemical, it's a compelling case if the enzyme-driven system lasts for weeks, not minutes. As more enzymes become commercially available, the push towards greener and more cost effective biotransformation's will increase, and continuous flow biocatalysis will likely to rapidly expand and diversify over the next few years.

Supplementary Material

Refer to Web version on PubMed Central for supplementary material.

References

1. Britton J and Raston CL, *Chem. Soc. Rev.*, 2017, 46, 1250–1271. [PubMed: 28106210]
2. Lévesque F and Seeberger PH, *Angew. Chem. Int. Edit.*, 2012, 51, 1706–1709.
3. Gutmann B, Cantillo D and Kappe CO, *Angew. Chem. Int. Edit.*, 2015, 54, 6688–6728.
4. Baumann M and Baxendale IR, *Beilstein J. Org. Chem.*, 2015, 11, 1194–1219. [PubMed: 26425178]
5. Britton J and Jamison TF, *Angew. Chem. Int. Edit.*, 2017, 129, 8949–8953.
6. Hartman RL and Jensen KF, *Lab Chip*, 2009, 9, 2495–2507. [PubMed: 19680575]
7. Malet-Sanz L and Susanne F, *J. Med. Chem.*, 2012, 55, 4062–4098. [PubMed: 22283413]
8. McQuade DT and Seeberger PH, *J. Org. Chem.*, 2013, 78, 6384–6389. [PubMed: 23750988]

9. Plutschack MB, Pieber B, Gilmore K and Seeberger PH, *Chem. Rev.*, 2017, 117, 11796–11893. [PubMed: 28570059]
10. Britton J and Jamison TF, *Eur. J. Org. Chem.*, 2017, 6566–6574.
11. Caaaayre JY, Renold P, Pitterna T and El QM, Google Patents, 2014.
12. Whittingham WG, Winn CL, Glithro H, Boussemghoune MA and Aspinall MB, Google Patents, 2011.
13. Buchholz A, Reiner W and Haas UJ, Google Patents, 2011.
14. Mathews CJ, Finney J, Scutt JN, Robinson L and Delaney JS, Google Patents, 2011.
15. Jeanmart SAM, Viner R, Taylor JB, Whittingham WG, Wailes JS, Targett SM, Mathews CJ and Muehlebach M, Google Patents, 2011.
16. Meyer KG, Owen WJ, Renga JM, Yao C, Nugent BM, Wilmot J, Li F and Bravo-Altamirano K, Google Patents, 2014.
17. Cantillo D and Kappe CO, *React. Chem. Eng.*, 2017, 2, 7–19.
18. Paseta L, Seoane B, Julve D, Sebastián V, Téllez C and Coronas J, *ACS Appl. Mater. Inter.*, 2013, 5, 9405–9410.
19. Bayliss PA, Ibarra IA, Perez E, Yang S, Tang CC, Poliakov M and Schroder M, *Green Chem.*, 2014, 16, 3796–3802.
20. Rubio-Martinez M, Batten MP, Polyzos A, Carey K-C, Mardel JI, Lim K-S and Hill MR, *Sci. Rep.*, 2014, 4, 5443. [PubMed: 24962145]
21. Rubio-Martinez M, Hadley TD, Batten MP, Constanti-Carey K, Barton T, Marley D, Mönch A, Lim K-S and Hill MR, *ChemSusChem*, 2016, 9, 938–941. [PubMed: 27075923]
22. Zhang Y, Jamison TF, Patel S and Mainolfi N, *Org. Lett.*, 2011, 13, 280–283. [PubMed: 21141809]
23. Bao J and Tranmer GK, *Chem. Commun.*, 2015, 51, 3037–3044.
24. Nuyts K, Ceulemans M, Parac-Vogt TN, Bultynck G and De Borggraeve WM, *Tetrahedron Lett.*, 2015, 56, 1687–1690.
25. Polyzos A, O'Brien M, Petersen TP, Baxendale IR and Ley SV, *Angew. Chem. Int. Edit.*, 2011, 50, 1190–1193.
26. Pastre JC, Browne DL, O'Brien M and Ley SV, *Org. Process. Res. Dev.*, 2013, 17, 1183–1191.
27. Yang L and Jensen KF, *Org. Process. Res. Dev.*, 2013, 17, 927–933.
28. Mallia CJ, Burton PM, Smith AMR, Walter GC and Baxendale IR, *Beilstein J. Org. Chem.*, 2016, 12, 1598–1607. [PubMed: 27559412]
29. Razzaq T, Glasnov TN and Kappe CO, *Eur. J. Org. Chem.*, 2009, DOI: 10.1002/ejoc.200900077, 1321–1325.
30. Glasnov TN and Kappe CO, *Chem. Eur. J.*, 2011, 17, 11956–11968. [PubMed: 21932289]
31. Ley SV, Fitzpatrick DE, Myers RM, Battilocchio C and Ingham RJ, *Angew. Chem. Int. Edit.*, 2015, 54, 10122–10136.
32. Gilmore K and Seeberger PH, *The Chemical Record*, 2014, 14, 410–418. [PubMed: 24890908]
33. Cambié D, Bottecchia C, Straathof NJW, Hessel V and Noël T, *Chem. Rev.*, 2016, 116, 10276–10341. [PubMed: 26935706]
34. Loubière K, Oelgemöller M, Aillet T, Dechy-Cabaret O and Prat L, *Chem. Eng. Process: Process Intensification*, 2016, 104, 120–132.
35. Seo H, Katcher MH and Jamison TF, *Nature Chem.*, 2016, 9, 453. [PubMed: 28430203]
36. Li H, Sheeran JW, Clausen AM, Fang Y-Q, Bio MM and Bader S, *Angew. Chem. Int. Edit.*, 2017, 56, 9425–9429.
37. Shu W, Pellegatti L, Oberli MA and Buchwald SL, *Angew. Chem. Int. Edit.*, 2011, 50, 10665–10669.
38. Koos P, Gross U, Polyzos A, O'Brien M, Baxendale I and Ley SV, *Org. Biomol. Chem.*, 2011, 9, 6903–6908. [PubMed: 21874192]
39. Mastronardi F, Gutmann B and Kappe CO, *Org. Lett.*, 2013, 15, 5590–5593. [PubMed: 24128181]
40. O'Brien M, Baxendale IR and Ley SV, *Org. Lett.*, 2010, 12, 1596–1598. [PubMed: 20218640]
41. Pieber B and Kappe CO, *Org. Lett.*, 2016, 18, 1076–1079. [PubMed: 26902154]

42. Roberge DM, Ducry L, Bieler N, Cretton P and Zimmermann B, *Chem. Eng. Technol*, 2005, 28, 318–323.
43. Adamo A, Beingsner RL, Behnam M, Chen J, Jamison TF, Jensen KF, Monbaliu J-CM, Myerson AS, Revalor EM, Snead DR, Stelzer T, Weeranoppanant N, Wong SY and Zhang P, *Science*, 2016, 352, 61–67. [PubMed: 27034366]
44. Perera D, Tucker JW, Brahmabhatt S, Helal CJ, Chong A, Farrell W, Richardson P and Sach NW, *Science*, 2018, 359, 429–434. [PubMed: 29371464]
45. Roberge DM, Zimmermann B, Rainone F, Gottsponer M, Eycholzer M and Kockmann N, *Org. Biomol. Chem*, 2008, 12, 905–910.
46. Schaber SD, Gerogiorgis DI, Ramachandran R, Evans JMB, Barton PI and Trout BL, *Ind. Eng. Chem. Res*, 2011, 50, 10083–10092.
47. Lee SL, O'Connor TF, Yang X, Cruz CN, Chatterjee S, Madurawe RD, Moore CMV, Yu LX and Woodcock J, *J. Pharm. Innov*, 2015, 10, 191–199.
48. Porta R, Benaglia M and Puglisi A, *Org. Process. Res. Dev*, 2016, 20, 2–25.
49. Poehlauer P, Manley J, Broxterman R, Gregertsen B and Ridemark M, *Org. Process. Res. Dev*, 2012, 16, 1586–1590.
50. Buchholz S, *Chem. Eng. Process: Process Intensification*, 2010, 49, 993–995.
51. Tamborini L, Fernandes P, Paradisi F and Molinari F, *Trends Biotechnol*, 2018, 36, 73–88. [PubMed: 29054312]
52. de Carvalho CCCR, *Biotech. Adv*, 2011, 29, 75–83.
53. Ishige T, Honda K and Shimizu S, *Curr. Opin. Chem. Biol*, 2005, 9, 174–180. [PubMed: 15811802]
54. Wachtmeister J and Rother D, *Curr. Opin. Biotech*, 2016, 42, 169–177. [PubMed: 27318259]
55. Klivanov AM, *Nature*, 2001, 409, 241. [PubMed: 11196652]
56. Klivanov AM, *Science*, 1983, 219, 722–727. [PubMed: 17814033]
57. W. G. M. Chi-Huey, *Angew. Chem. Int. Edit.*, in English, 1985, 24, 617–638.
58. Jones JB and DeSantis G, *Account. Chem. Res*, 1999, 32, 99–107.
59. DeSantis G and Jones JB, *Curr. Opin. Biotechnol*, 1999, 10, 324–330. [PubMed: 10449313]
60. Jones JB and Pliura DH, *Canadian J. Chem*, 1981, 59, 2921–2925.
61. Toone EJ, Werth MJ and Jones JB, *J. Am. Chem. Soc*, 1990, 112, 4946–4952.
62. Schüürmann J, Quehl P, Festel G and Jose J, *Appl. Microbiol. Biot*, 2014, 98, 8031–8046.
63. Tsai D-Y, Tsai Y-J, Yen C-H, Ouyang C-Y and Yeh Y-C, *RSC Adv*, 2015, 5, 87998–88001.
64. Gustavsson M, Hörnström D, Lundh S, Belotserkovsky J and Larsson G, *Sci. Rep*, 2016, 6, 36117. [PubMed: 27782179]
65. Fukuda H, Hama S, Tamalampudi S and Noda H, *Trends Biotechnol*, 2008, 26, 668–673. [PubMed: 18976825]
66. Zhu Y, in *Bioprocessing for Value-Added Products from Renewable Resources*, Elsevier, Amsterdam, 2007, pp. 373–396.
67. Lin B and Tao Y, *Microb. Cell Fact*, 2017, 16, 106. [PubMed: 28610636]
68. Schrewe M, Julsing MK, Buhler B and Schmid A, *Chem. Soc. Rev*, 2013, 42, 6346–6377. [PubMed: 23475180]
69. Ni Y and Chen RR, *Biotechnol. Bioeng*, 2004, 87, 804–811. [PubMed: 15329939]
70. Chen RR, *Appl. Microbiol. Biot*, 2007, 74, 730–738.
71. Lam CMC, Suárez Diez M, Godinho M and Martins dos Santos VAP, *FEBS Letters*, 2012, 586, 2184–2190. [PubMed: 22710181]
72. Lee S, *Encyclopedia of Chemical Processing, Volume 1*, Taylor & Francis Group, New York, 2006.
73. Baneyx F, *Curr. Opin. Biotech*, 1999, 10, 411–421. [PubMed: 10508629]
74. Overton TW, *Drug Discovery Today*, 2014, 19, 590–601. [PubMed: 24246684]
75. Rosano GL and Ceccarelli EA, *Front. Microbiol*, 2014, 5. [PubMed: 24523715]
76. Papaneophytou CP and Kontopidis G, *Protein Express. Purif*, 2014, 94, 22–32.
77. Terpe K, *Appl. Microbiol. Biot*, 2006, 72, 211.

78. Robichon C, Luo J, Causey TB, Benner JS and Samuelson JC, *Appl. Environ. Microb*, 2011, 77, 4634–4646.
79. Kapoor M and Gupta MN, *Process Biochem*, 2012, 47, 555–569.
80. Sharma UK, Sharma N, Kumar R, Kumar R and Sinha AK, *Org. Lett*, 2009, 11, 4846–4848. [PubMed: 19788267]
81. Svedendahl M, Hult K and Berglund P, *J. Am. Chem. Soc*, 2005, 127, 17988–17989. [PubMed: 16366534]
82. Ding Y, Xiang X, Gu M, Xu H, Huang H and Hu Y, *Bioproc. Biosyst. Eng*, 2016, 39, 125–131.
83. Yang F, Wang Z, Wang H, Zhang H, Yue H and Wang L, *RSC Adv*, 2014, 4, 25633–25636.
84. Guezane-Lakoud S, Toffano M and Aribi-Zouiouche L, *Heteroatom Chem*, 2017, 28, e21408.
85. Rodrigues RC, Ortiz C, Berenguer-Murcia A, Torres R and Fernandez-Lafuente R, *Chem. Soc. Rev*, 2013, 42, 6290–6307. [PubMed: 23059445]
86. Rosevear A, *J. Chem. Technol. Biot*, 1984, 34, 127–150.
87. Sheldon RA and van Pelt S, *Chem. Soc. Rev*, 2013, 42, 6223–6235. [PubMed: 23532151]
88. Magner E, *Chem. Soc. Rev*, 2013, 42, 6213–6222. [PubMed: 23306669]
89. Liese A and Hilterhaus L, *Chem. Soc. Rev*, 2013, 42, 6236–6249. [PubMed: 23446771]
90. Secundo F, *Chem. Soc. Rev*, 2013, 42, 6250–6261. [PubMed: 23482973]
91. Hartmann M and Kostrov X, *Chem. Soc. Rev*, 2013, 42, 6277–6289. [PubMed: 23765193]
92. Sheldon RA, *Adv. Syn. Catal*, 2007, 349, 1289–1307.
93. Datta S, Christena LR and Rajaram YRS, *3 Biotech*, 2013, 3, 1–9.
94. Bickerstaff GF, in *Immobilization of Enzymes and Cells*, ed. Bickerstaff GF, Humana Press, Totowa, NJ, 1997, DOI: 10.1385/0-89603-386-4:1, pp. 1–11.
95. Birnbaum S, in *Advances in Molecular and Cell Biology*, eds. Bittar EE, Danielsson B and Bülow L, Elsevier, 1996, vol. 15, pp. 136–139.
96. Jesionowski T, Zdarta J and Krajewska B, *Adsorption*, 2014, 20, 801–821.
97. Cristóvão RO, Tavares APM, Brígida AI, Loureiro JM, Boaventura RAR, Macedo EA and Coelho MAZ, *J. Mol. Cat B: Enzymatic*, 2011, 72, 6–12.
98. Brígida AIS, Pinheiro ÁDT, Ferreira ALO and Gonçalves LRB, *Appl. Biochem. Biotech*, 2008, 146, 173–187.
99. Chernoglazov VM, Ermolova OV and Klyosov AA, *Enzyme Microb. Tech*, 1988, 10, 503–507.
100. Šekuljica NŽ, Prlainovi NŽ, Jovanovi JR, Stefanovi AB, Djoki VR, Mijin DŽ and Kneževi - Jugovi ZD, *Bioproc. Biosyst. Eng*, 2016, 39, 461–472.
101. Tanaskovi S, Jakoveti J, Joki B, Grbav i S, Drvenica I, Prlainovi N, Lukovi N and Kneževi - Jugovi Z, *Appl. Clay Sci*, 2017, 135, 103–111.
102. Yiu HHP, Wright PA and Botting NP, *J. Mol. Cat B: Enzymatic*, 2001, 15, 81–92.
103. Deere J, Magner E, Wall JG and Hodnett BK, *J. Phys. Chem B*, 2002, 106, 7340–7347.
104. Vinu A, Murugesan V and Hartmann M, *J. Phys. Chem. B*, 2004, 108, 7323–7330.
105. Yan A-X, Li X-W and Ye Y-H, *Appl. Biochem. Biotech*, 2002, 101, 113–129.
106. Al-Duri B and Yong YP, *J. Mol. Cat. B: Enzymatic*, 1997, 3, 177–188.
107. Porath J and Axén R, in *Method. Enzymol*, Academic Press, 1976, vol. 44, pp. 19–45.
108. Britton J, Raston CL and Weiss GA, *Chem. Commun*, 2016, 52, 10159–10162.
109. Fu J, Reinhold J and Woodbury NW, *PLOS ONE*, 2011, 6, e18692. [PubMed: 21494577]
110. Sirisha VL, Jain A and Jain A, in *Advances in Food and Nutrition Research*, eds. Kim S-K and Toldrá F, Academic Press, 2016, vol. 79, pp. 179–211. [PubMed: 27770861]
111. Kim HP, Byun SM, Yeom YI and Kim SW, *J. Pharm. Sci*, 1983, 72, 225–228. [PubMed: 6221088]
112. Zhang D, Hegab HE, Lvov Y, Dale Snow L and Palmer J, *SpringerPlus*, 2016, 5, 48. [PubMed: 26835228]
113. Ma H-Z, Yu X-W, Song C, Xue Q.-I. and Jiang B, *J. Mol. Cat B: Enzymatic*, 2016, 127, 76–81.
114. Wang X-Y, Jiang X-P, Li Y, Zeng S and Zhang Y-W, *Int. J. Biol. Macromol*, 2015, 75, 44–50. [PubMed: 25603148]

115. Zang L, Qiu J, Wu X, Zhang W, Sakai E and Wei Y, *Ind. Eng. Chem. Res.*, 2014, 53, 3448–3454.
116. Sánchez-Ramírez J, Martínez-Hernández JL, Segura-Ceniceros P, López G, Saade H, Medina-Morales MA, Ramos-González R, Aguilar CN and Ilyina A, *Bioproc. Biosyst. Eng.*, 2017, 40, 9–22.
117. de Souza SP, de Almeida RAD, Garcia GG, Leão RAC, Bassut J, de Souza ROMA and Itabaiana I, Jr., *J. Chem. Technol. Biotechnol.*, 2018, 93, 105–111.
118. Li X, Li D, Wang W, Durrani R, Yang B and Wang Y, *Journal of Molecular Catalysis B: Enzymatic*, 2016, 133, 154–160.
119. Marín-Navarro J, Talens-Perales D, Oude-Vrielink A, Cañada FJ and Polaina J, *World Journal of Microbiology and Biotechnology*, 2014, 30, 989–998. [PubMed: 24122101]
120. Zhou X, Mikhailopulo IA, Cruz Bournazou MN and Neubauer P, *J. Mol. Catal. B: Enzymatic*, 2015, 115, 119–127.
121. Li W, Wen H, Shi Q and Zheng G, *Process Biochemistry*, 2016, 51, 270–276.
122. Shang C-Y, Li W-X, Jiang F and Zhang R-F, *J. Mol. Cat B: Enzymatic*, 2015, 113, 9–13.
123. Shang C-Y, Li W-X and Zhang R-F, *Enzyme Microb. Tech.*, 2014, 61–62, 28–34.
124. Britton J, Dyer RP, Majumdar S, Raston CL and Weiss GA, *Angew. Chem. Int. Edit.*, 2017, 56, 2296–2301.
125. Spriestersbach A, Kubicek J, Schäfer F, Block H and Maertens B, in *Method Enzymol.*, ed. Lorsch JR, Academic Press, 2015, vol. 559, pp. 1–15.
126. Shi QH, Tian Y, Dong XY, Bai S and Sun Y, *Biochem. Eng. J.*, 2003, 16, 317–322.
127. Carlsson J, Gabel D, Larsson E, Pontén J and Westermark B, *In Vitro*, 1979, 15, 844–850. [PubMed: 583464]
128. Shen Q, Yang R, Hua X, Ye F, Zhang W and Zhao W, *Process Biochem.*, 2011, 46, 1565–1571.
129. Wen H, Nallathambi V, Chakraborty D and Barton Calabrese S, *Microchimica Acta*, 2011, 175, 283–289.
130. Wang Z-G, Wan L-S, Liu Z-M, Huang X-J and Xu Z-K, *J. Mol. Cat B: Enzymatic*, 2009, 56, 189–195.
131. Betigeri SS and Neau SH, *Biomaterials*, 2002, 23, 3627–3636. [PubMed: 12109688]
132. Ispas C, Sokolov I and Andreescu S, *Anal. Bioanal. Chem.*, 2009, 393, 543–554. [PubMed: 18642104]
133. Erdemir S and Yilmaz M, *J. Incl. Phenom. Macro.*, 2012, 72, 189–196.
134. Jegannathan KR, Jun-Yee L, Chan E-S and Ravindra P, *Fuel*, 2010, 89, 2272–2277.
135. Lee CY and Chang HN, *Biotechnol. Lett.*, 1990, 12, 23–28.
136. Schiraldi C, Di Lernia I, Giuliano M, Generoso M, D’Agostino A and De Rosa M, *J. Ind. Microbiol. Biot.*, 2003, 30, 302–307.
137. Matsuda T, Watanabe K, Kamitanaka T, Harada T and Nakamura K, *Chem. Commun.*, 2003, DOI: 10.1039/B301452E, 1198–1199.
138. Genari AN, Passos FV and Passos FML, *J. Dairy Sci.*, 2003, 86, 2783–2789. [PubMed: 14507014]
139. Mo Y and Jensen KF, *React. Chem. Eng.*, 2016, 1, 501–507.
140. Browne DL, Deadman BJ, Ashe R, Baxendale IR and Ley SV, *Org. Process. Res. Dev.*, 2011, 15, 693–697.
141. Pieber B, Shalom M, Antonietti M, Seeberger PH and Gilmore K, *Angew. Chem. Int. Edit.*, DOI: 10.1002/anie.201712568, DOI: 10.1002/anie.201712568.
142. Tan AWI, Fischbach M, Huebner H, Buchholz R, Hummel W, Dausmann T, Wandrey C and Liese A, *Appl. Microbiol. Biot.*, 2006, 71, 289–293.
143. Kurbanoglu EB, Zilbeyaz K, Kurbanoglu NI, Ozdal M, Taskin M and Algur OF, *Tetrahedron: Asymmetry*, 2010, 21, 461–464.
144. Al’myasheva NR, Kopitsyn DS, Vinokurov VA and Novikov AA, *Chem. Tech. Fuels Oil+*, 2015, 50, 449–452.
145. Chen G, Liu J, Yao J, Qi Y and Yan B, *Energ. Convers. Manage.*, 2017, 138, 556–564.
146. Xiao MAN, Qi C and Obbard JP, *GCB Bioenergy*, 2011, 3, 293–298.

147. Tamborini L, Romano D, Pinto A, Contente M, Iannuzzi MC, Conti P and Molinari F, *Tetrahedron Lett*, 2013, 54, 6090–6093.
148. de Oliveira Lopes R, Ribeiro JB, Silva de Miranda A, Vieira da Silva GV, Miranda LSM, Ramos Leal IC and Mendonça RO de Souza Alves, *Tetrahedron*, 2014, 70, 3239–3242.
149. Hara F, Nakashima T and Fukuda H, *J. Am. Oil. Chem. Soc.*, 1997, 74, 1129–1132.
150. Hoshino A and Isono Y, *Biodegradation*, 2002, 13, 141–147. [PubMed: 12449316]
151. Kumar A, Dhar K, Kanwar SS and Arora PK, *Biol. Proced. Online*, 2016, 18, 2. [PubMed: 26766927]
152. Kamal MZ, Yedavalli P, Deshmukh MV and Rao NM, *Prot. Sci.*, 2013, 22, 904–915.
153. Cao SG, Feng Y, Liu ZB, Ding ZT and Cheng YH, *Appl. Biochem. Biotech.*, 1992, 32, 7–13.
154. Adlercreutz P, *Chem. Soc. Rev.*, 2013, 42, 6406–6436. [PubMed: 23403895]
155. Sánchez A, delRío JL, Valero F, Lafuente J, Faus I and Solà C, *J. Biotechnol.*, 2000, 84, 1–12.
156. Gitlesen T, Bauer M and Adlercreutz P, *Biochimica et Biophysica Acta (BBA) - Lipids and Lipid Metabolism*, 1997, 1345, 188–196. [PubMed: 9106498]
157. Woodcock LL, Wiles C, Greenway GM, Watts P, Wells A and Eyley S, *Biocatal. Biotransfor.*, 2008, 26, 466–472.
158. Wiles C, Hammond MJ and Watts P, *Beilstein J. Org. Chem.*, 2009, 5, 27. [PubMed: 19590744]
159. Kundu S, Bhangale AS, Wallace WE, Flynn KM, Guttman CM, Gross RA and Beers KL, *J. Am. Chem. Soc.*, 2011, 133, 6006–6011. [PubMed: 21438577]
160. Porcar R, Sans V, Ríos-Lombardía N, Gotor-Fernández V, Gotor V, Burguete MI, García-Verdugo E and Luis SV, *ACS Catal.*, 2012, 2, 1976–1983.
161. Britton J and Jamison TF, *Nature Protoc.*, 2017, 12, 2423. [PubMed: 29072707]
162. Junior II, Flores MC, Sutuli FK, Leite SGF, de M. Miranda LS Leal ICR and de Souza ROMA, *Org. Process. Res. Dev.*, 2012, 16, 1098–1101.
163. Le Joubioux F, Bridiau N, Sanekli M, Graber M and Maugard T, *J. Mol. Cat B: Enzymatic*, 2014, 109, 143–153.
164. Brahma A, Musio B, Ismayilova U, Nikbin N, Kamptmann SB, Siegert P, Jeromin GE, Let SV and Pohl M, *Synlett*, 2015, 27, 262–266.
165. Saranya P, Ramani K and Sekaran G, *RSC Adv*, 2014, 4, 10680–10692.
166. Wang J, Gu S-S, Cui H-S, Wu X-Y and Wu F-A, *Bioresource Technol.*, 2014, 158, 39–47.
167. Ro H-S and Kim H-S, *Enzyme Microb. Tech.*, 1991, 13, 920–924.
168. Wang AA, Chen W and Mulchandani A, *Biotechnol. Bioeng.*, 2005, 91, 379–386. [PubMed: 15892051]
169. Mohr S, Fisher K, Scrutton NS, Goddard NJ and Fielden PR, *Lab Chip*, 2010, 10, 1929–1936. [PubMed: 20526519]
170. Tudorache M, Mahalu D, Teodorescu C, Stan R, Bala C and Parvulescu VI, *J. Mol. Cat B: Enzymatic*, 2011, 69, 133–139.
171. Babich L, Hartog AF, van der Horst MA and Wever R, *Chem. Eur. J.*, 2012, 18, 6604–6609. [PubMed: 22505143]
172. Lawrence J, O'Sullivan B, Lye GJ, Wohlgemuth R and Szita N, *J. Mol. Cat B: Enzymatic*, 2013, 95, 111–117.
173. Tomaszewski B, Lloyd RC, Warr AJ, Buehler K and Schmid A, *ChemCatChem*, 2014, 6, 2567–2576.
174. Andrade LH, Kroutil W and Jamison TF, *Org. Lett.*, 2014, 16, 6092–6095. [PubMed: 25394227]
175. Peschke T, Skoupi M, Burgahn T, Gallus S, Ahmed I, Rabe KS and Niemeyer CM, *ACS Catal.*, 2017, 7, 7866–7872.
176. Benítez-Mateos AI, SanlSebastian E, Ríos-Lombardía N, Morís F, González-Sabín J and López-Gallego F, *Chem. Eur. J.*, 2017, 23, 16843–16852. [PubMed: 28940802]
177. Planchestainer M, Contente ML, Cassidy J, Molinari F, Tamborini L and Paradisi F, *Green Chem.*, 2017, 19, 372–375.
178. Contente ML, Dall'Oglio F, Tamborini L, Molinari F and Paradisi F, *ChemCatChem*, 2017, 9, 3843–3848.

179. Dreßen A, Hilberath T, Mackfeld U, Rudat J and Pohl M, *J. Biotechnol*, 2017, 258, 158–166. [PubMed: 28472673]
180. Sayer LH, Florence GJ and Smith TK, *React. Chem. Eng*, 2017, 2, 44–49.
181. Gruber P, Carvalho F, Marques MPC, O’Sullivan B, Subrizi F, Dobrijevic D, Ward J, Hailes HC, Fernandes P, Wohlgemuth R, Baganz F and Szita N, *Biotechnol. Bioeng*, 2018, 115, 586–596. [PubMed: 28986983]
182. DelVitis V, Dall’Oglio F, Pinto A, DelMicheli C, Molinari F, Conti P, Romano D and Tamborini L, *ChemistryOpen*, 2017, 6, 668–673. [PubMed: 29046862]
183. Tang X, Allemann RK and Wirth T, *Eur. J. Org. Chem*, 2017, 2, 414–418.
184. Jones E, McClean K, Housden S, Gasparini G and Archer I, *Chem. Eng. Res. Des*, 2012, 90, 726–731.
185. Karande R, Schmid A and Buehler K, *Adv. Syn. Catal*, 2011, 353, 2511–2521.
186. Valikhani D, Bolivar JM, Viefhues M, McLroy DN, Vrouwe EX and Nidetzky B, *ACS Appl. Mater. Inter*, 2017, 9, 34641–34649.
187. Peris E, Okafor O, Kulcinskaja E, Goodridge R, Luis SV, Garcia-Verdugo E, O’Reilly E and Sans V, *Green Chem*, 2017, 19, 5345–5349.
188. Zor C, Reeve HA, Quinson J, Thompson LA, Lonsdale TH, Dillon F, Grobert N and Vincent KA, *Chem. Commun*, 2017, 53, 9839–9841.
189. Koeller KM and Wong CH, *Nature*, 2001, 409, 232–240. [PubMed: 11196651]
190. Chenault HK, Simon ES and Whitesides GM, *Biotechnol. Genet Eng*, 1988, 6, 221–270.
191. Chenault HK and Whitesides GM, *Appl. Biochem. Biotech*, 1987, 14, 147–197.
192. Zhao H and van der Donk WA, *Curr. Opin. Biotechnol*, 2003, 14, 583–589. [PubMed: 14662386]
193. Schmid A, Dordick JS, Hauer B, Kiener A, Wubbolts M and Witholt B, *Nature*, 2001, 409, 258–268. [PubMed: 11196655]
194. Chenault HK and Whitesides GM, *Appl. Biochem. Biotechnol*, 1987, 14, 147–197. [PubMed: 3304160]
195. Leonida MD, *Curr. Med. Chem*, 2001, 8, 345–369. [PubMed: 11172694]
196. van der Donk WA and Zhao H, *Curr. Opin. Biotechnol*, 2003, 14, 421–426. [PubMed: 12943852]
197. Fassouane A, Laval JM, Moiroux J and Bourdillon C, *Biotechnol. Bioeng*, 1990, 35, 935–939. [PubMed: 18592598]
198. Yoon SK, Choban ER, Kane C, Tzedakis T and Kenis PJ, *J. Am. Chem. Soc*, 2005, 127, 10466–10467. [PubMed: 16045315]
199. Kochius S, Park JB, Ley C, Konst P, Hollmann F, Schrader J and Holtmann D, *J. Mol. Catal. B:Enzyme*, 2014, 103, 94–99.
200. Ruinatscha R, Buehler K and Schmid A, *J. Mol. Catal. B: Enzyme*, 2014, 103, 100–105.
201. Mauritz KA and Moore RB, *Chem Rev*, 2004, 104, 4535–4585. [PubMed: 15669162]
202. Beauchamp J and Vieille C, *Bioengineered*, 2015, 6, 106–110. [PubMed: 25611453]
203. El-Zahab B, Donnelly D and Wang P, *Biotechnol. Bioeng*, 2008, 99, 508–514. [PubMed: 17680680]
204. Ji X, Su Z, Wang P, Ma G and Zhang S, *ACS Nano*, 2015, 9, 4600–4610. [PubMed: 25857747]
205. Gestrelius S, MÅNsson M-O and Mosbach K, *Eur. J. Biochem*, 1975, 57, 529–535. [PubMed: 170114]
206. Ji X, Wang P, Su Z, Ma G and Zhang S, *J. Mater. Chem. B*, 2014, 2, 181–190.
207. Fu J, Yang YR, Johnson-Buck A, Liu M, Liu Y, Walter NG, Woodbury NW and Yan H, *Nature Nanotechnol*, 2014, 9, 531. [PubMed: 24859813]
208. Velasco-Lozano S, Benítez-Mateos AI and López-Gallego F, *Angew. Chem. Int. Edit*, 2017, 56, 771–775.
209. Paiva A, Vidinha P, Angelova M, Rebocho S, Barreiros S and Brunner G, *The Journal of Supercritical Fluids*, 2011, 55, 963–970.
210. Tamborini L, Romano D, Pinto A, Bertolani A, Molinari F and Conti P, *J. Mol. Cat. B: Enzymatic*, 2012, 84, 78–82.
211. Mesiano AJ, Beckman EJ and Russell AJ, *Chem Rev*, 1999, 99, 623–634. [PubMed: 11848995]

212. Fricks AT, Oestreicher EG, Filho LC, Feihmann AC, Cordeiro Y, Dariva C and Antunes OAC, *The Journal of Supercritical Fluids*, 2009, 50, 162–168.
213. Lozano P, Garcia-Verdugo E, Karbass N, Montague K, De Diego T, Burguete MI and Luis SV, *Green Chem.*, 2010, 12, 1803–1810.
214. Burguete MI, Galindo F, Garcia-Verdugo E, Karbass N and Luis SV, *Chem. Commun.*, 2007, DOI: 10.1039/B704611A, 3086–3088.
215. Karbass N, Sans V, Garcia-Verdugo E, Burguete MI and Luis SV, *Chem. Commun.*, 2006, DOI: 10.1039/B603224A, 3095–3097.
216. Burguete MI, Erythropel H, Garcia-Verdugo E, Luis SV and Sans V, *Green Chem.*, 2008, 10, 401–407.
217. Burguete MI, García-Verdugo E, Garcia-Villar I, Gelat F, Licence P, Luis SV and Sans V, *J. Catal.*, 2010, 269, 150–160.
218. Cimporescu A, Todea A, Badea V, Paul C and Peter F, *Process Biochemistry*, 2016, 51, 2076–2083.
219. Moisa ME, Spelmezan CG, Paul C, Bartha-Vari JH, Bencze LC, Irimie FD, Paizs C, Peter F and Tosa MI, *RSC Adv.*, 2017, 7, 52977–52987.
220. Ursoiu A, Paul C, Kurtán T and Péter F, *Molecules*, 2012, 17, 13045. [PubMed: 23124473]
221. Ungurean M, Paul C and Peter F, *Bioproc. Biosyst Eng.*, 2013, 36, 1327–1338.
222. Ma B-D, Yu H-L, Pan J and Xu J-H, *Biochem. Eng. J.*, 2016, 107, 45–51.
223. Falus P, Cerioli L, Bajnóczi G, Boros Z, Weiser D, Nagy J, Tessaro D, Servi S and Poppe L, *Adv. Syn. Catal.*, 2016, 358, 1608–1617.
224. Hugentobler KG, Rasparini M, Thompson LA, Jolley KE, Blacker AJ and Turner NJ, *Org. Process. Res. Dev.*, 2017, 21, 195–199.
225. Manoel EA, Pais KC, Flores MC, e Miranda L. S. d. M., Coelho MAZ, Simas ABC, Freire DMG and de Souza ROMA, *J. Mol. Cat B: Enzymatic*, 2013, 87, 139–143.
226. de Miranda AS, Miranda LSM and de Souza ROMA, *Org. Biomol. Chem.*, 2013, 11, 3332–3336. [PubMed: 23558581]


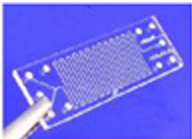

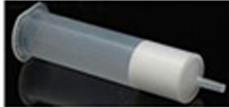
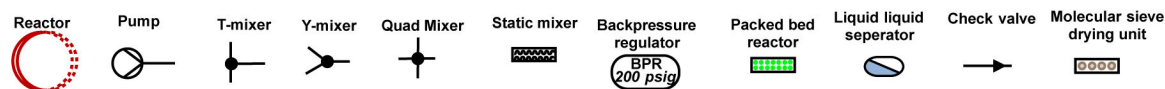
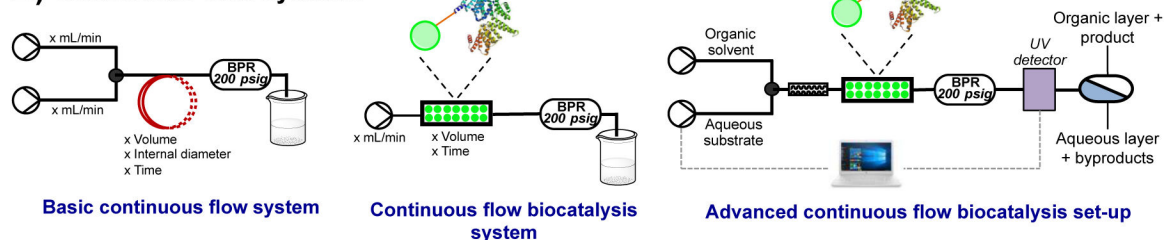
				
Reactor type	PFA	Microfluidic chip	Packed bed reactor	Cartridges
Cost per reactor	\$150 per 50 ft.	~\$100 per chip ^[a]	~\$150 (6ft. Tubing ~\$10)	~\$5-20 each

Figure 1. Continuous flow reactors used for continuous flow synthesis and biocatalysis. The prices given are estimates from recent experience.

A) Continuous flow legend



B) Continuous flow systems



Basic continuous flow system

Continuous flow biocatalysis system

Advanced continuous flow biocatalysis set-up

C) Continuous flow pumps



Semi-continuous flow pumps

Brands include

- Harvard apparatus (~\$5k)
- Syringe Pump Pro (~\$800)

Advantages:

- Low flow rates
- Low flow rate variability
- Most labs have one
- High chemical tolerance

Disadvantages:

- Finite volumes in syringes
- Bulky and space consuming
- Hard to use high flow rates
- Hard to scale



True continuous flow pumps

Brands include

- Syrris (~\$20k + ~\$100's for syringes)
- MilligAT (~\$5k)
- Vapourtec

Advantages:

- No need to refill syringes
- Easier to translate to industry
- Lots of experiments in a run
- Many brands on the market

Disadvantages:

- Some cannot handle pressure
- Expensive
- Hard to fix
- Uneven flow rate at pressure

Figure 2. Continuous flow basics and equipment.

A) The continuous flow systems depicted in this Review will use the legend shown here. B) Several different schematics of continuous flow systems. The first continuous flow system would be used for a synthetic transformation using two pumps to mix fluids before entering the reactor. The fluid then passes through the reactor before exiting through a backpressure regulator into the collection flask. The variables indicated in the scheme should be quoted (flow rate, reactor volume, internal diameter of the reactor tubing, and reactor temperature) in manuscripts. The second system is a simple continuous flow biocatalysis experiment. Here, a substrate solution is pumped through a packed bed reactor housing immobilized enzymes. The solution passes through the reactor to be modified before exiting into a collection flask. The third system is an advanced experimental set-up. Here, an organic solvent (such as ethyl acetate) is pumped through the packed bed reactor with the substrate solution. The organic phase dissolves the product to accelerate the enzymatic reaction, and a UV detector that can provide information back to the pumps monitors the out flow. Additionally, an in-line separator is used to separate the aqueous layer from the organic. In theory, this approach can provide a pure stream of product in the organic layer. C) Both semi-continuous and continuous pumps are shown. The benefits and disadvantages are described and a rough price given. The high price of continuous flow pumps often limits the construction of larger continuous flow systems. The cost indicated (\$, USD) may vary amongst supplier and country.

			
<p>Reactor coils</p>	<p>Mixers</p>	<p>Liquid-liquid separator and backpressure regulator</p>	<p>Packed bed reactor / mixer</p>
<p>Advantages</p>	<p>Advantages</p>	<p>Advantages</p>	<p>Advantages</p>
<ul style="list-style-type: none"> • Quick to construct • Cost effective • Handles many conditions • Simply heated or cooled • Commercially available materials 	<ul style="list-style-type: none"> • Screws into the system • Effective in most situations • No expertise needed • Commercially available • Can be modified for customizability 	<ul style="list-style-type: none"> • Screws into the system • Very easy to use • Vast amount of literature • Commercially available • Handles many flow rates • Variable backpressure – set by the user unlike other brands • Backpressure regulator can handle certain solids 	<ul style="list-style-type: none"> • Easy to make in lab • Easy to change the contents • High pressures possible • Modification is easy • Commercially available parts
<p>Disadvantages</p>	<p>Disadvantages</p>	<p>Disadvantages</p>	<p>Disadvantages</p>
<ul style="list-style-type: none"> • Heated and cooled in an oil bath - can be messy • Only several sizes available • Hard to spot leaks • Can be fouled easily • Small chemicals can diffuse out of the tubing 	<ul style="list-style-type: none"> • Blocked with precipitate easily • Heating causes the ferrules to swell inside • Can't see what is happening inside • Exposure to certain chemicals will leave them brittle 	<ul style="list-style-type: none"> • Becomes blocked as supports swell • Product can get caught on the support or chemicals • Potentially hard to scale • Can get high backpressure with compacted material (~1000 psi). 	<ul style="list-style-type: none"> • Becomes blocked as supports swell • Product can get caught on the support or chemicals • Potentially hard to scale • Can get high backpressure with compacted material (~1000 psi).
<p>Cost</p>	<p>Cost</p>	<p>Cost</p>	<p>Cost</p>
<p>~\$150 per 50 ft. of tubing from Idex Health & Science</p>	<p>~\$25 per mixer from Idex Health & Science</p>	<p>~\$3 to 5k per unit from Zaiput Flow Technology</p>	<p>~\$150 with materials from Idex Health & Science and Grainger</p>

Figure 3. Advantages and disadvantages of common continuous flow equipment.

Here, the advantages and disadvantages of each piece of modular continuous flow equipment are described from our personal experience. The cost indicated (\$, USD) may vary amongst supplier and country.

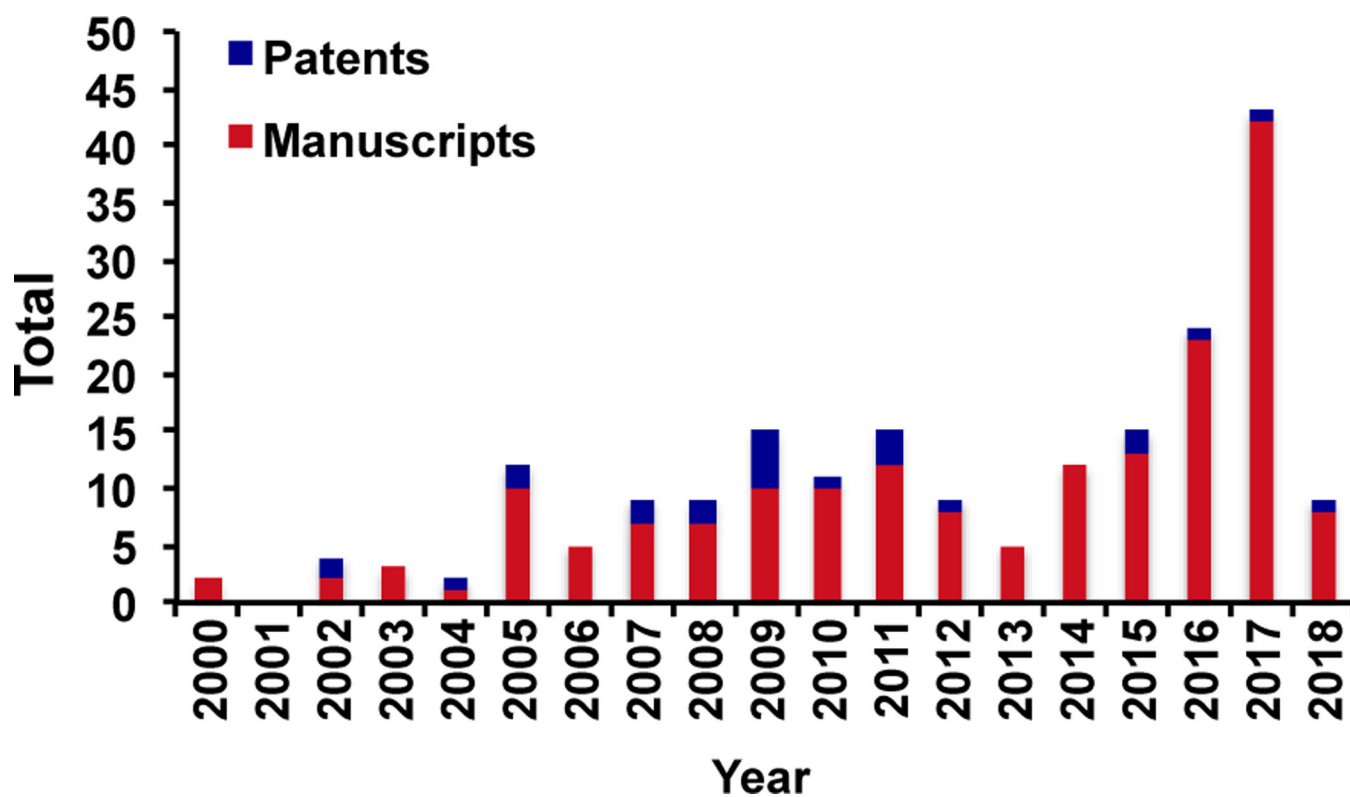


Figure 4.
The total number of patents and publications in continuous flow biocatalysis since 2000. This graph was constructed using data from Scifinder with the terms “*continuous flow biocatalysis*”. Data was analyzed to January 2018.

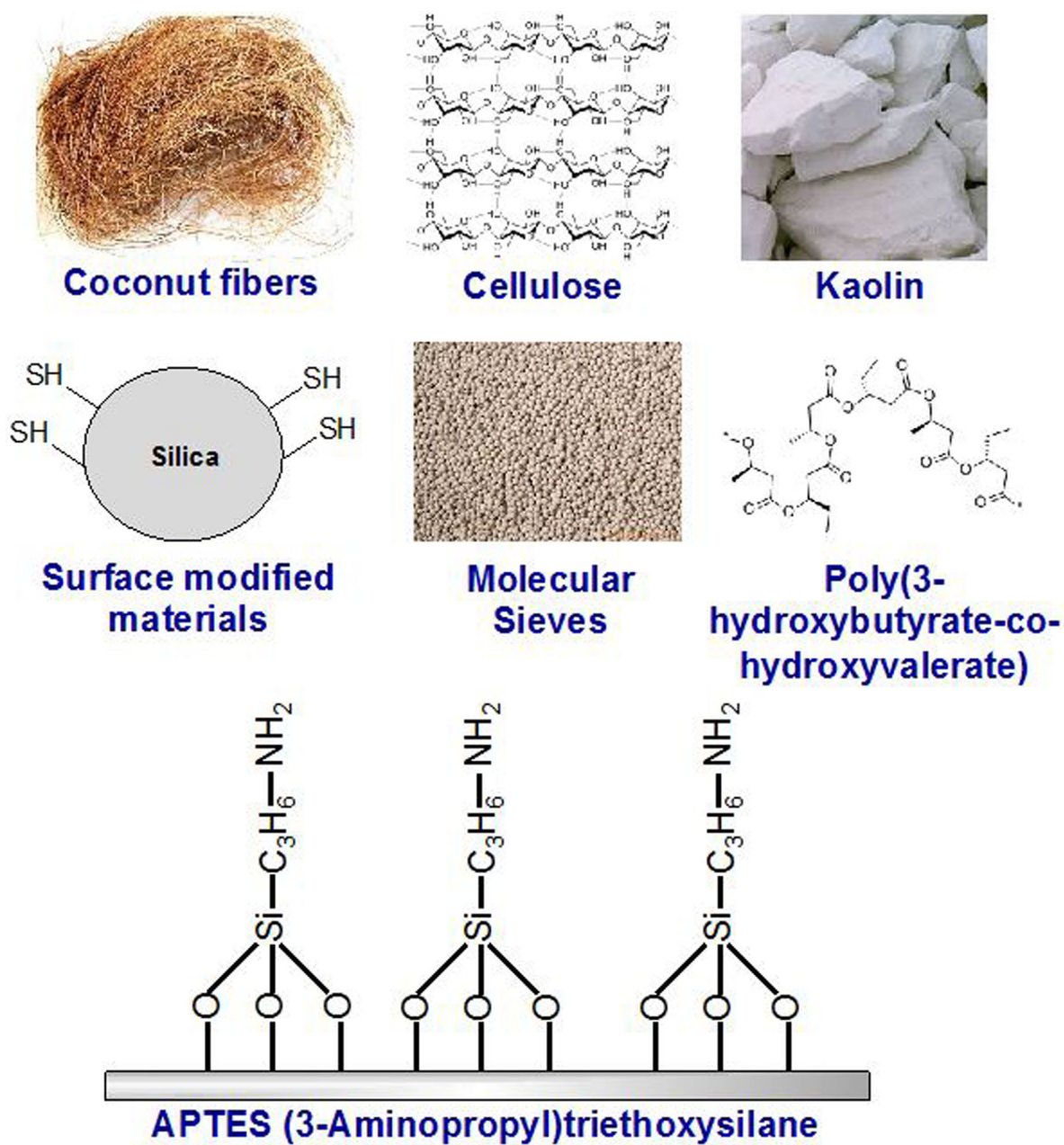


Figure 5.
Examples of immobilization materials used for adsorption.

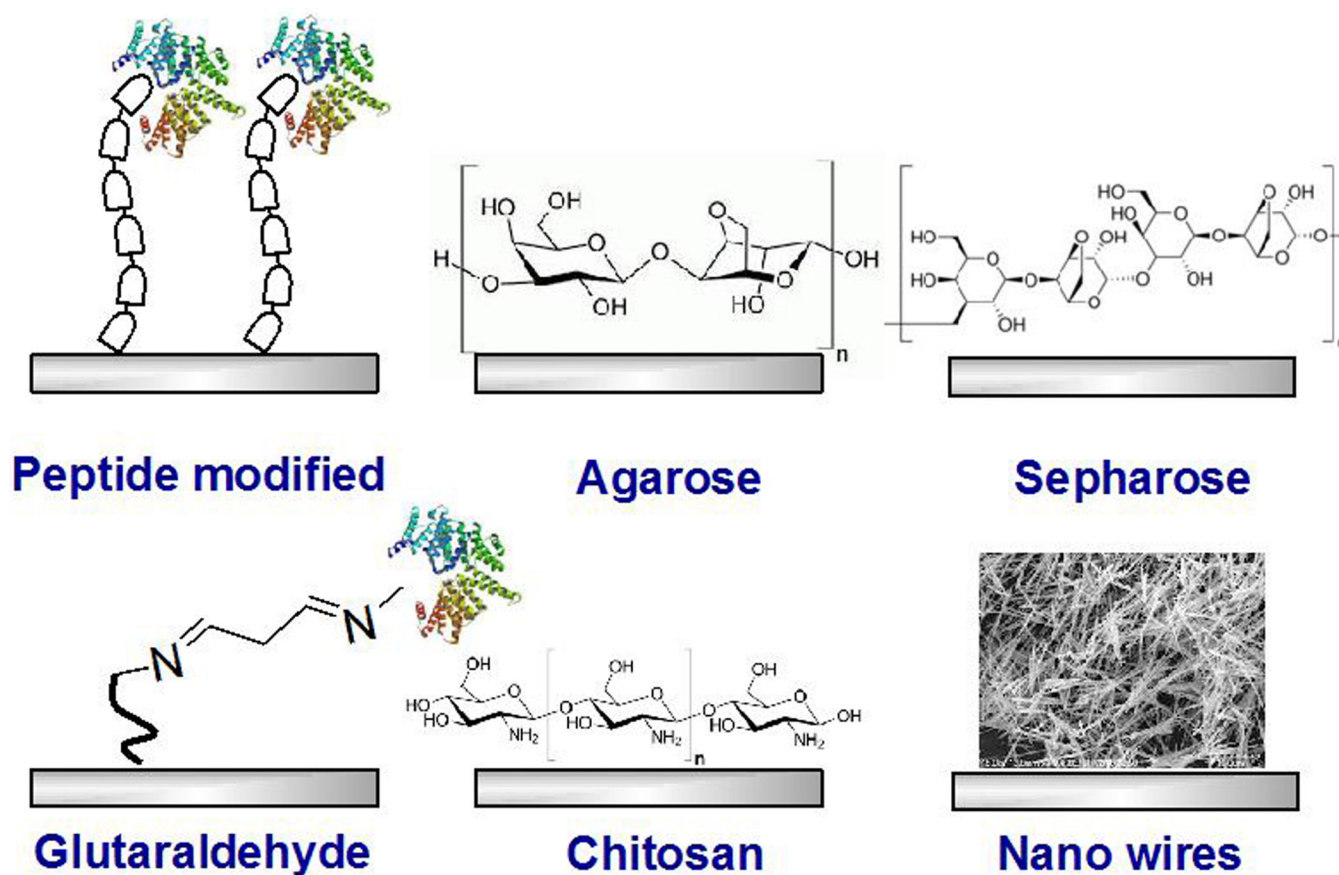


Figure 6.
Examples of materials for covalent immobilization.

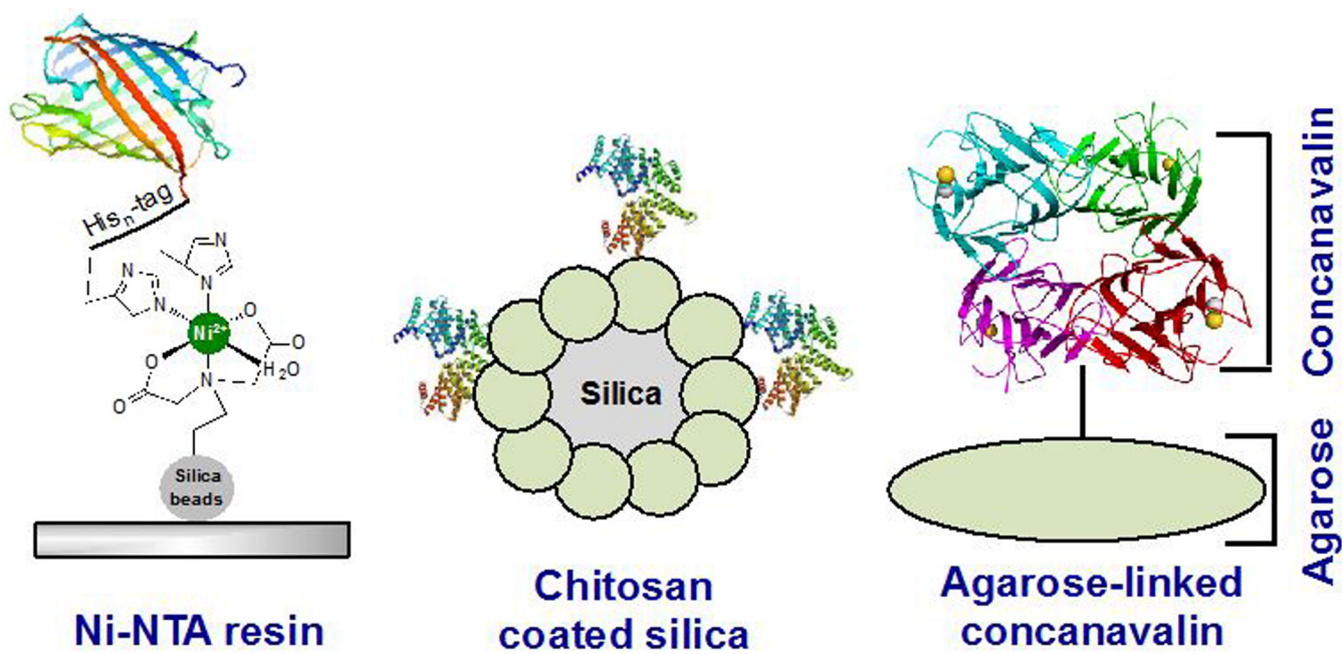


Figure 7.
Examples of affinity immobilization.

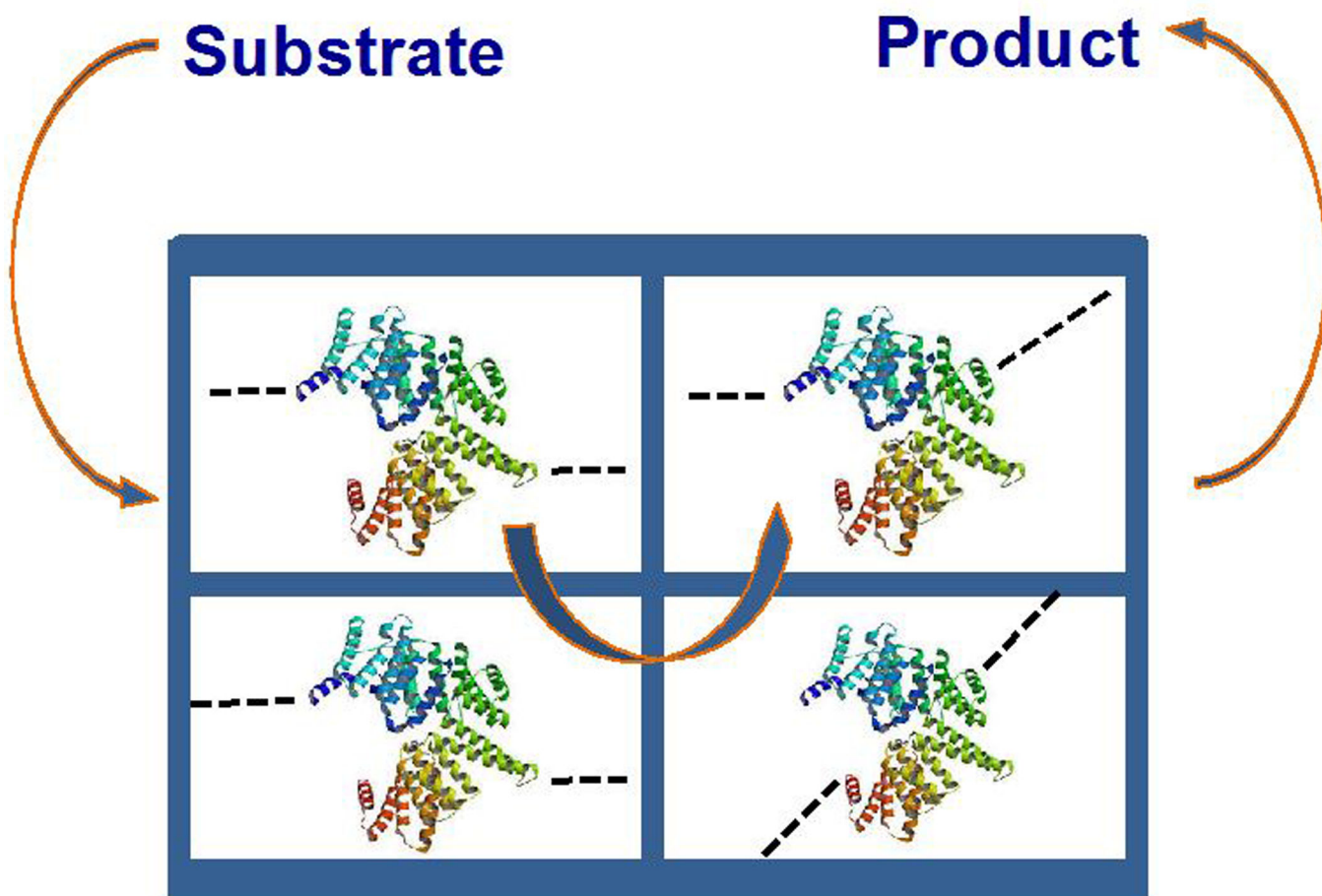


Figure 8.
Encapsulation immobilization.

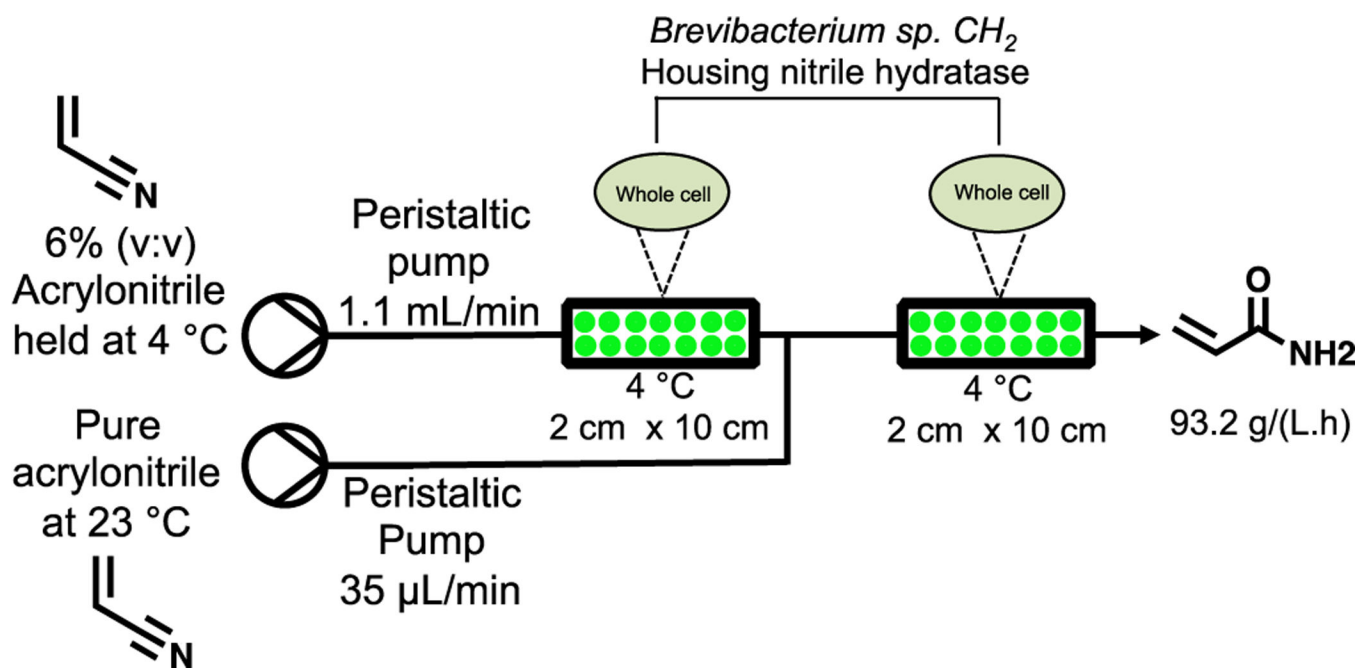


Figure 9. Whole cell continuous flow synthesis of acrylamide using two packed bed reactors housing *Brevibacterium sp. CH₂* expressing nitrile hydratase.¹³⁵

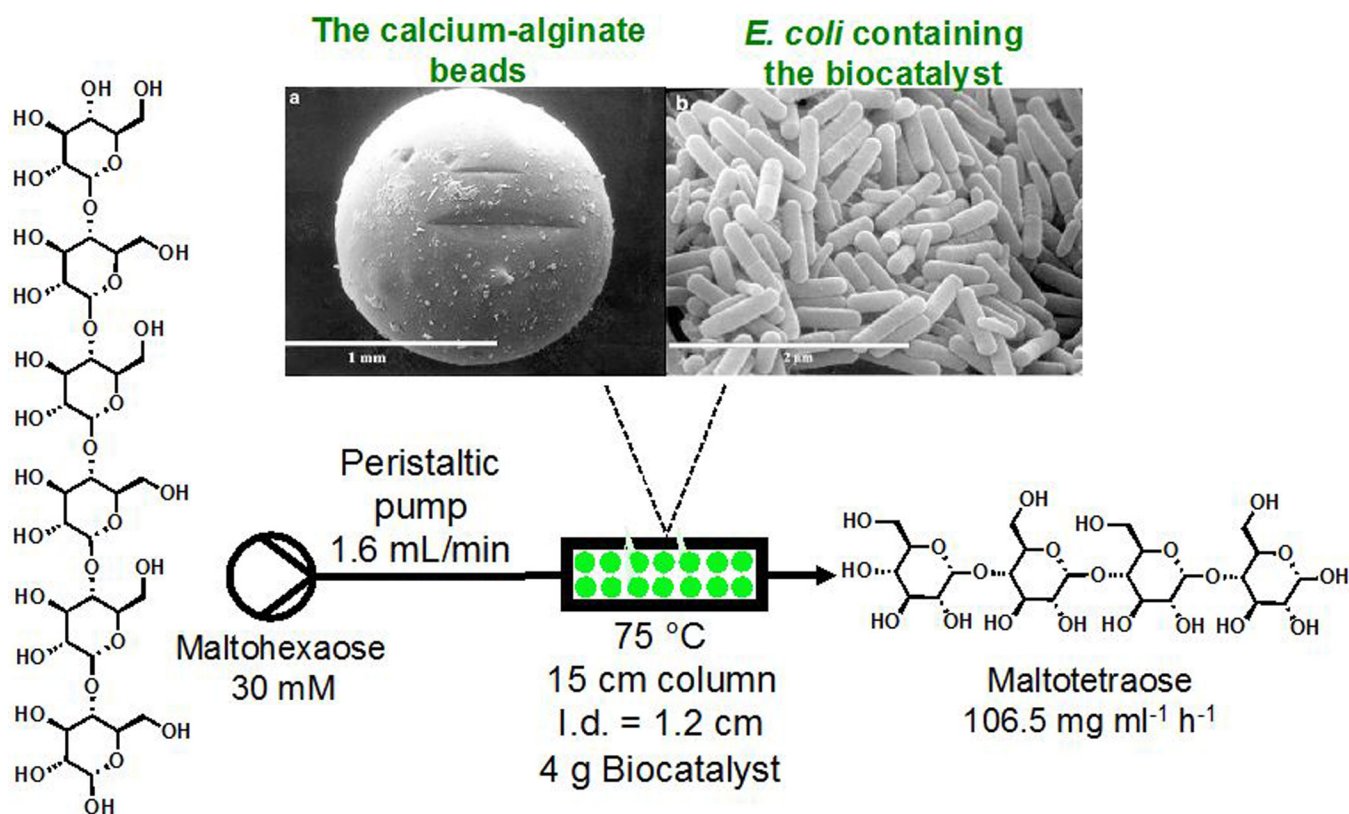


Figure 10. Whole cell continuous flow synthesis of maltotetraose using a packed bed reactor containing immobilized *E. coli* cells on calcium-alginate beads.¹³⁶ Images were used with permission from Springer, Nature – 2018.

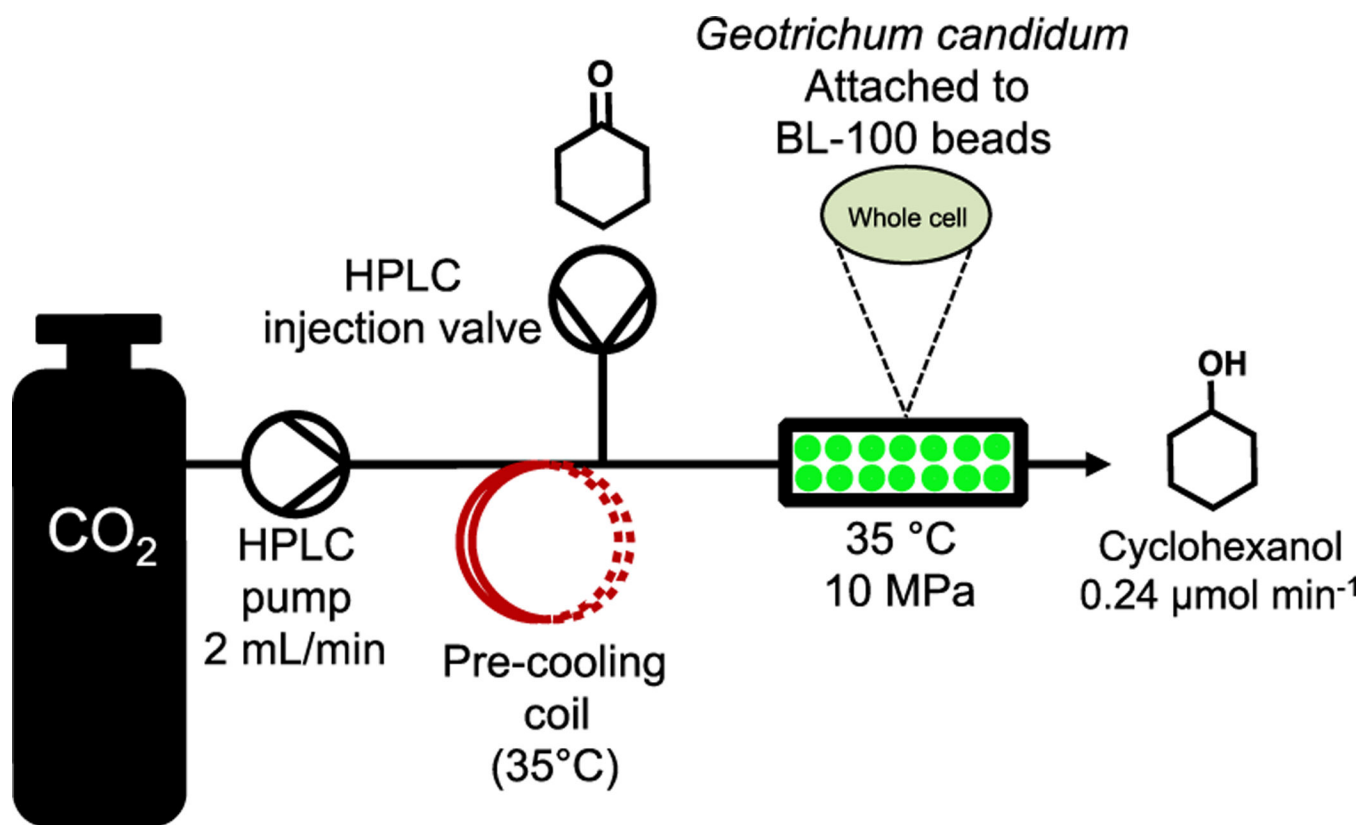


Figure 11. Whole cell continuous flow synthesis of cyclohexanol using immobilized *Geotrichum candidum* on BL-100 beads with super critical CO_2 .¹³⁷

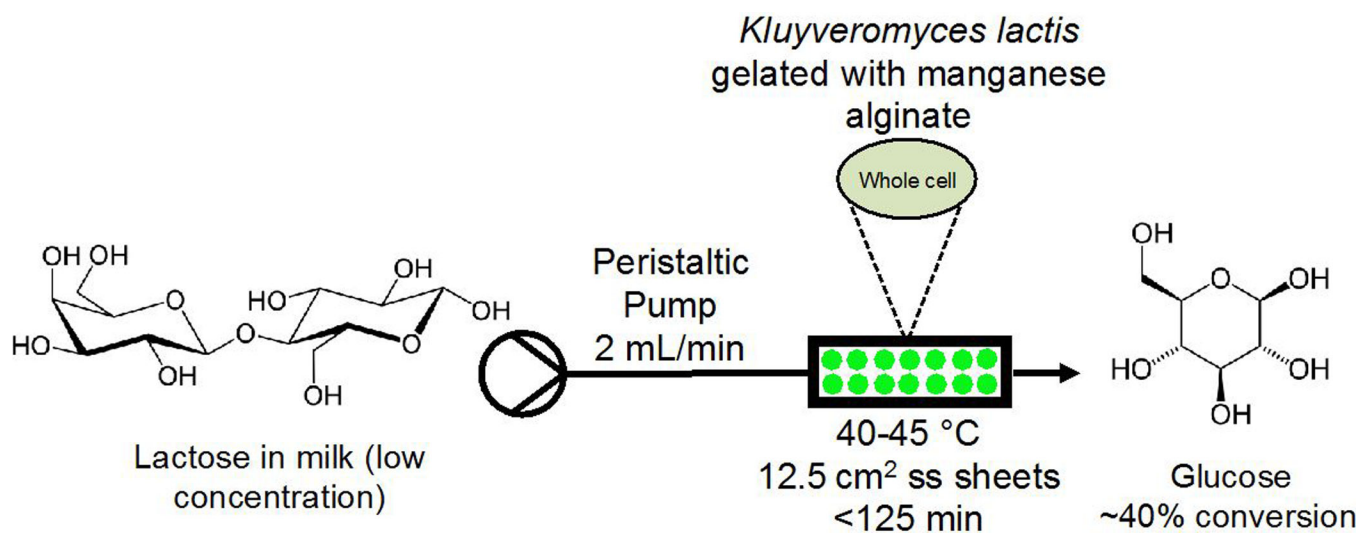


Figure 12. Whole cell continuous flow hydrolysis of lactose using immobilized *Kluyveromyces lactis* on alginate. ss= stainless steel.¹³⁸

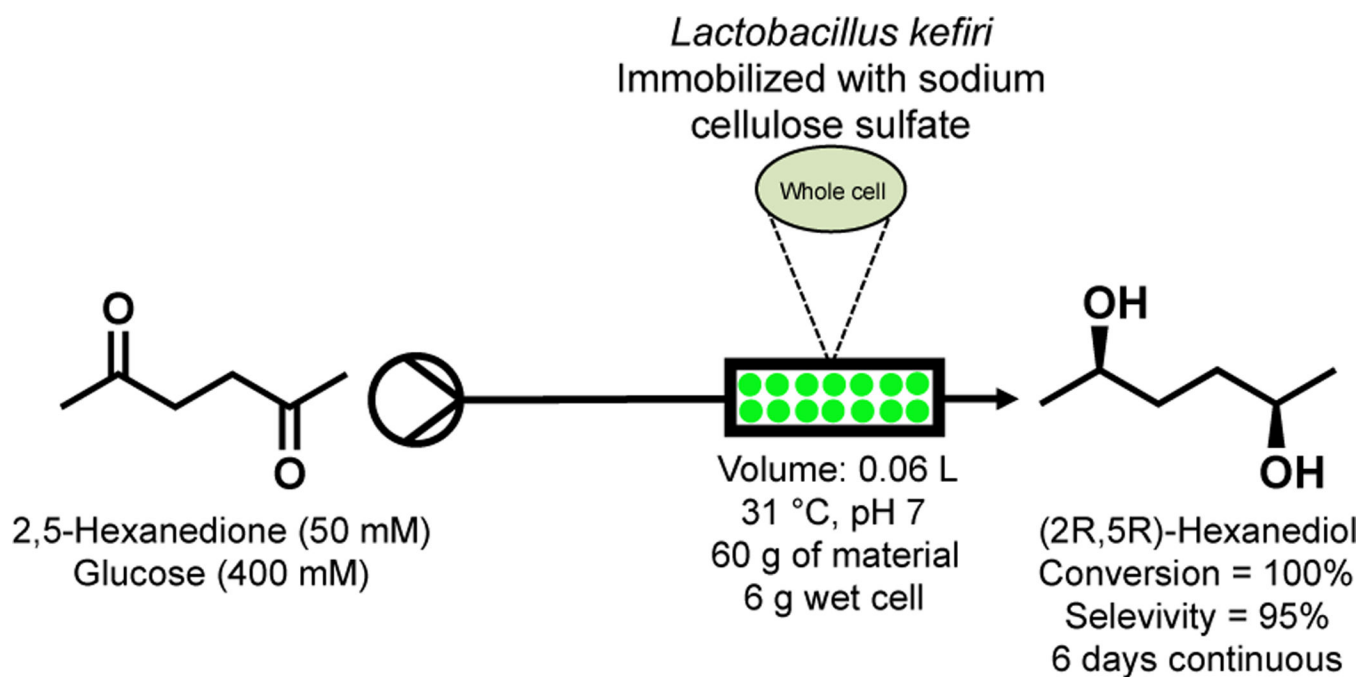


Figure 13. Whole cell continuous flow reduction of 2,5-hexanedione to (2R,5R)-hexanediol using immobilized *Lactobacillus kefir*. Flow rates and pump type were omitted in the original publication.¹⁴²

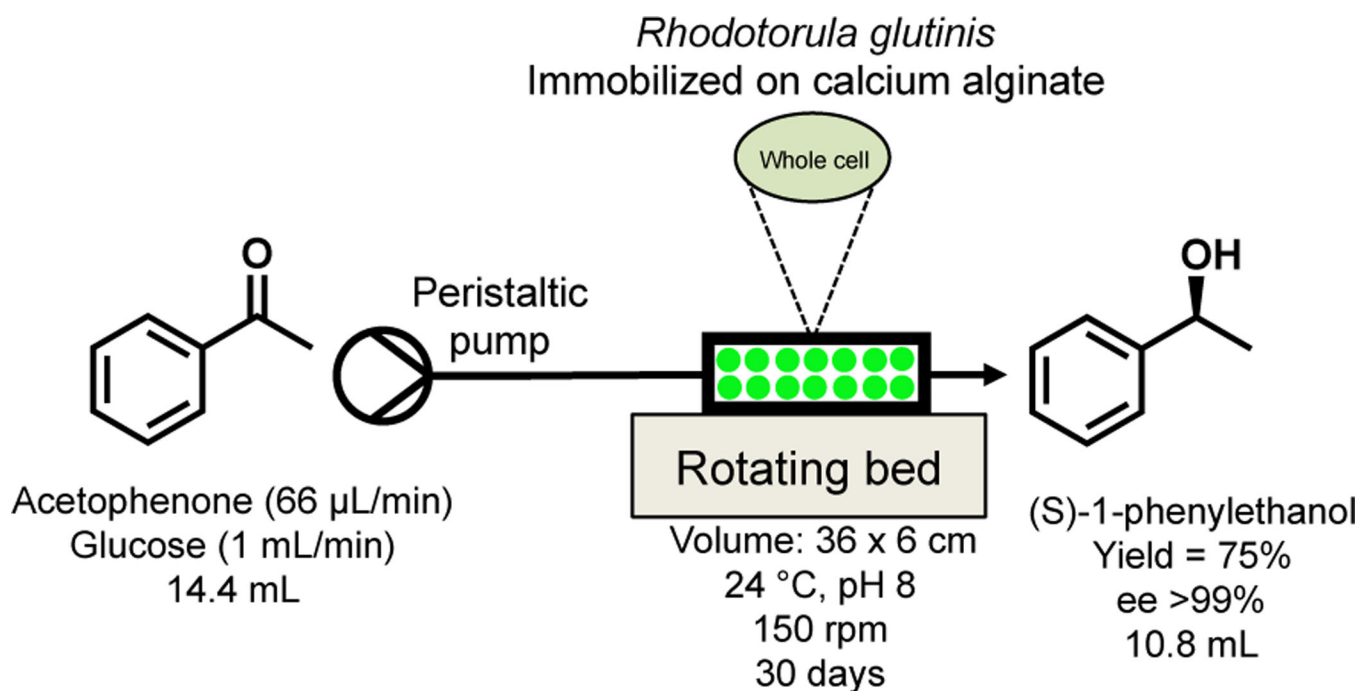


Figure 14. Whole cell continuous flow reduction of acetophenone to (*S*)-1-phenylethanol using immobilized *Rhodotorula glutinis* on calcium alginate.¹⁴³

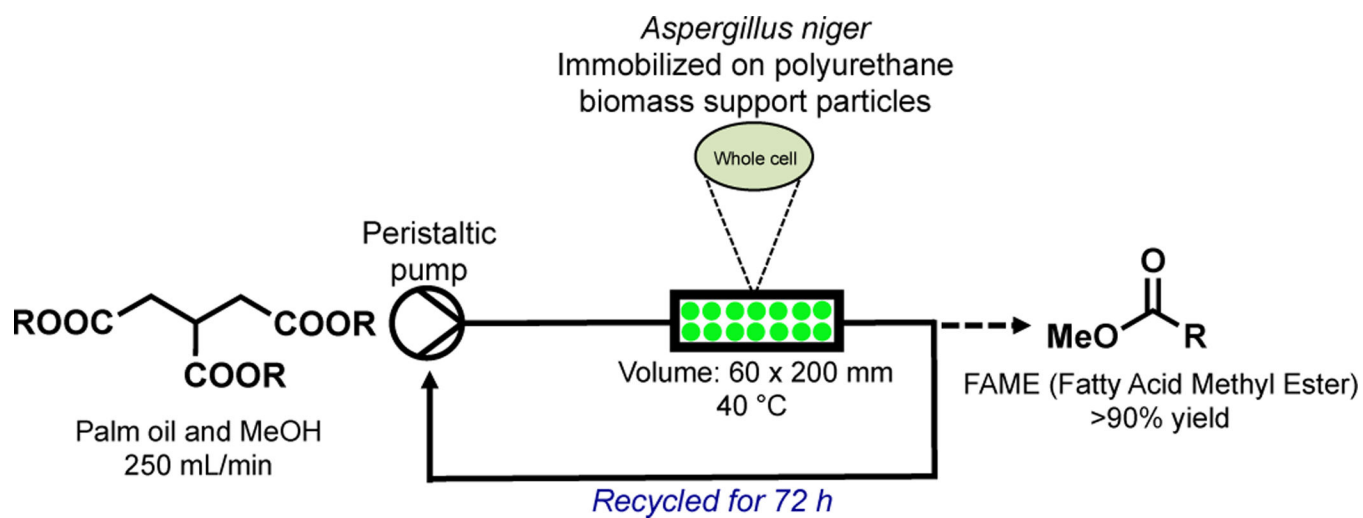


Figure 15. Whole cell continuous flow synthesis of biodiesel from palm oil using *Aspergillus niger* immobilized on polyurethane support particles.¹⁴⁶

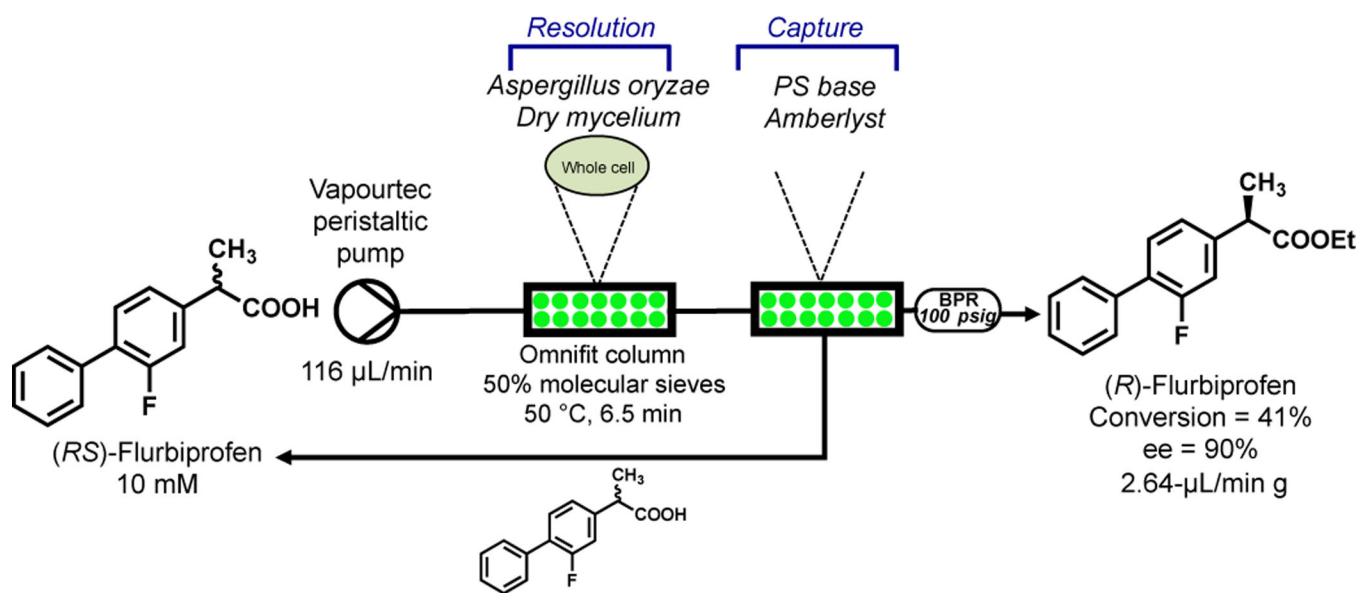


Figure 16. Whole cell continuous flow resolution of (*R,S*)-flurbiprofen using dry mycelium of *Aspergillus oryzae* in a Vapourtec R2+/R4 reactor.¹⁴⁷

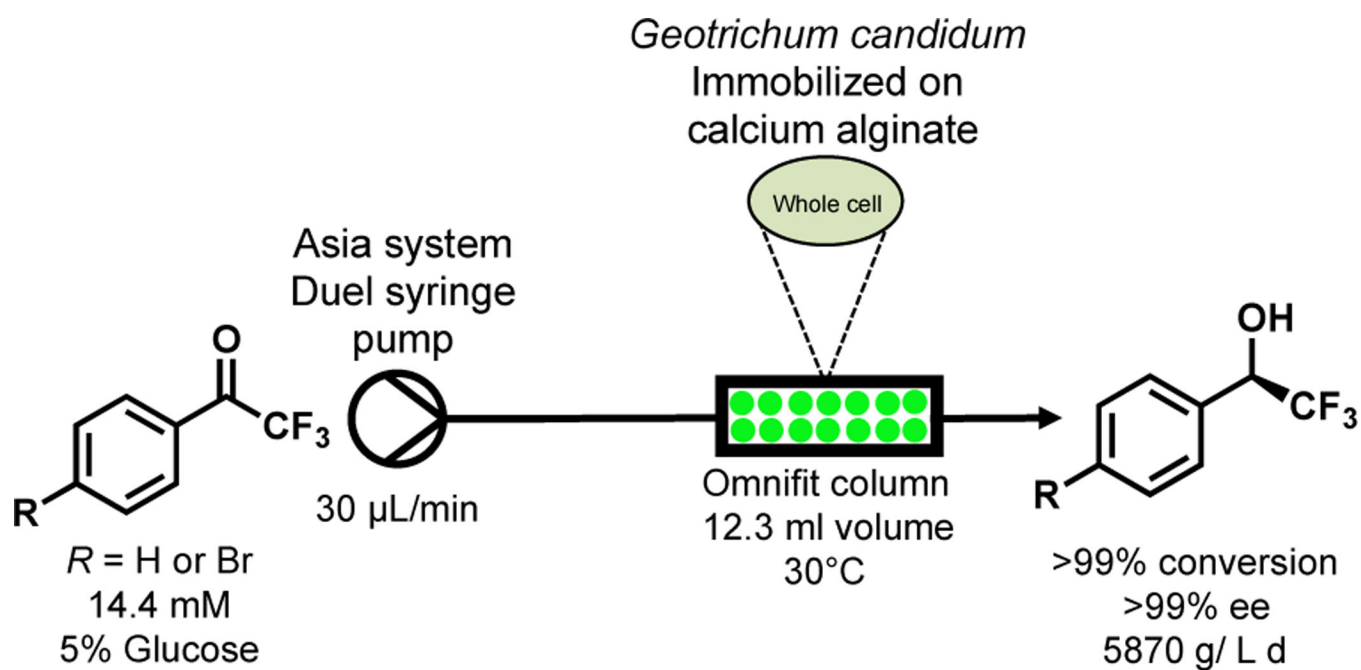


Figure 17. Whole cell continuous flow reduction of fluorinated acetophenone analogues using immobilized *Geotrichum candidum* on calcium alginate.¹⁴⁸

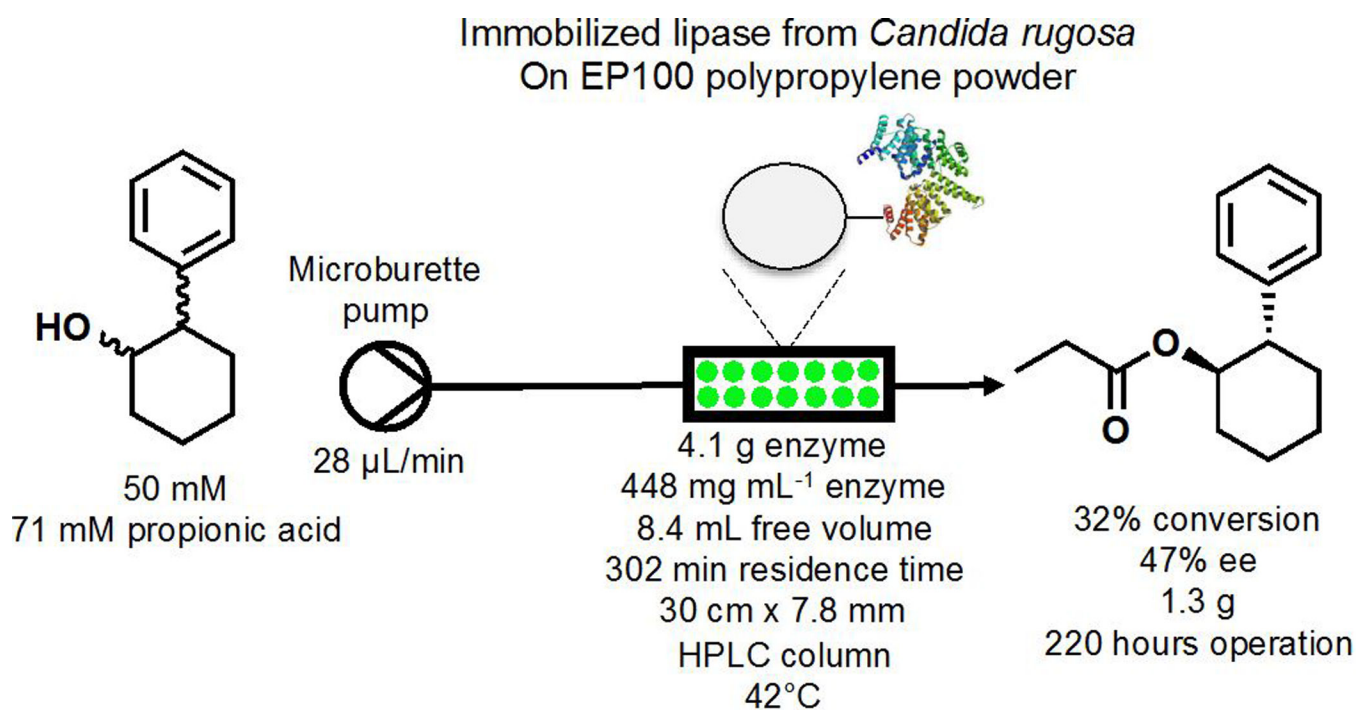


Figure 18. Continuous flow enantioselective esterification of *rac-trans*-2-phenyl-1-cyclohexanol using an immobilized lipase expressed in *Candida rugosa*.¹⁵⁶

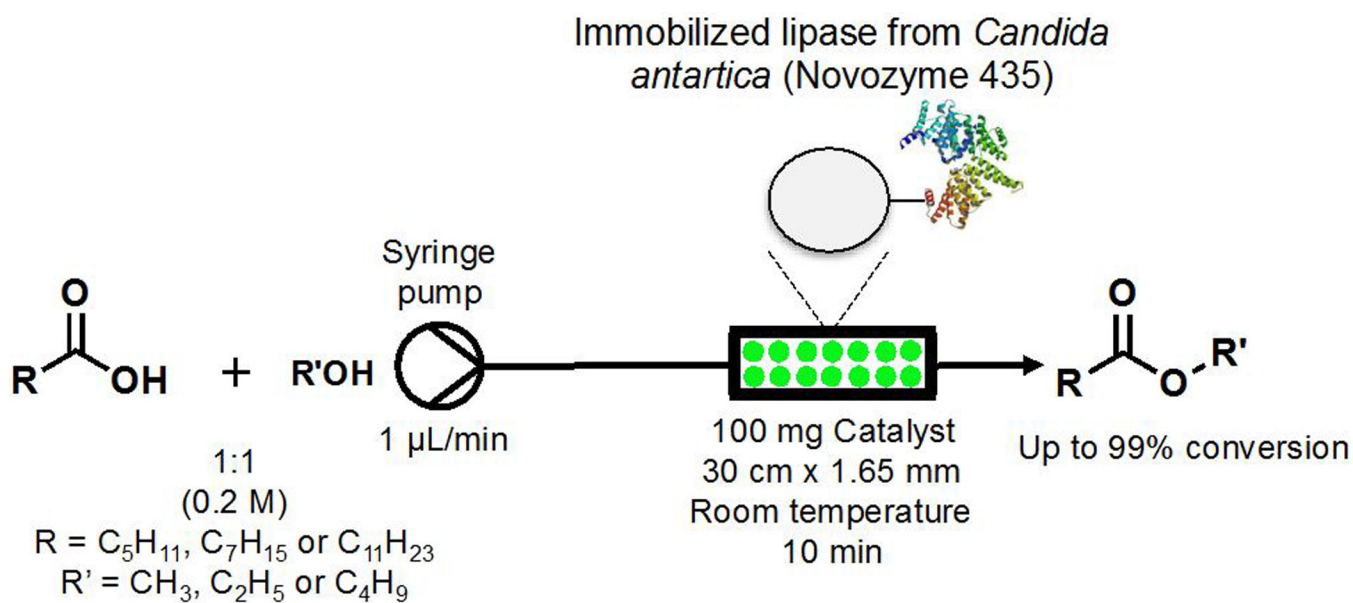


Figure 19. Continuous flow synthesis of alkyl esters using Novozyme 435 in a packed bed reactor.¹⁵⁷

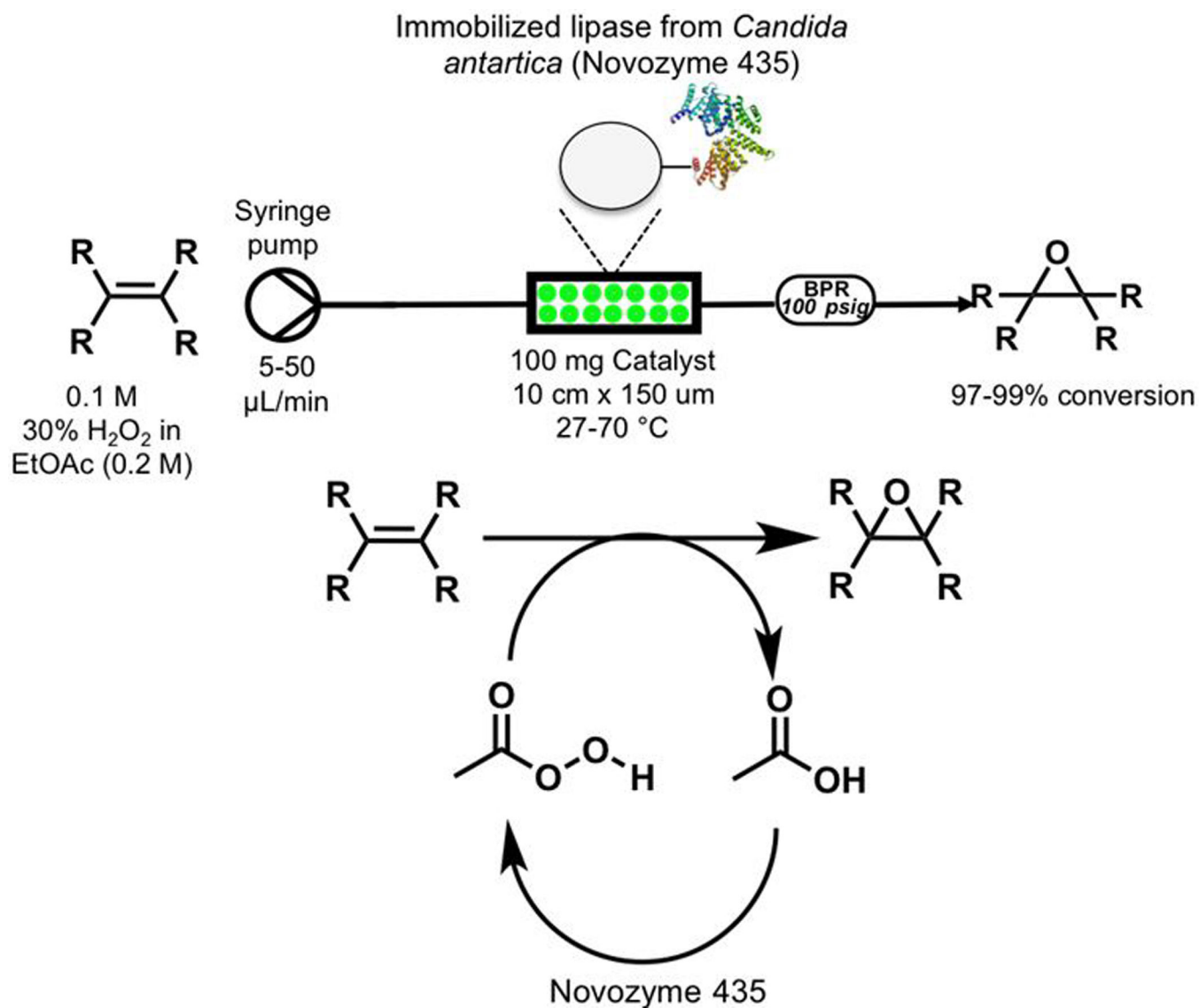


Figure 20. Continuous flow epoxidation using Novozyme 435 in a packed bed reactor with hydrogen peroxide as the initial oxygen source.¹⁵⁸

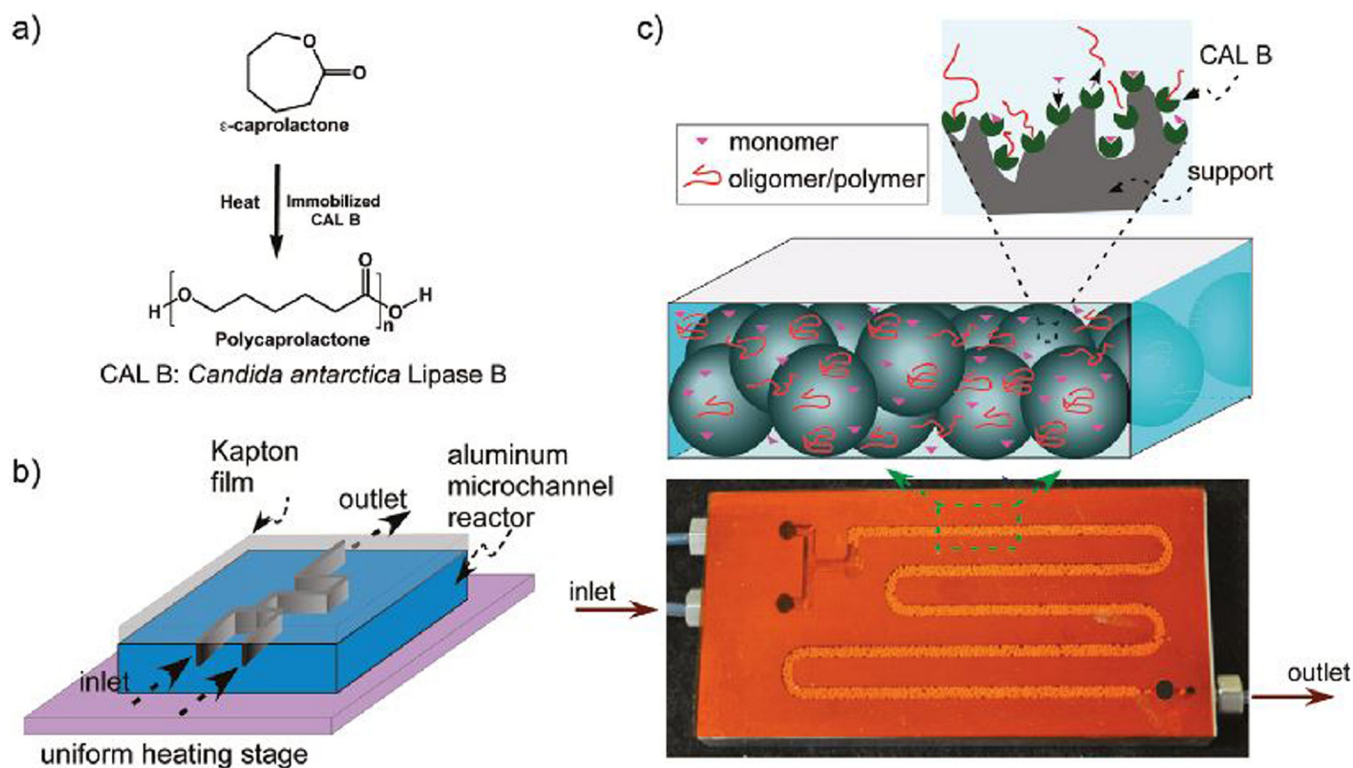


Figure 21. Continuous flow ring opening polymerization of ϵ -caprolactone using Novozyme 435 in a microfluidic device.¹⁵⁹ This figure was with permission. Copyright (2018) American Chemical Society.

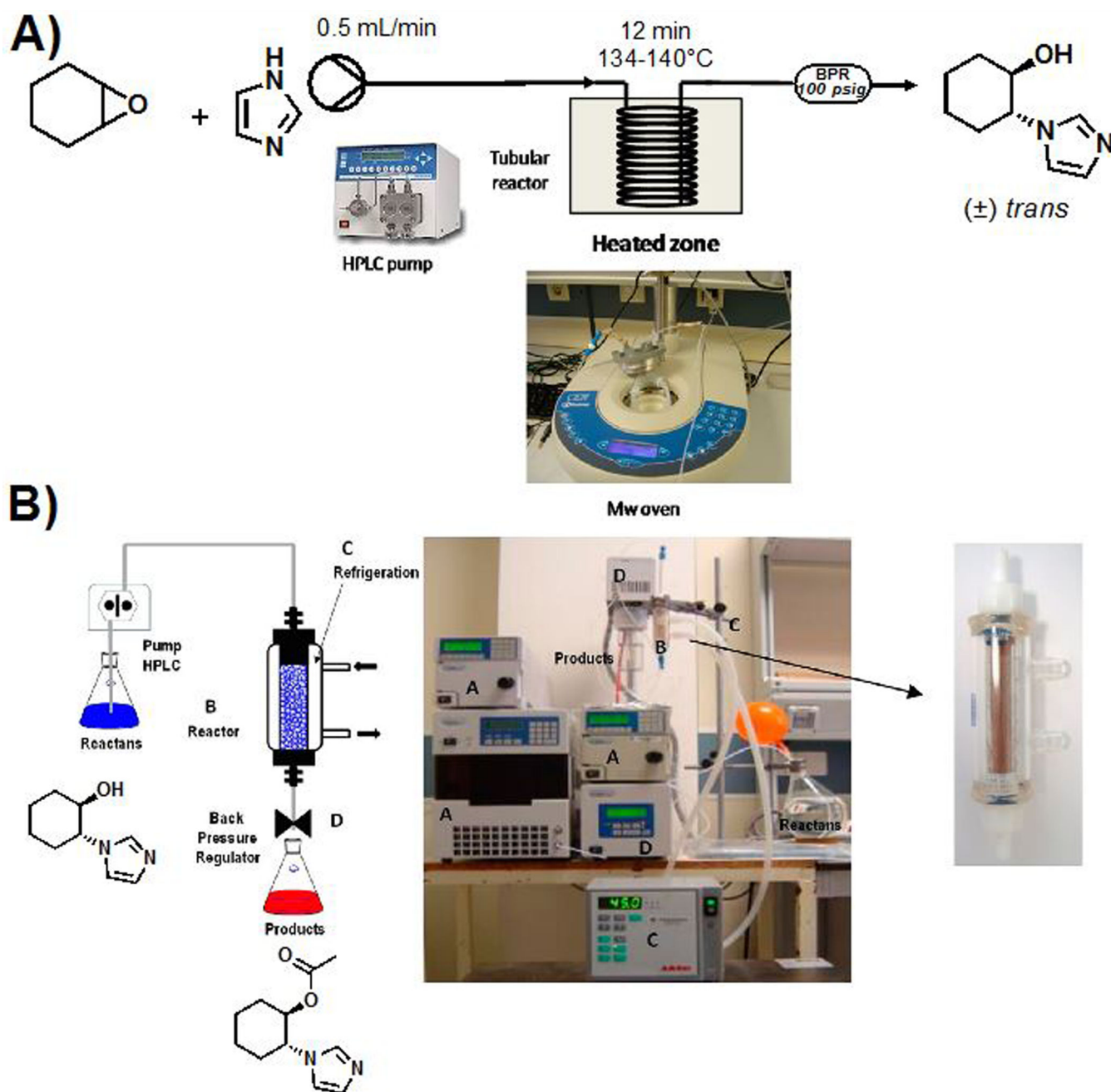


Figure 22.

A two-step continuous flow process that involves high temperature ring opening and then chiral resolution of the product by Novozyme 435. **A)** The chemoenzymatic synthesis. Here, a HPLC pump passes the reaction mixture through a reactor coil placed in a bench-top microwave reactor to implement a fast ring opening. **B)** The second step of the process is the chiral resolution of the *trans* product through use of Novozyme 435. This figure was used with permission. Copyright (2018) American Chemical Society.¹⁶⁰ Mw=microwave.

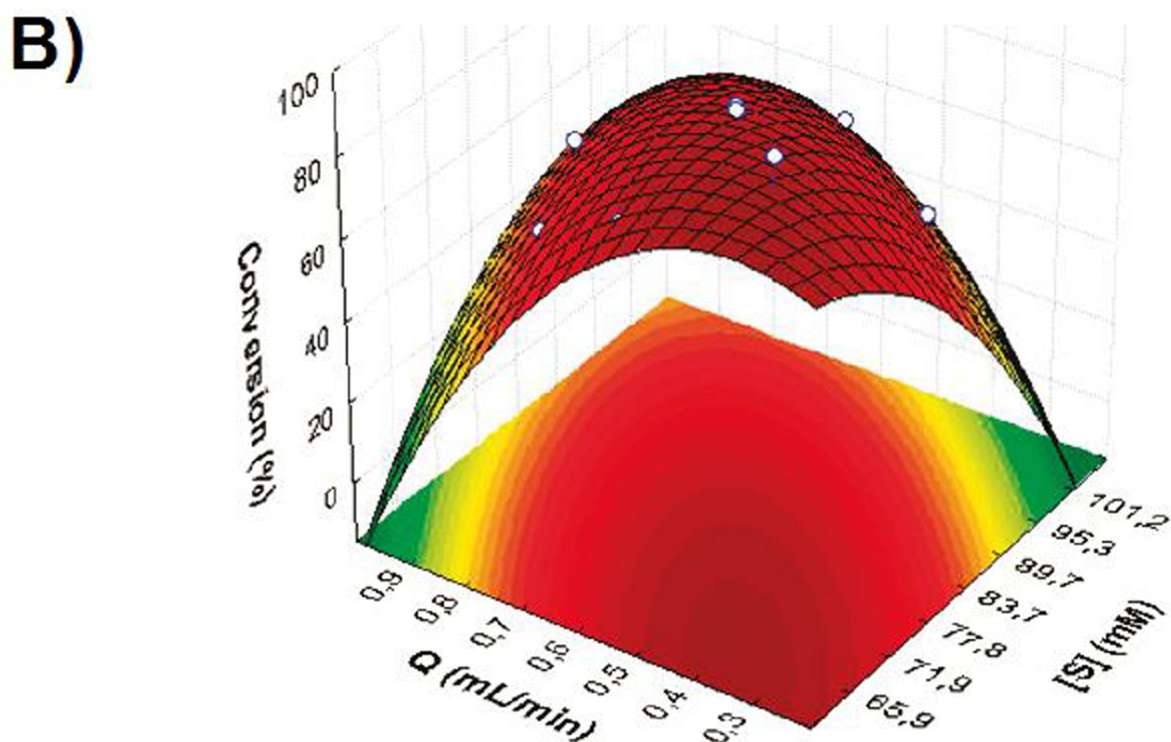
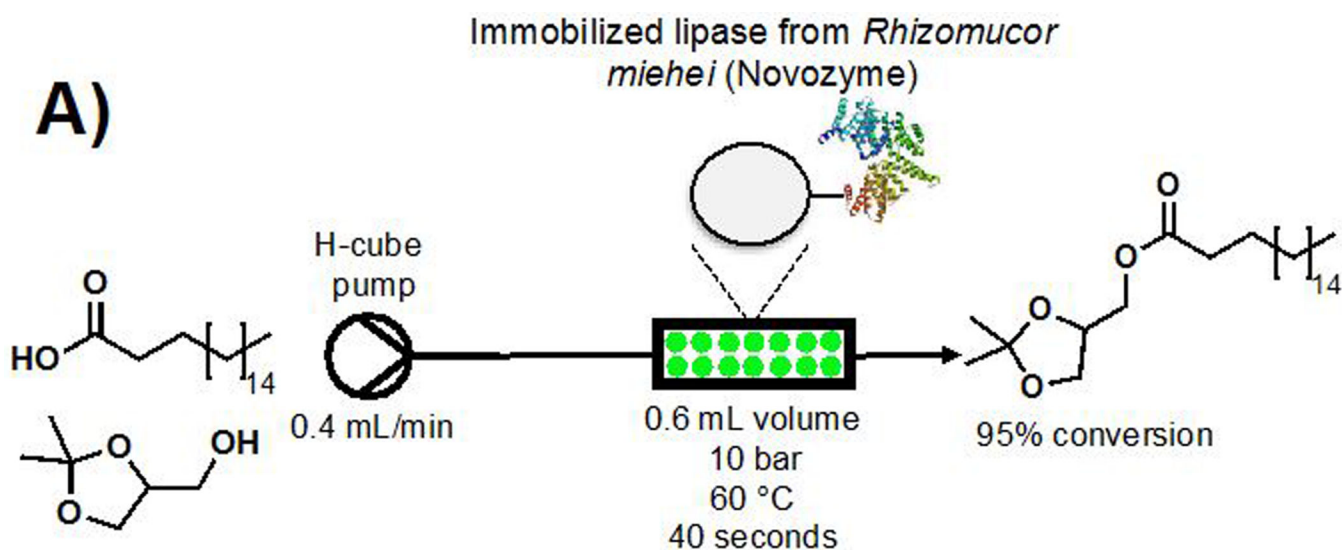


Figure 23. Continuous flow esterification using an immobilized lipase from *Rhizomucor miehei*. **A)** The continuous flow system used a packed bed reactor of protein. **B)** The 3-D plot of the response surface methodology (RSM). In this plot, Q=flow rate and [s]= concentration of substrate. This figure was used with permission.¹⁶² Copyright (2018) American Chemical Society.

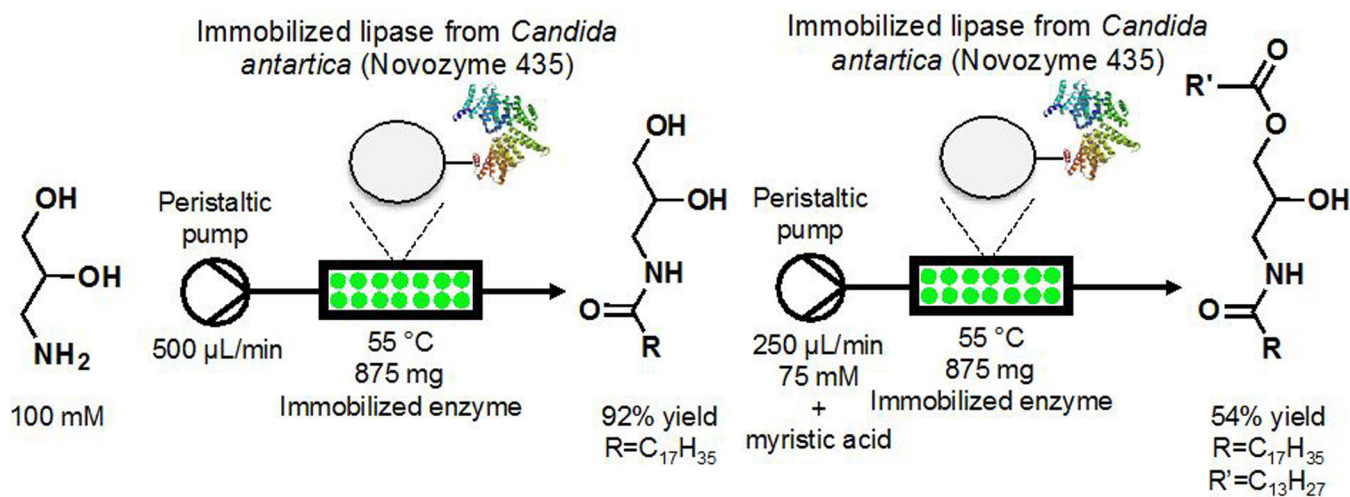


Figure 24. Continuous flow amidation and esterification of 3-amino-1,2-propanediol using Novozyme 435 in the production of ceramides.¹⁶³

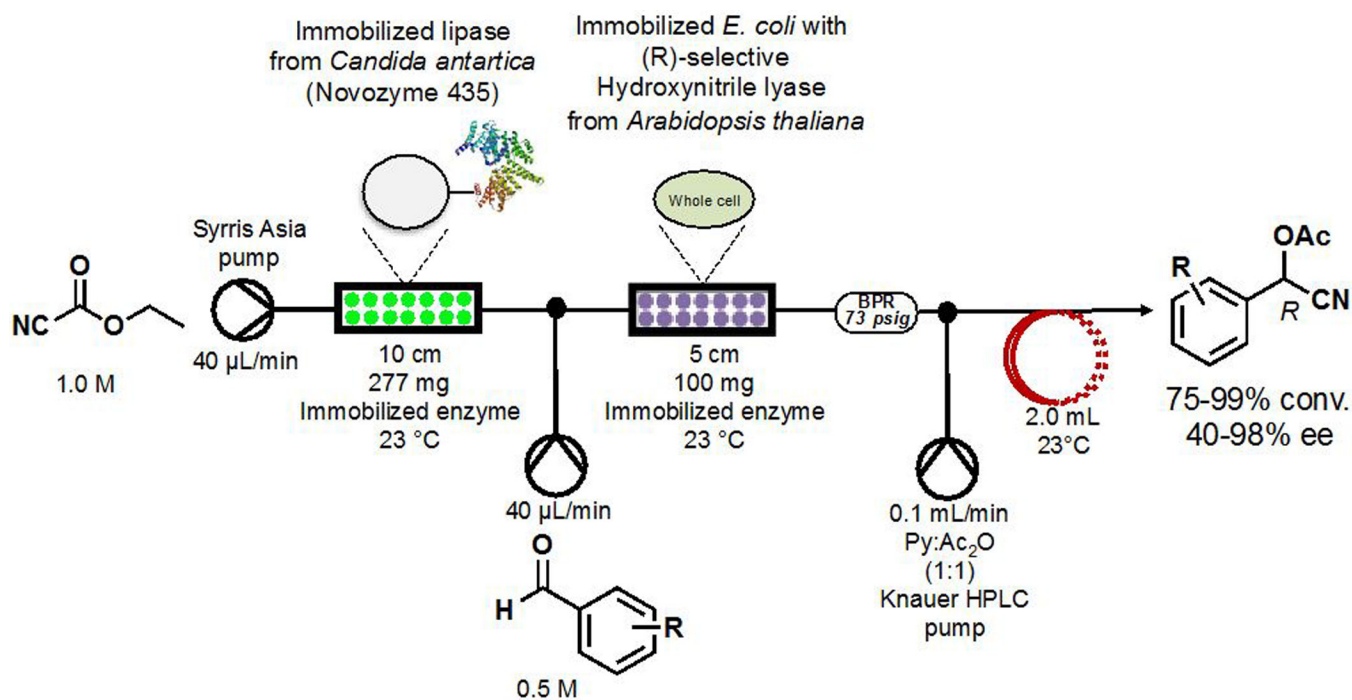


Figure 25. The multi-step chemoenzymatic synthesis of chiral cyanohydrins using Novozyme 435, a (*R*)-selective hydroxynitrile lyase, and a room temperature chemical acylation.¹⁶⁴ For the range of chemical functionality present for R, see the original publication.

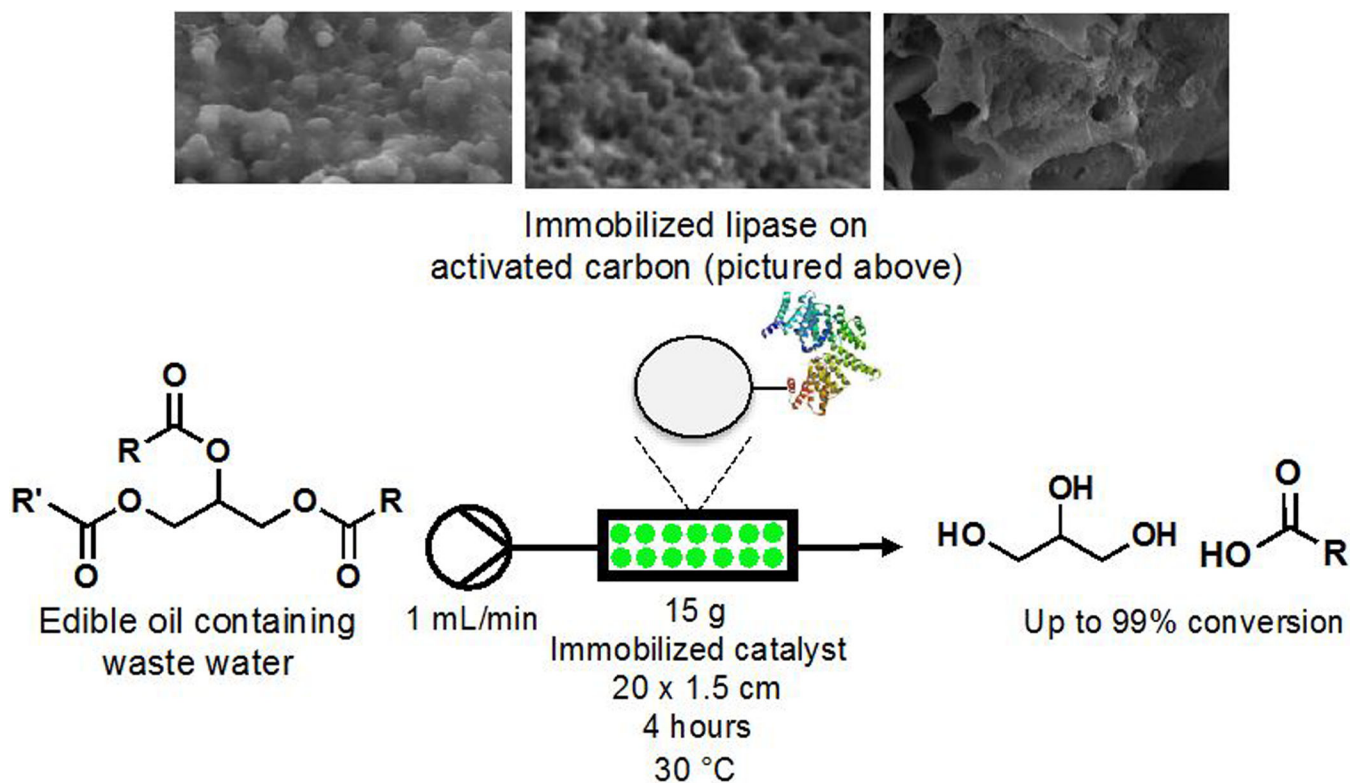


Figure 26.

Waste water treatment using an immobilized lipase on activated carbon to hydrolyze fats and oils in continuous flow.¹⁶⁵ The top photographs are SEM images of the immobilized enzyme on the activated carbon. The photographs used in this figure were reproduced with permission from the Royal Society of Chemistry (2018).¹⁶⁵

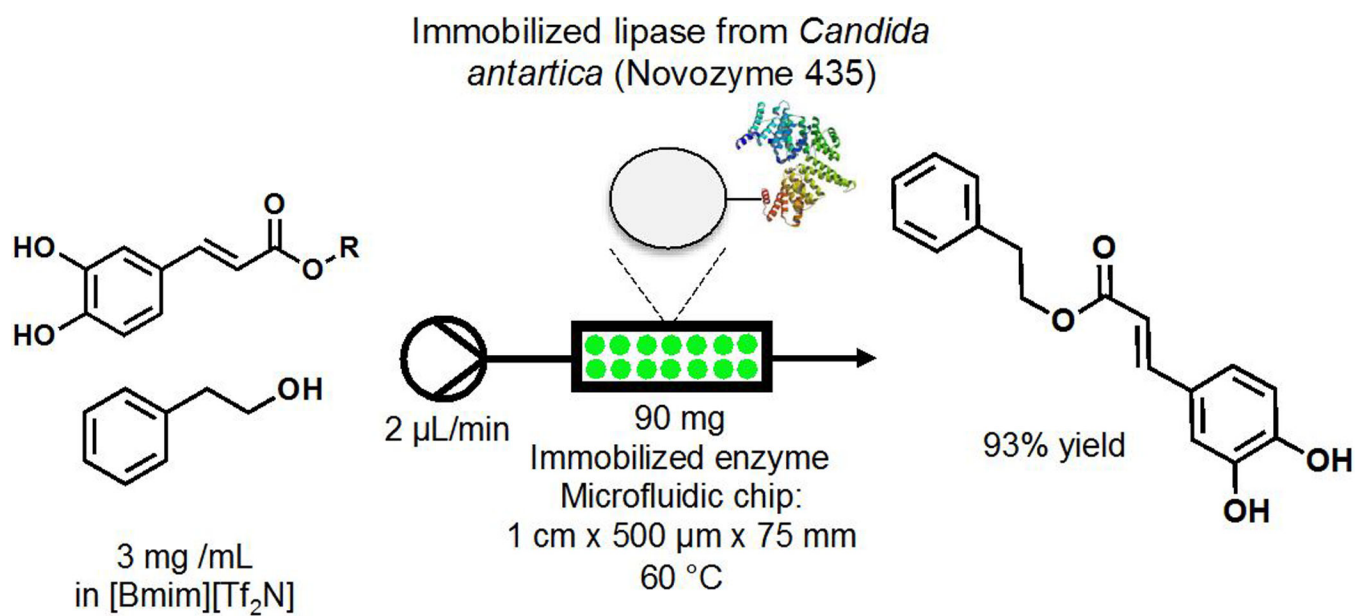


Figure 27. Continuous flow synthesis of caffeic acid phenylethyl ester (CAPE) using immobilized Novozyme 435 in a microfluidic chip.¹⁶⁶

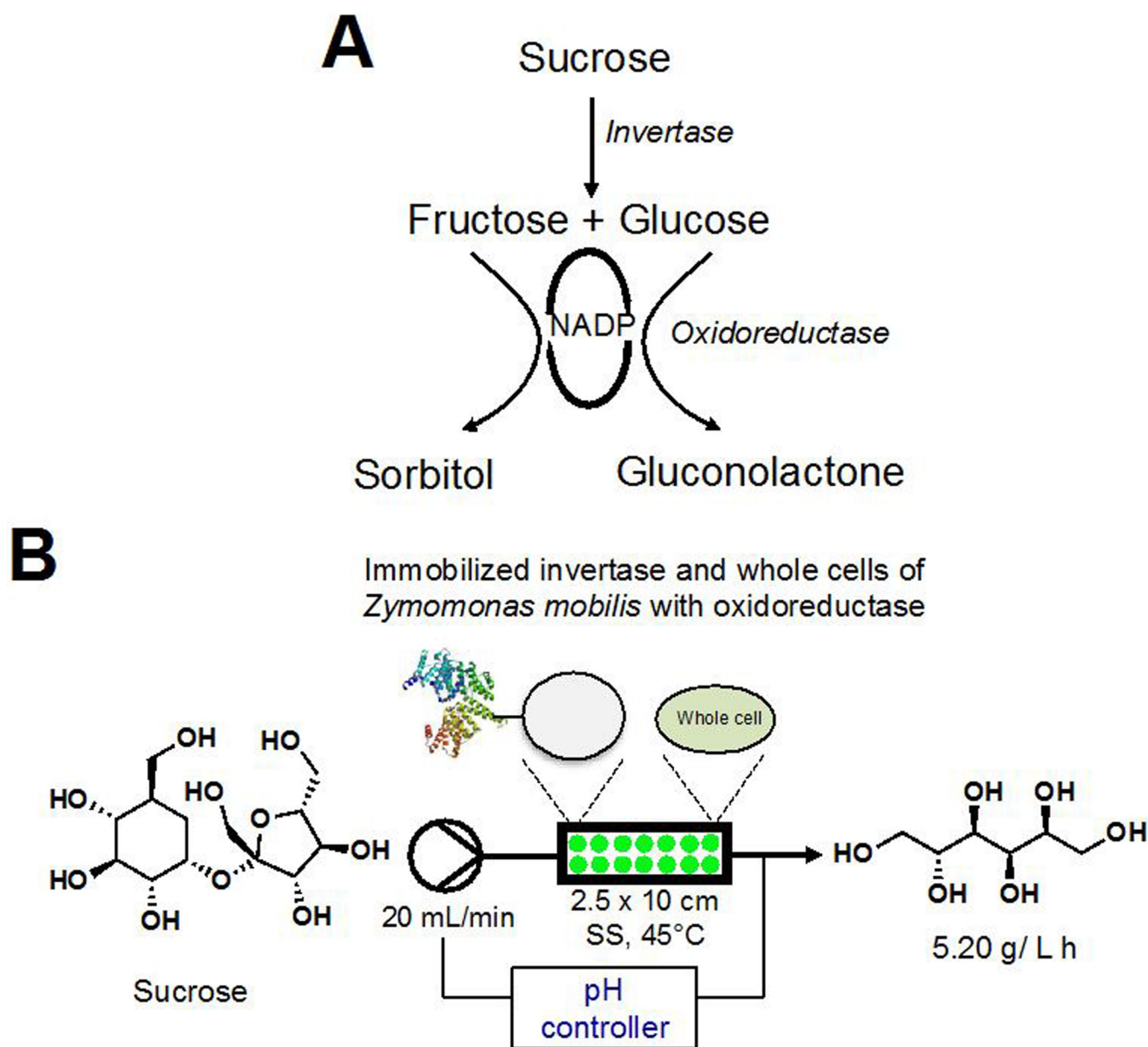


Figure 28.

A continuous flow synthesis of sorbitol using a co-immobilized packed bed reactor of purified invertase and oxidoreductase contained within *Zymomonas mobilis*. **A)** The exploited biochemical transformation in this system. **B)** The continuous flow set-up.¹⁶⁷

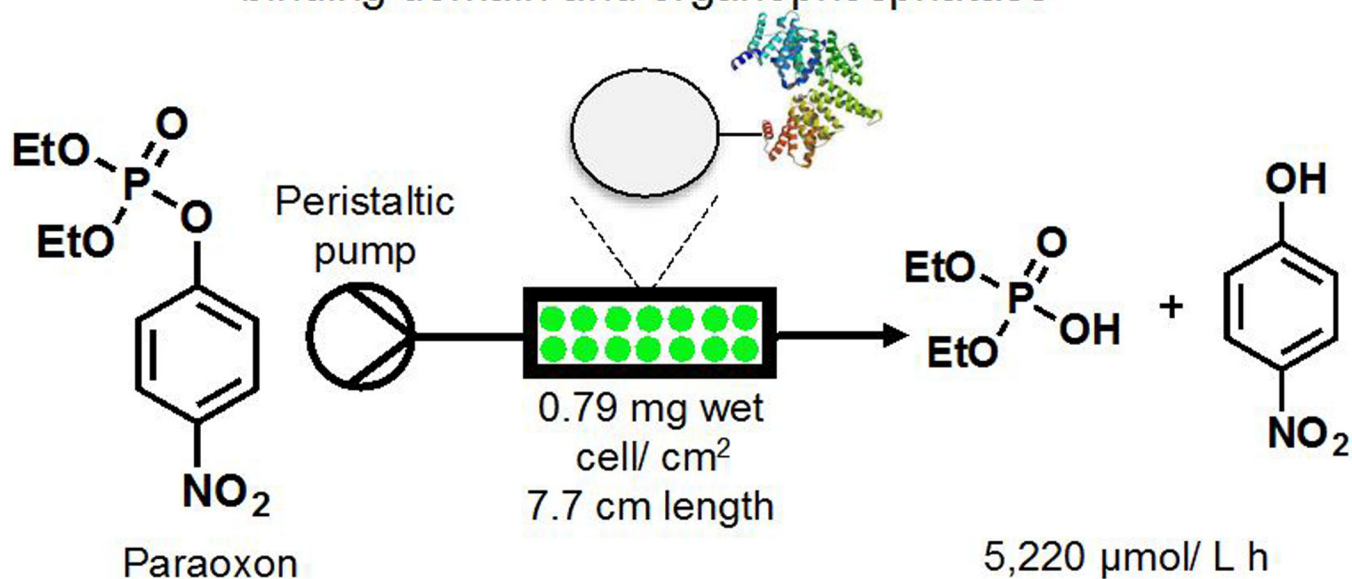
Immobilized *E. coli* expressing a cellulose binding domain and organophosphatase

Figure 29.

A continuous flow degradation of paraoxon using immobilized organophosphatase immobilized onto cellulose fibers using a cellulose-binding domain.¹⁶⁸

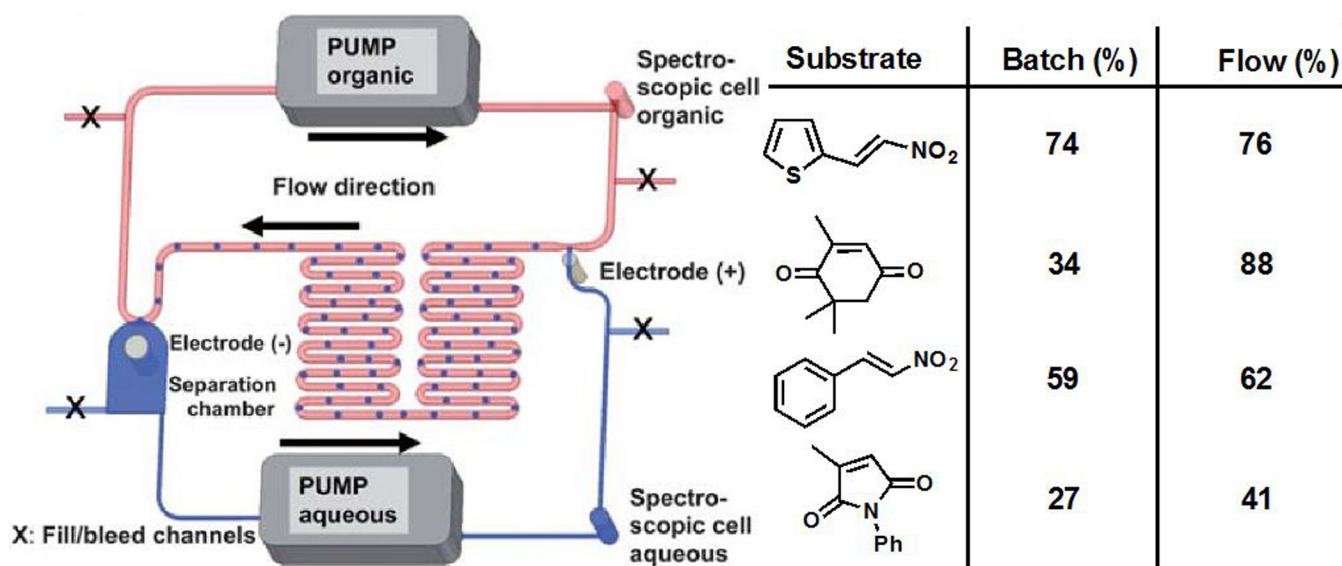


Figure 30.

Continuous flow reduction using penicillamine tetranitrate reductase in a biphasic continuous flow reactor. UV optics was purchased from Ocean Optics, and measurements were collected at one to five minute intervals. The photographs used in this figure were reproduced with permission from the Royal Society of Chemistry (2018).¹⁶⁹

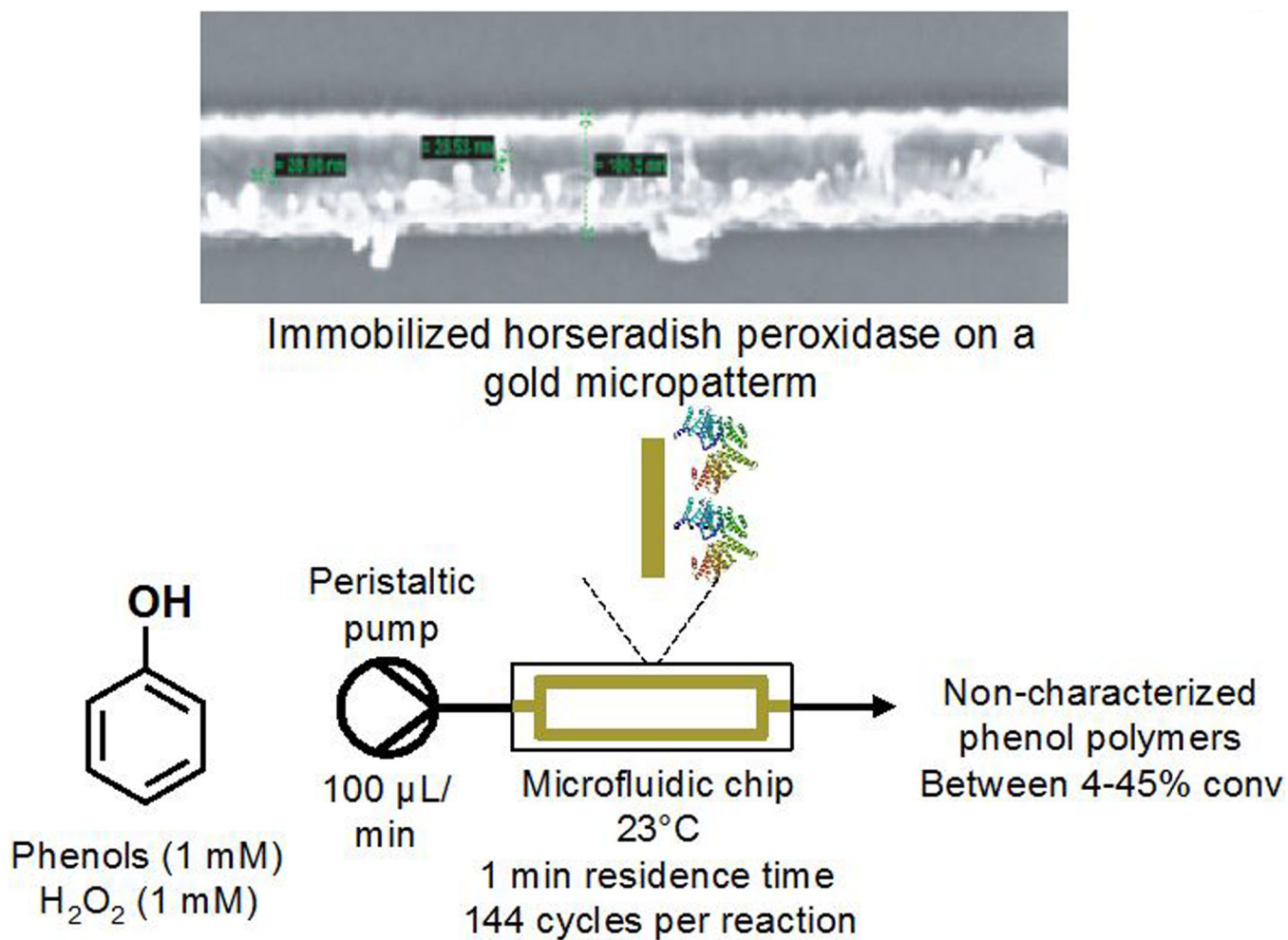


Figure 31. Continuous flow oxidation of phenols into phenol-containing polymers using horseradish peroxidase. The photographs used in this figure were reproduced with permission from Elsevier (2018).¹⁷⁰

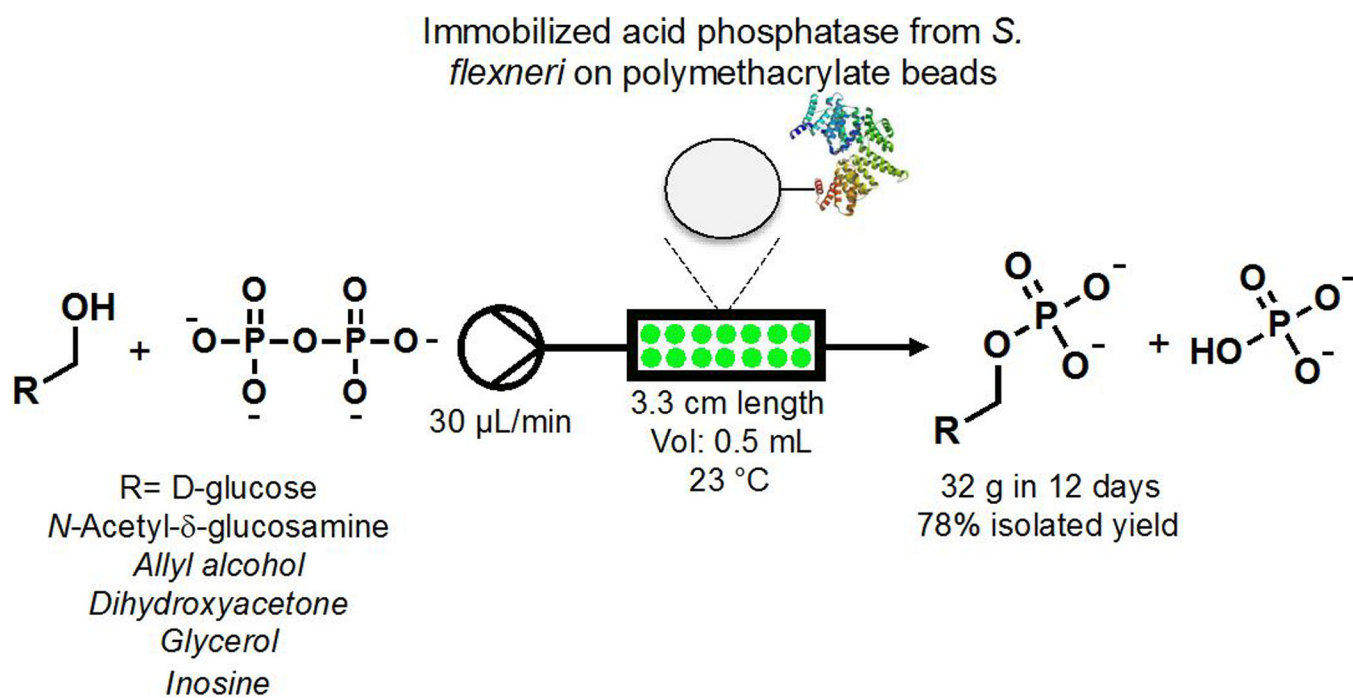


Figure 32. Continuous flow phosphorylation using acid phosphatase immobilized into polymethacrylate beads.¹⁷¹

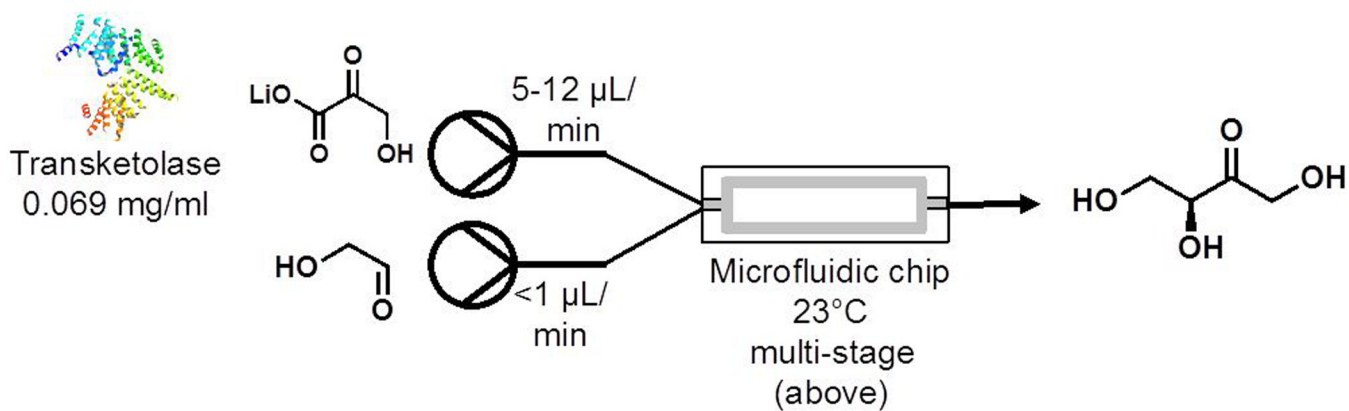
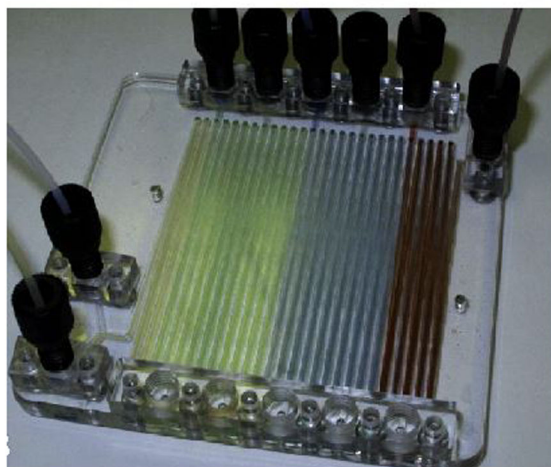
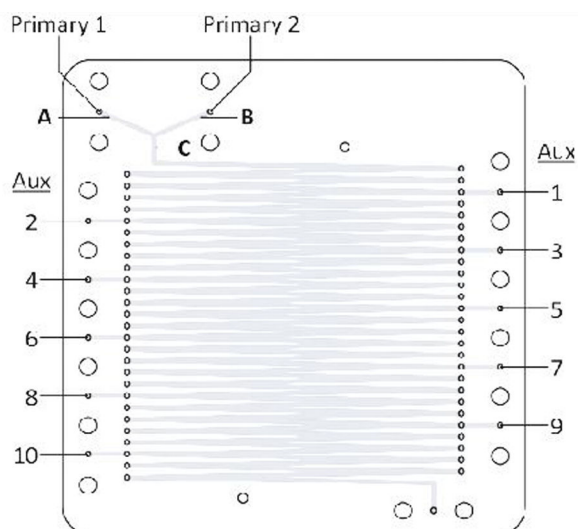


Figure 33. Continuous flow C-C bond formation using wild-type transketolase. This reaction does not use immobilized enzyme. Additionally, the Mg^{2+} (9.8 mM) and thiamine diphosphate (2.4 mM) present in the reaction mixture have been omitted for clarity. The photographs used in this figure were reproduced with permission from Elsevier (2018).¹⁷²

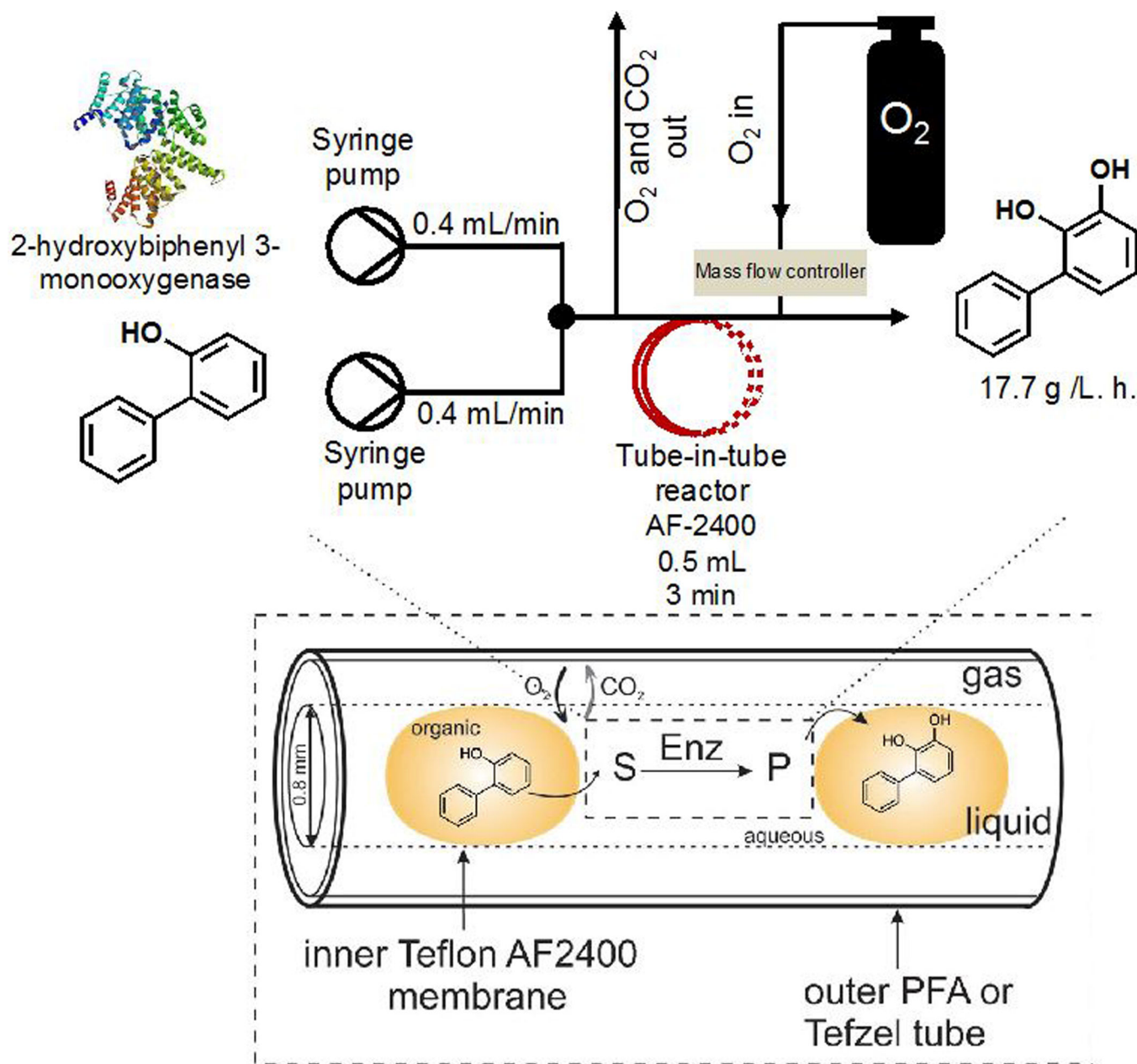


Figure 34. Continuous flow oxygenation using a tube-in-tube reactor with 2-hydroxybiphenyl 3-monoxygenase and O₂. The lower schematic used in this figure were reproduced from the original manuscript.¹⁷³ The photographs used in this figure were reproduced with permission from John Wiley and Sons (2018).¹⁷³

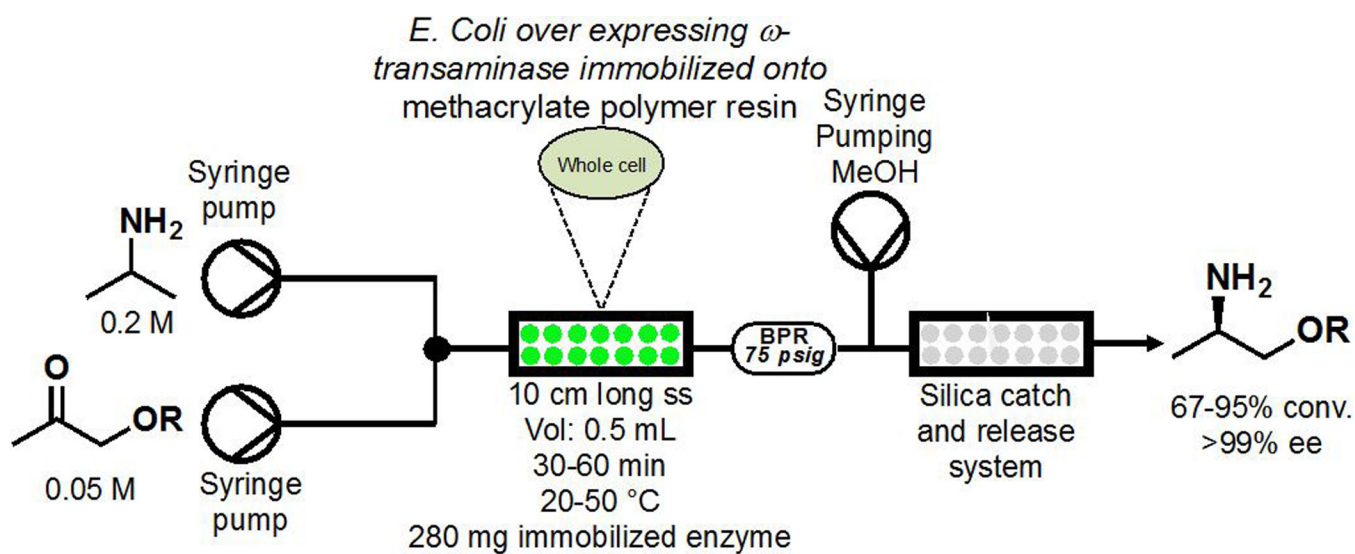


Figure 35. Continuous flow synthesis of optically pure amines using immobilized *E. coli* cells on methacrylate polymer resin overexpressing ω -transaminase.¹⁷⁴

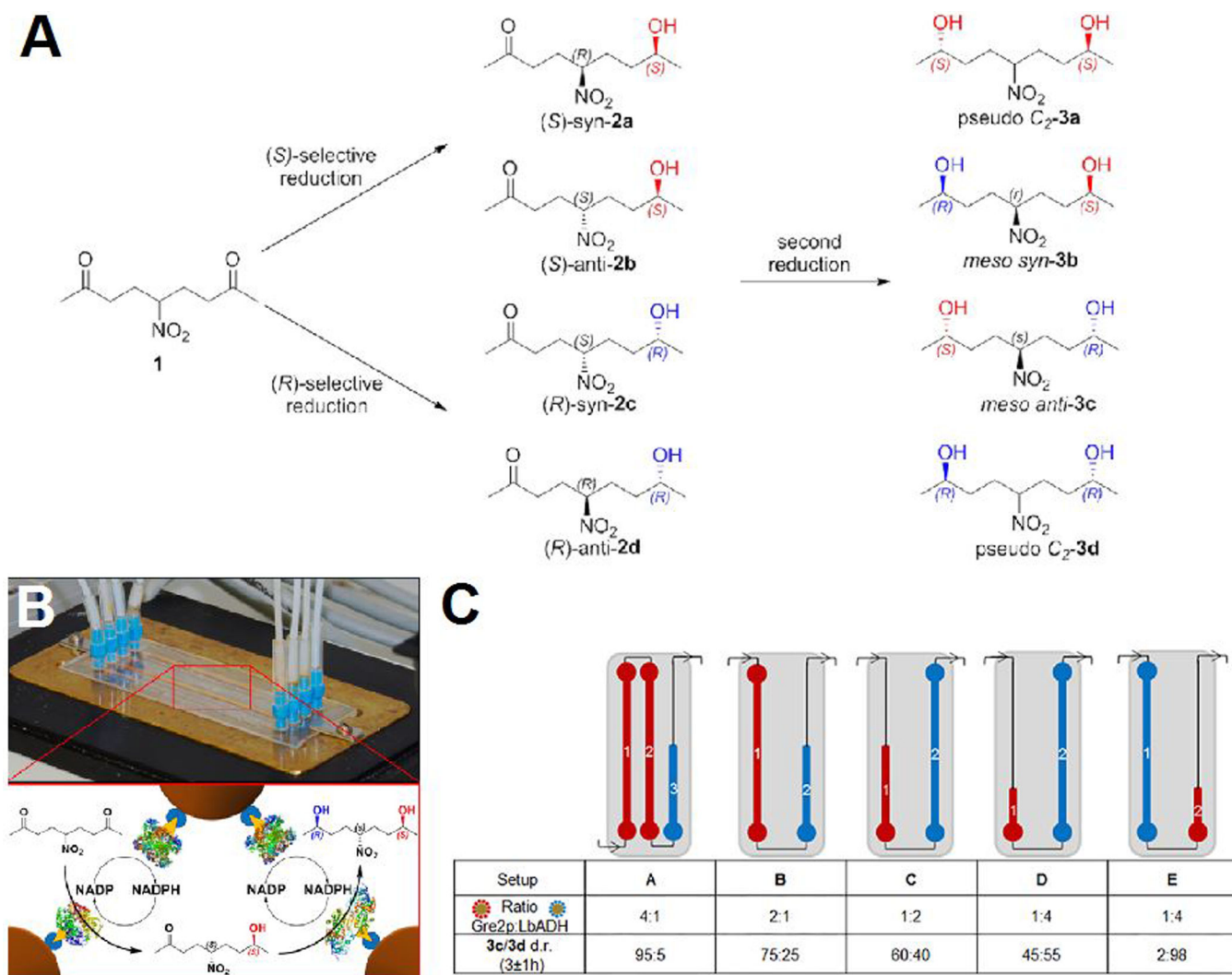


Figure 36.

Continuous flow synthesis of different meso-compounds using a three-enzyme continuous flow system. **A**) The molecules possible through double reduction of starting compound **1**. **B**) The microfluidic set up showing the two enzymes involved in this multi-step process. Not shown is the third enzyme (glucose 1-dehydrogenase) involved in co-factor regeneration. **C**) The effect of immobilizing either the (*S*)-selective or (*R*)-selective reductase at different points of the micro reactor and its effect on the ratio of compounds **3c/3d**. For additional information and larger images, please see the original publication. This figure was used with permission.¹⁷⁵ Copyright (2018) American Chemical Society.

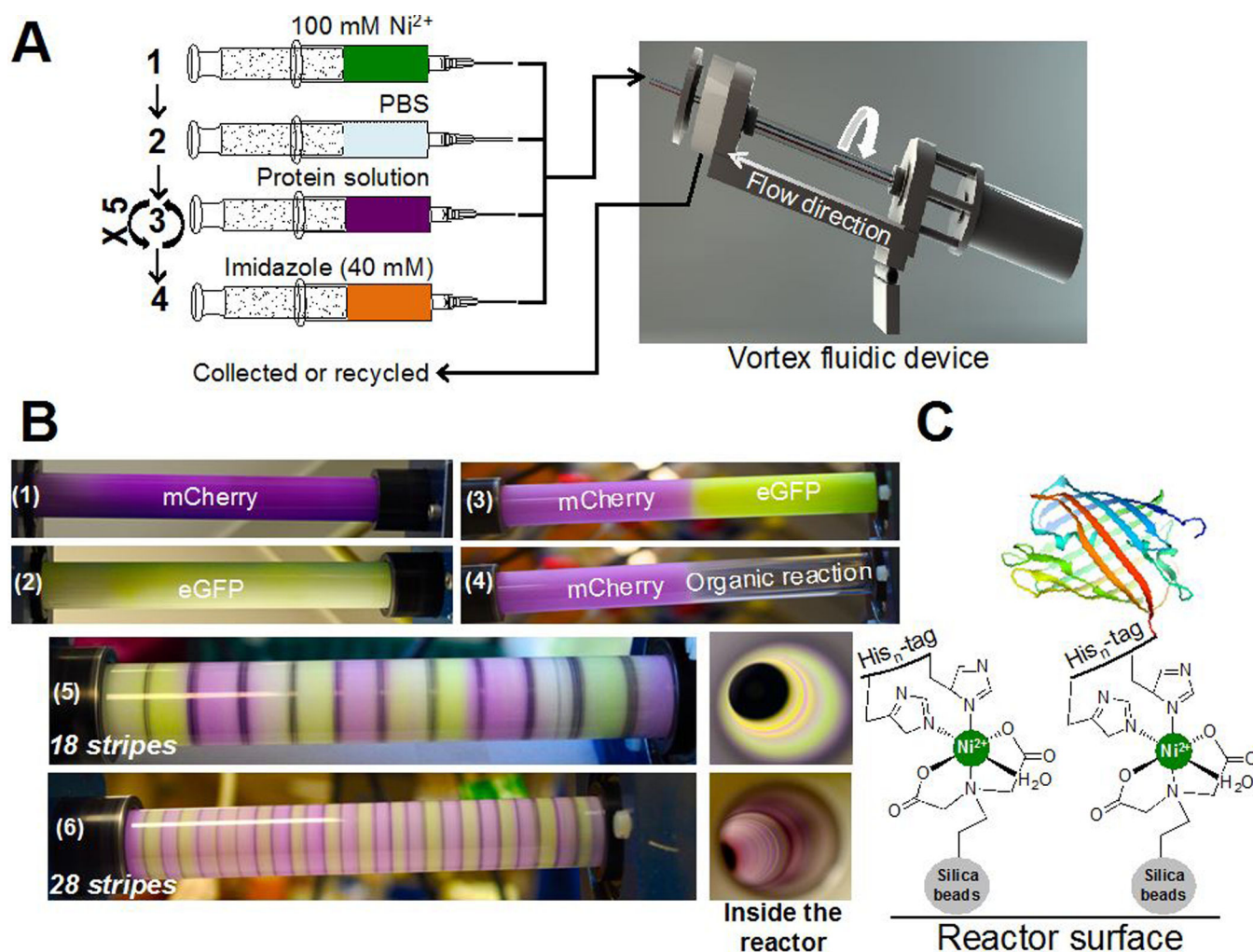


Figure 37. Multi-step continuous flow biocatalysis using thin films and IMAC-based attachment. **A)** The continuous operation allowing protein purification and immobilization in ten minutes from cell lysate. First the column is charged with Ni²⁺, then PBS rinses out any residual Ni²⁺. The cell lysate is then recycled through the reactor five times before the immobilized protein is washed with a low concentration of imidazole. **B)** The different stripes and patterns possible when using this methodology. **C)** The enzyme immobilization mode utilizing polyhistidine tags on the protein.¹²⁴ This figure was used with permission. Copyright (2018) John Wiley and Sons.

Ketoreductase from *Lactobacillus kefir*
co-immobilized with NADPH on porous
agarose beads

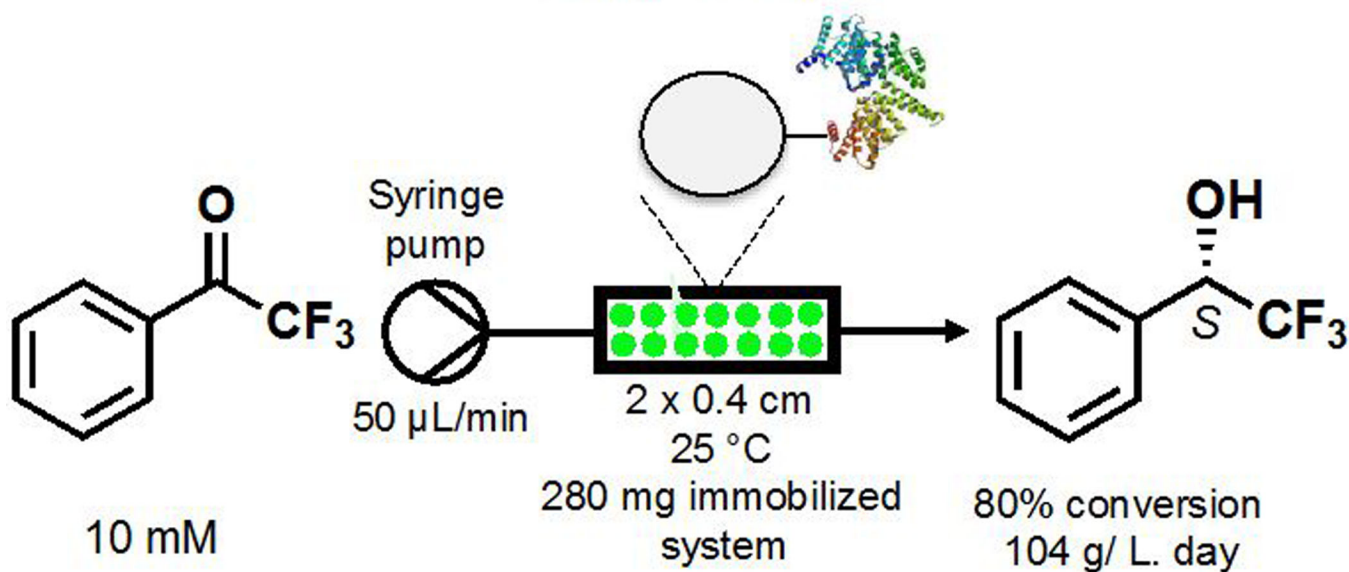


Figure 38. Continuous flow biocatalysis using a ketoreductase and NADP(H) co-immobilized into porous agarose beads. Under these conditions, the ketoreductase yielded the (*S*)-enantiomer, however; all other substrates yielded the (*R*)-enantiomer. IPA was used to regenerate the co-factor.¹⁷⁶

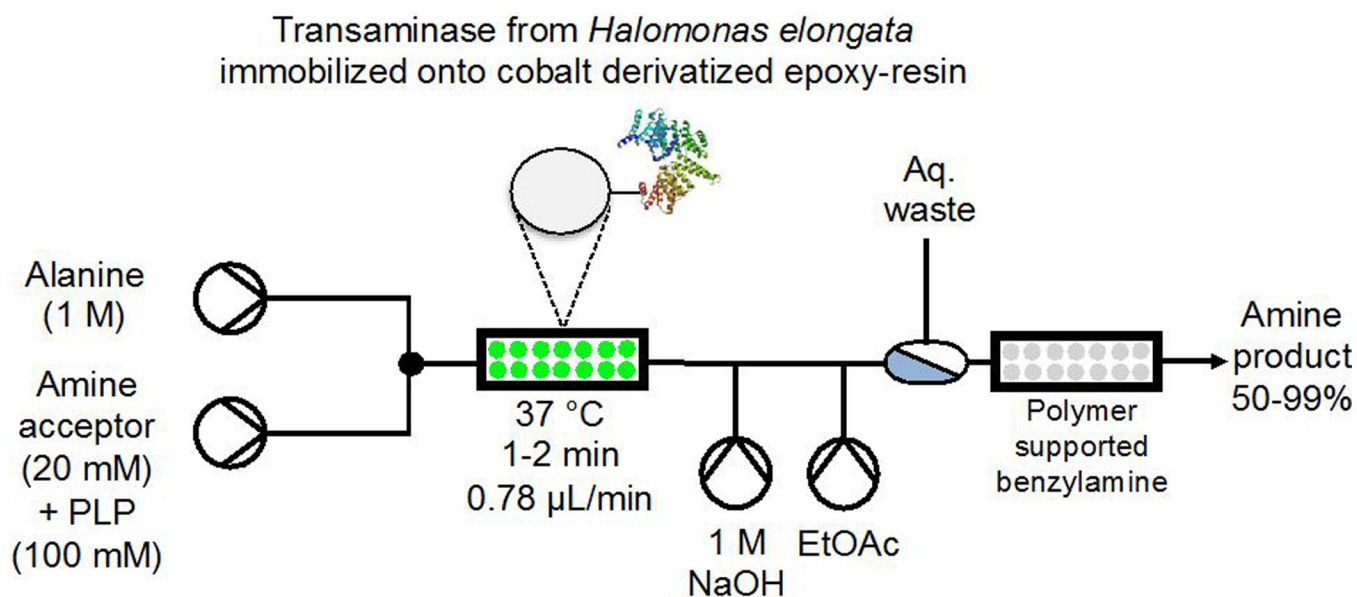


Figure 39.

Continuous flow synthesis of amines from alanine as an amine source and an aldehyde amine acceptor using immobilized purified transaminase on cobalt-derivatized epoxy-resin. Additionally, this example uses a Zaiput Flow technologies liquid-liquid separator and polymer supported benzylamine to purify the reaction mixture and provide a means of recycling any unreacted substrate.¹⁷⁷

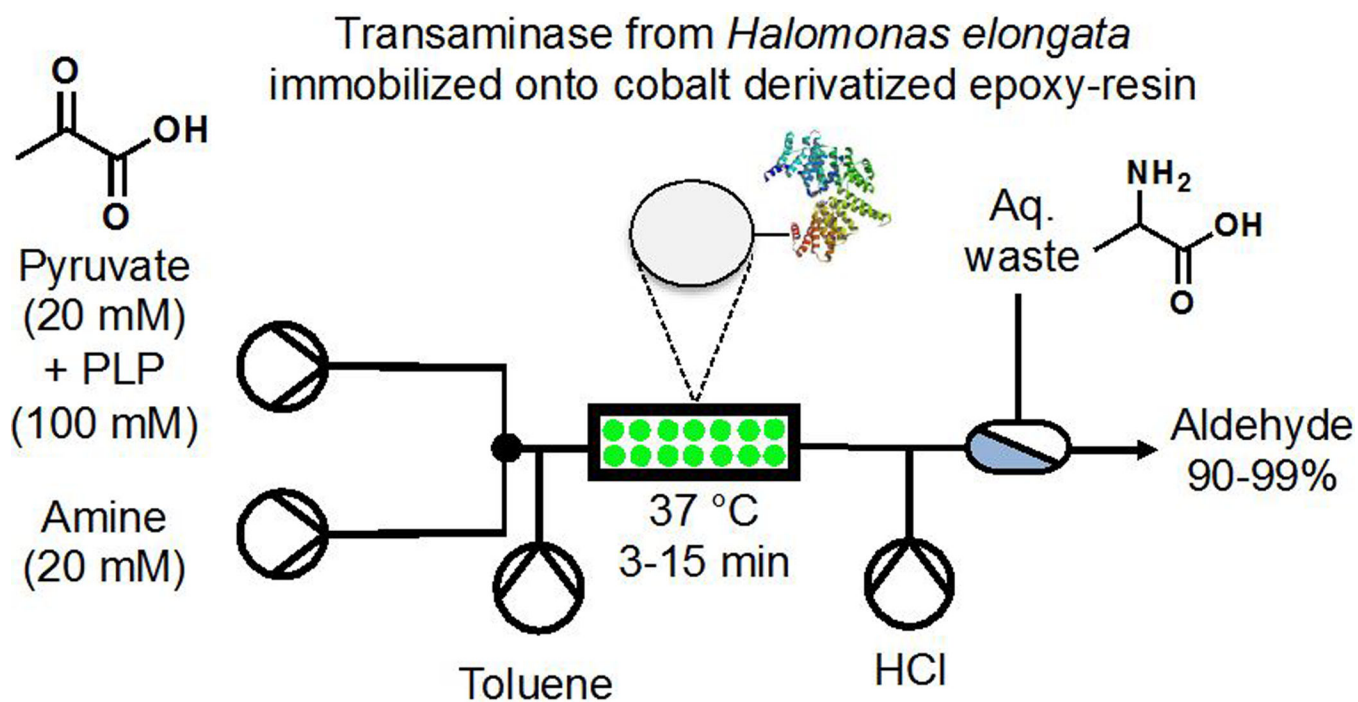


Figure 40.

Continuous flow synthesis of aldehydes using immobilized purified transaminase on cobalt-derivatized epoxy-resin. Here, a toluene stream is added to the reaction mixture (50:50 v:v) to ensure the aldehyde is not immobilized onto the packed bed reactor. Simple acidification of the effluent stream with HCl allows a biphasic liquid-liquid extraction with a Zaiput liquid-liquid separator.¹⁷⁸

Phenylalanine ammonia lyase from *Aradidopsis thaliana* containing a carbohydrate binding module immobilized onto Avicel

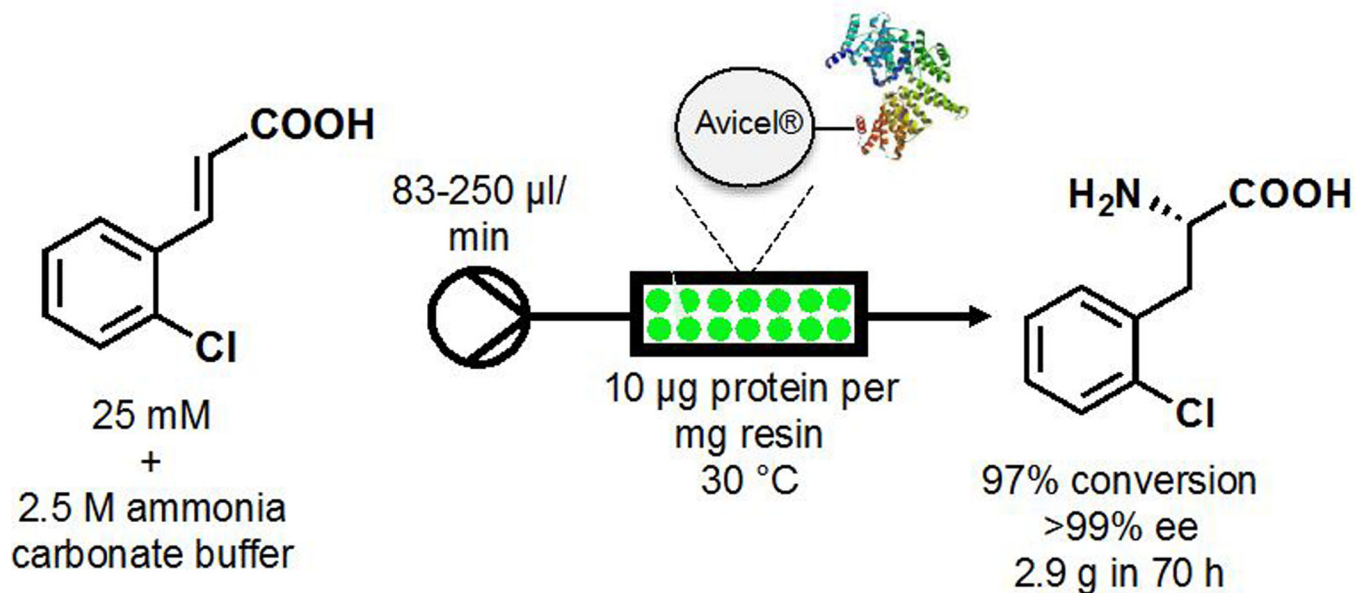


Figure 41. Continuous flow synthesis of a (*S*)-phenylalanine derivative using phenylalanine ammonia lyase from *Aradidopsis thaliana*. The enzyme was expressed with a carbohydrate-binding domain at the C-terminus of the protein allowing rapid immobilization onto a carbohydrate based resin (Avicel).¹⁷⁹

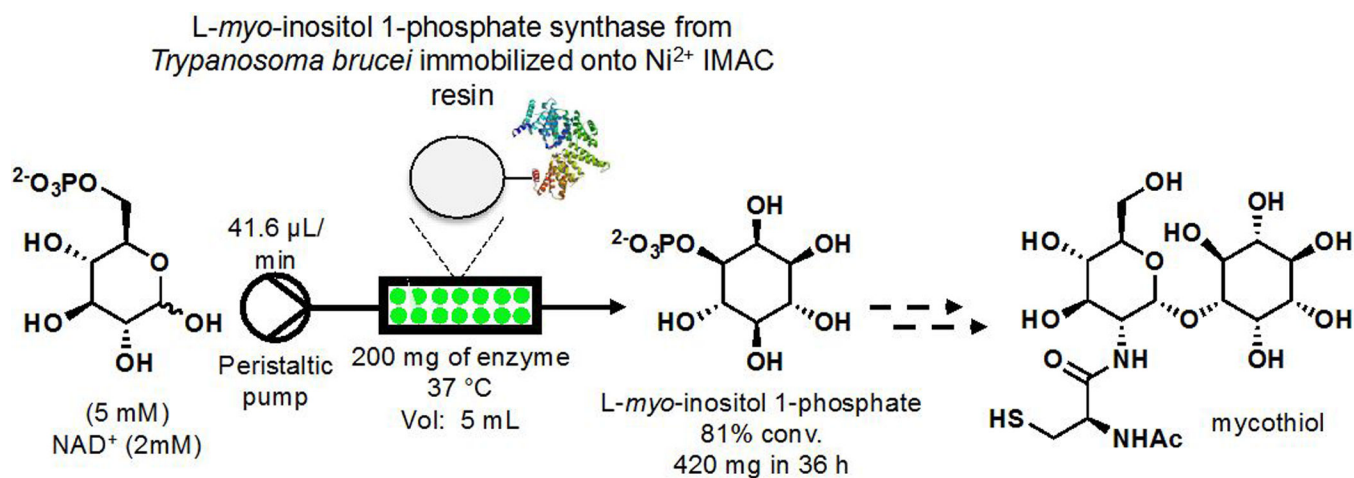


Figure 42. Continuous flow synthesis of (*L*)-*myo*-inositol 1-phosphate using (*L*)-*myo*-inositol 1-phosphate synthase from *Trypanosoma brucei* immobilized onto IMAC resin.¹⁸⁰

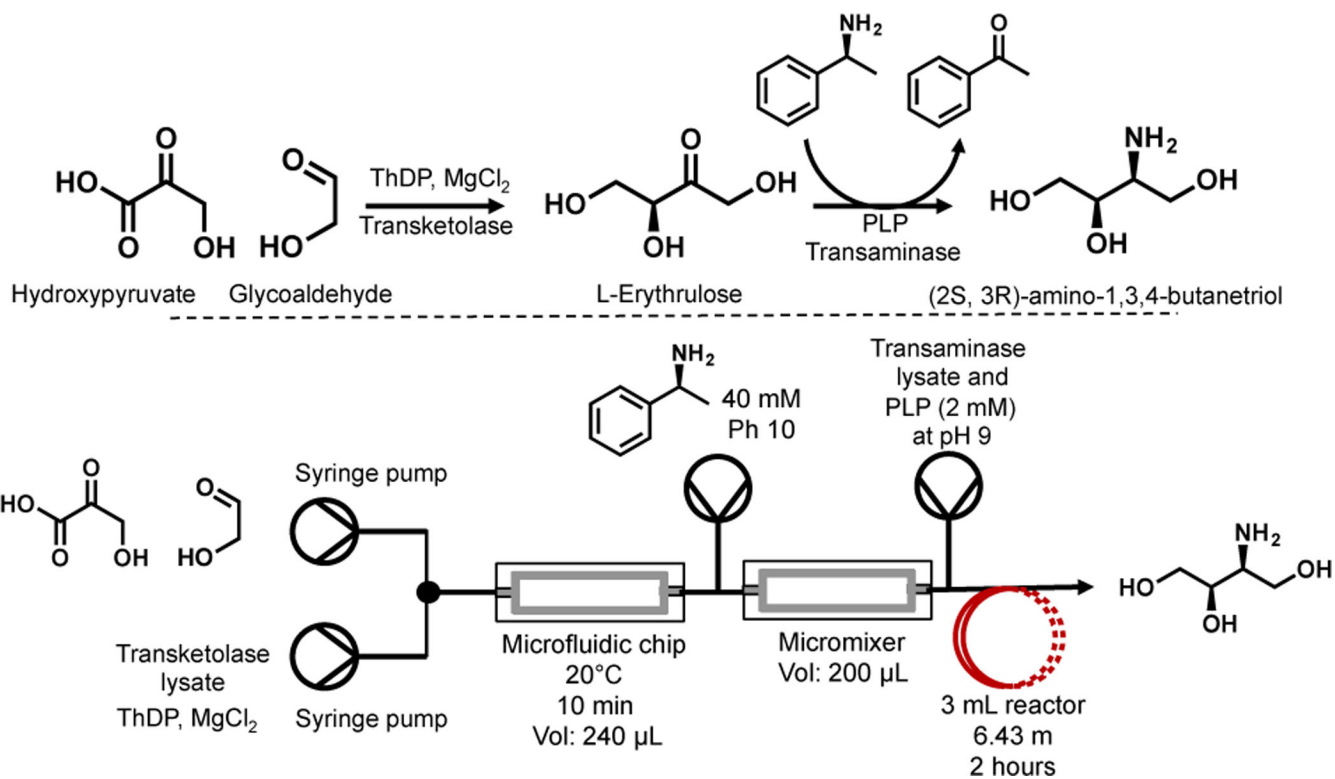


Figure 43. Multi-step continuous flow synthesis of (2*S*,3*R*)-amino-1,3,4-butanetriol using a transketolase and transaminase in cascading continuous flow reactors.¹⁸¹

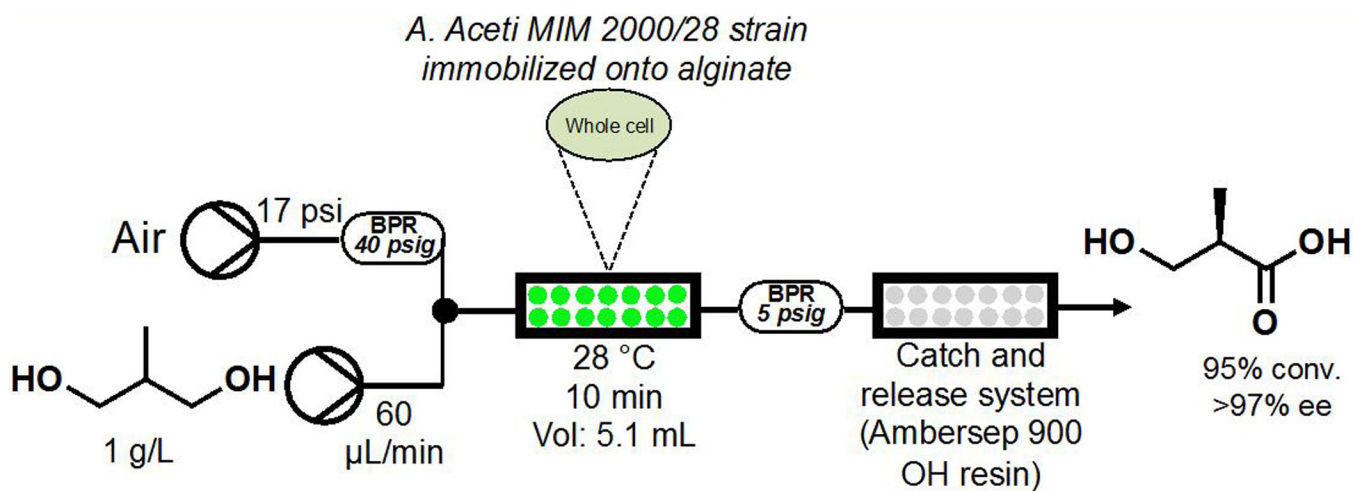


Figure 44. Continuous flow oxidation of 2-methyl-1,3-propanediol using whole cells of *Acetobacter aceti* MIM 2000/28 immobilized onto alginate.¹⁸²

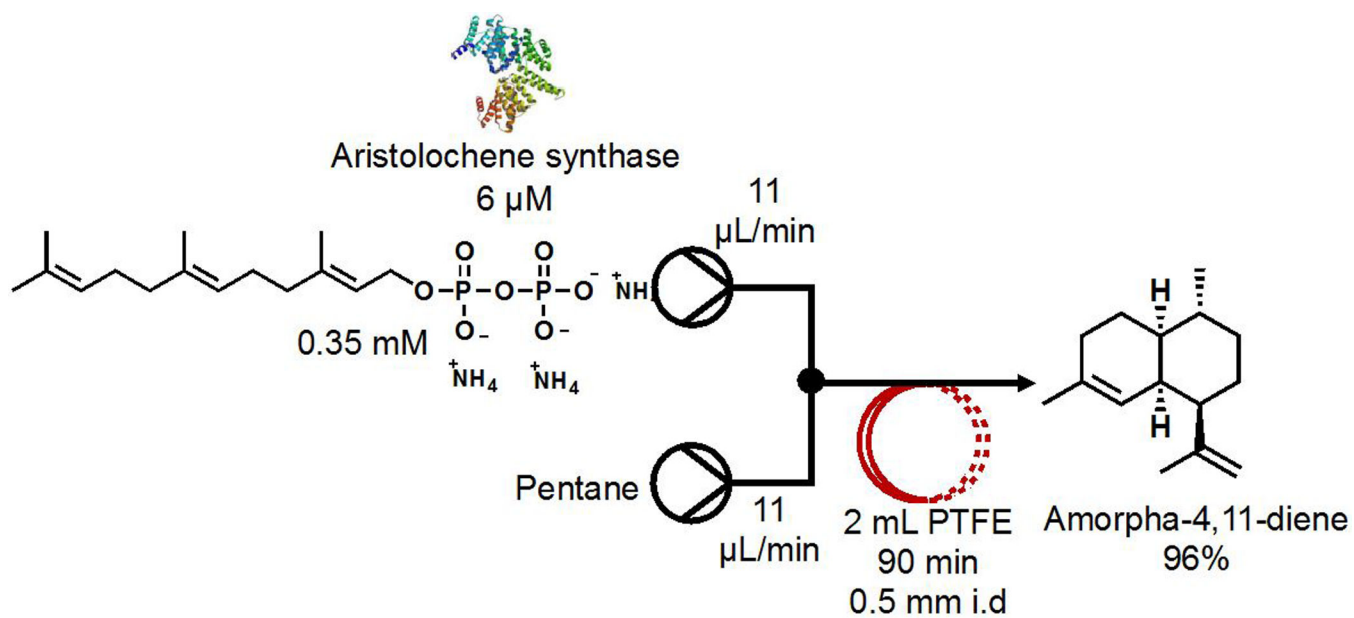


Figure 45. Continuous flow synthesis of the terpene amorpha-4,11-diene using a biphasic system comprised of buffer and pentane.¹⁸³

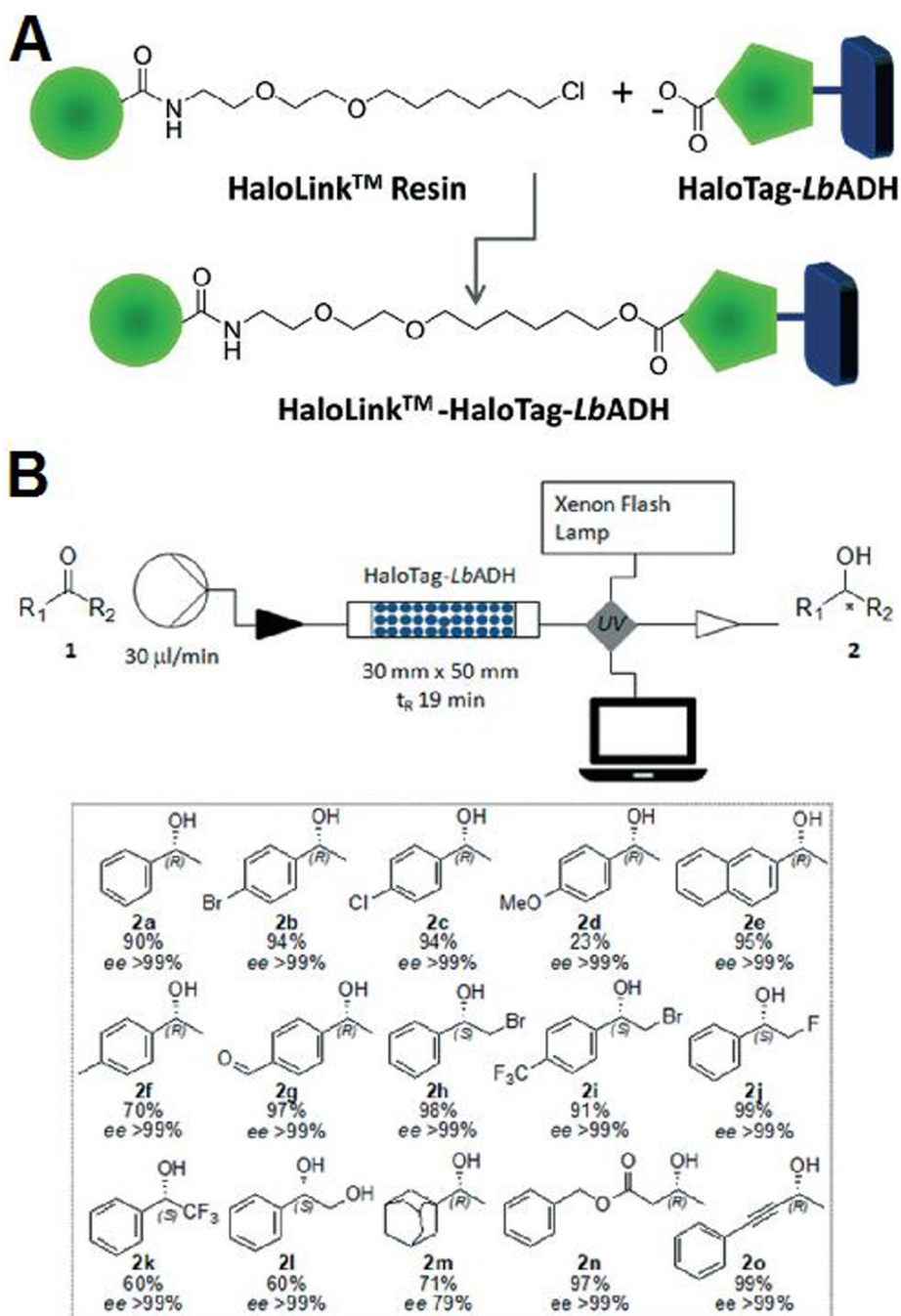


Figure 46. Continuous flow asymmetric reduction of ketones using an alcohol dehydrogenase immobilized onto HaloLink resin. The UV monitoring equipment was purchased from UniQsis Ltd. The photographs used in this figure were reproduced with permission from The Royal Society of Chemistry (2018).¹⁸³

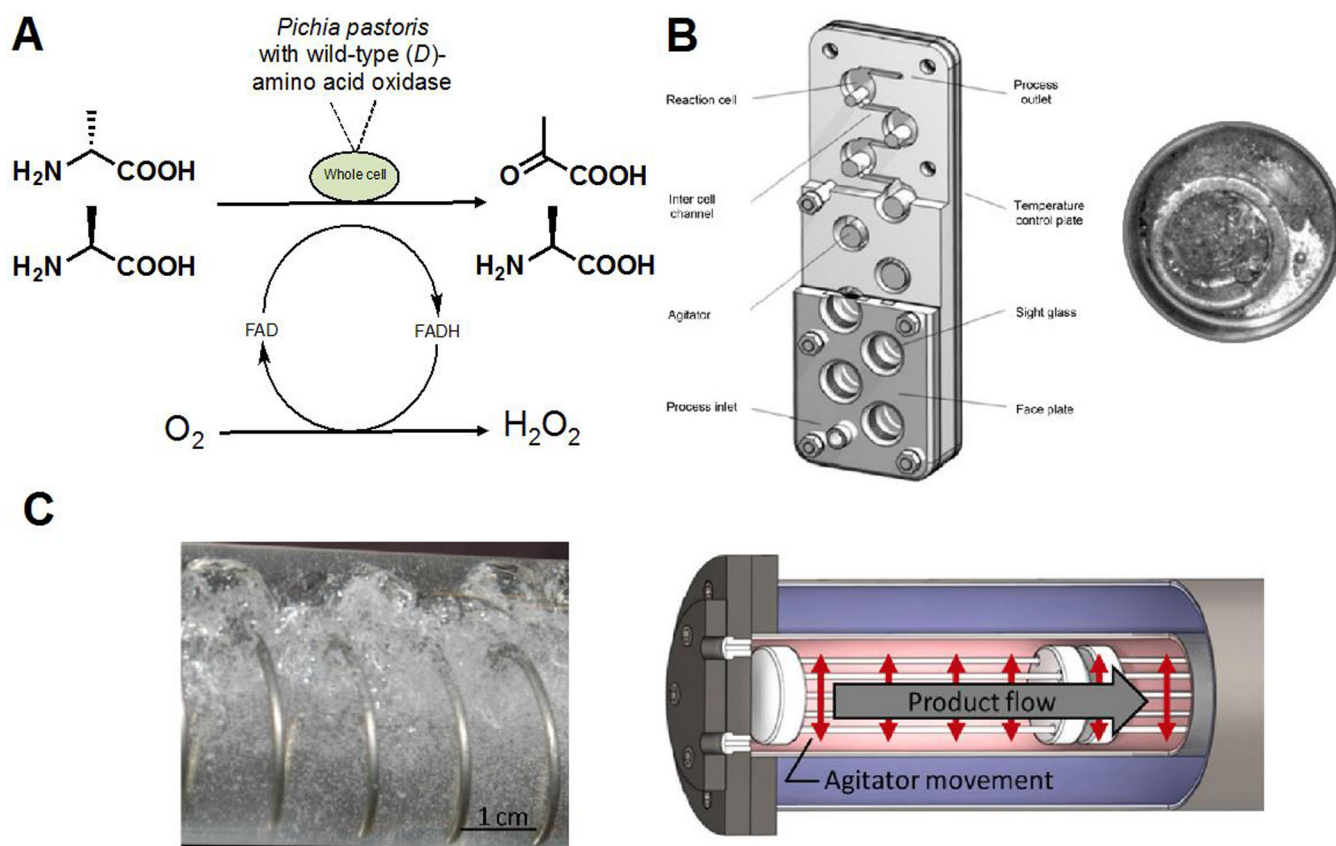


Figure 47. Chiral resolution of (*D*)- and (*L*)-alanine using whole cells with wild type (*D*)-amino acid oxidase. In this example, a batch vs. continuous flow experiment is done. **A**) The biocatalytic system used in both the continuous flow and batch experiment. Note that oxygen is required in the transformation. **B**) The Coflore agitated cell reactor (Coflore ACR) and a close up photograph of one of the agitators. **C**) The Coflore agitated tube reactor (Coflore ACR) with a close up photograph of the agitator movement. The photographs used in this figure were reproduced with permission from Science Direct (2018).¹⁸⁴

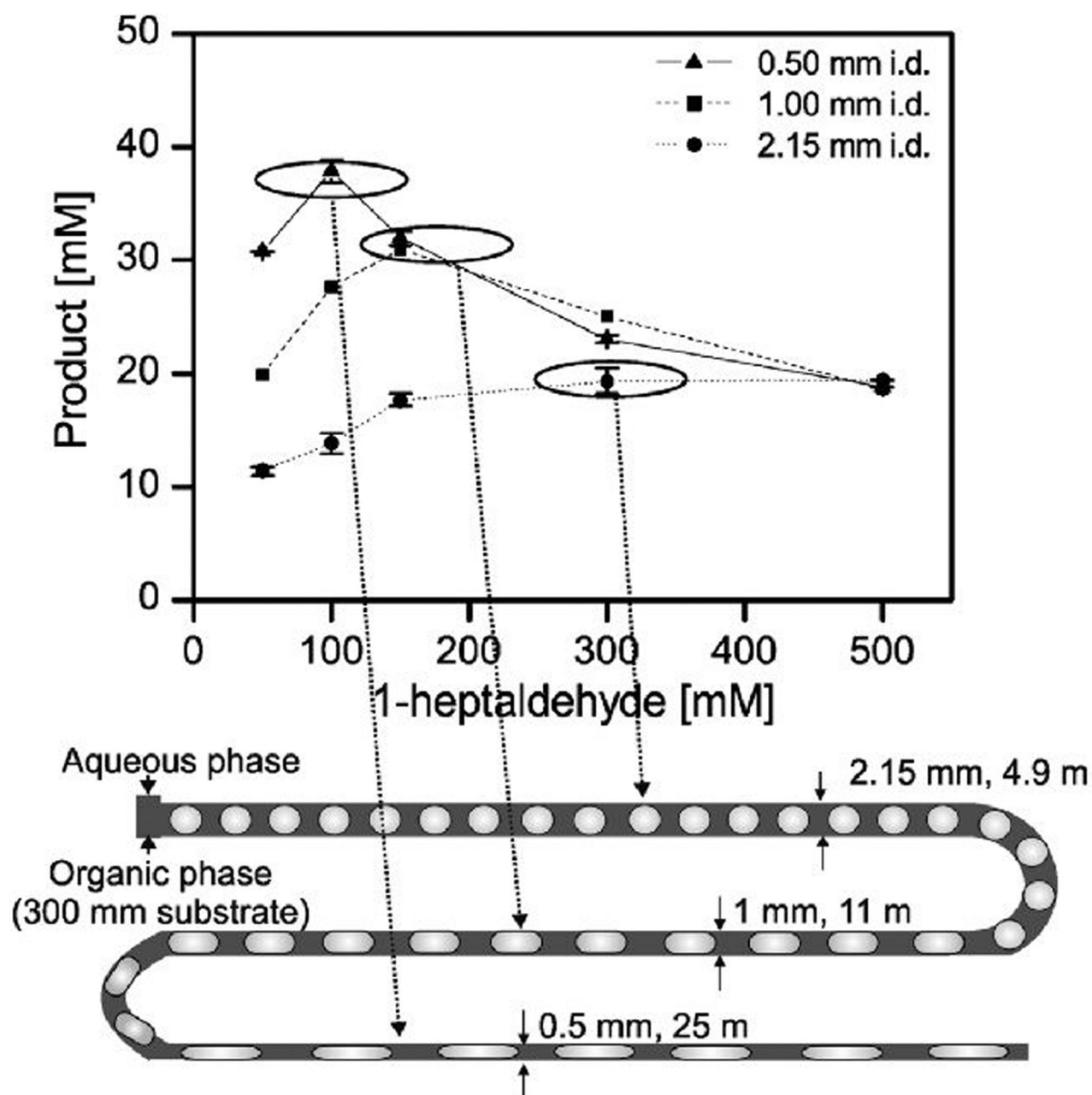


Figure 48.

The variable diameter tube reactor for reducing 1-heptaldehyde to 1-heptanol using a thermophilic alcohol dehydrogenase. The larger diameter tubing (2.15 mm i.d.) at the start of the continuous flow system is more effective with higher substrate concentrations (300 mM) compared to the smaller diameter tubing (1.00 and 0.50 mm i.d.) that is more effective operating under lower substrate concentrations (~100–200 mM). This figure was used with permission. Copyright (2018) John Wiley & Sons.¹⁸⁵

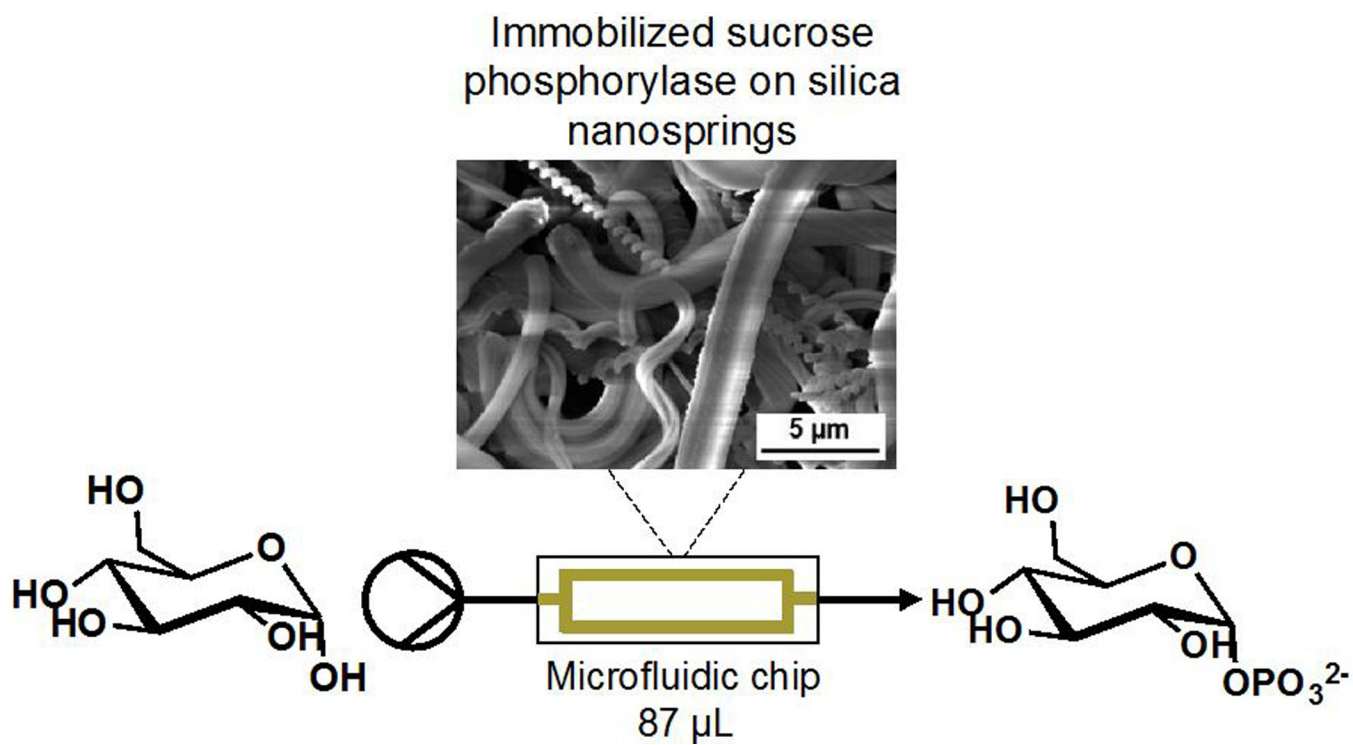


Figure 49. Continuous flow phosphorylation of glucose using immobilized sucrose phosphorylase. The enzyme was immobilized onto silica springs using a silica-binding domain. Interestingly, the reaction was improved 10-fold in an 87 μL volume microfluidic chip.¹⁸⁶ This figure was used with permission.¹⁸⁶ Copyright (2018) American Chemical Society.

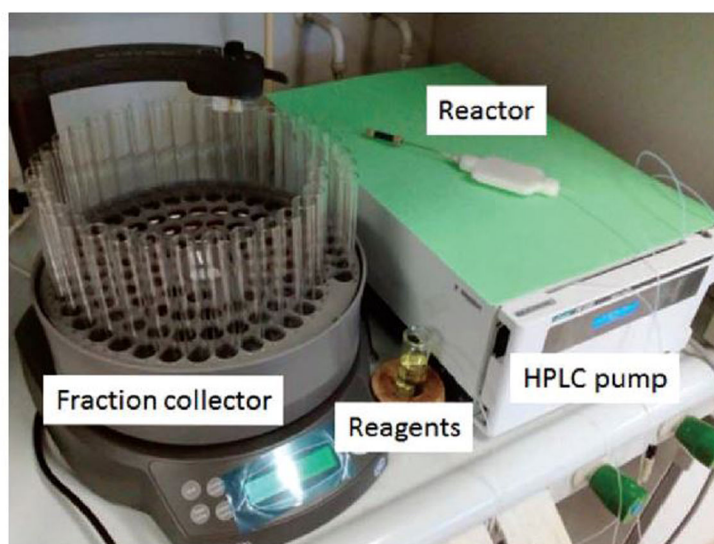
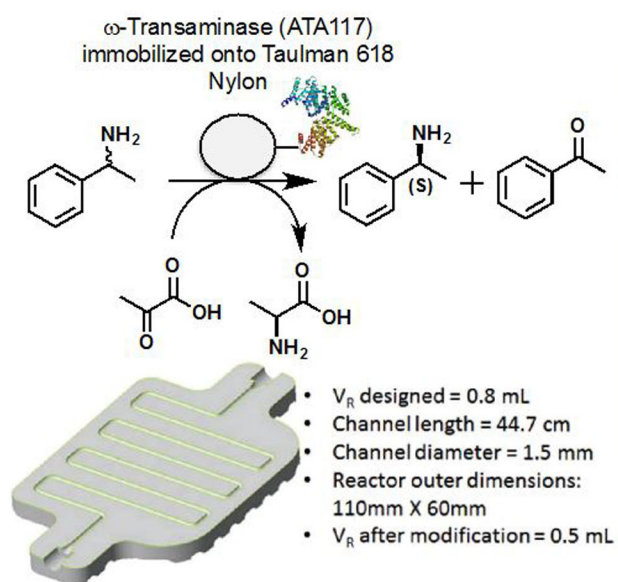


Figure 50.

Continuous flow kinetic resolution of (*rac*)-methylbenzylamine using a (*R*)-selective ω -transaminase immobilized onto the surface of 3D printed reactor constructed from Nylon Taulman 618. The photographs used in this figure were reproduced with permission from The Royal Society of Chemistry (2018).¹⁸⁷

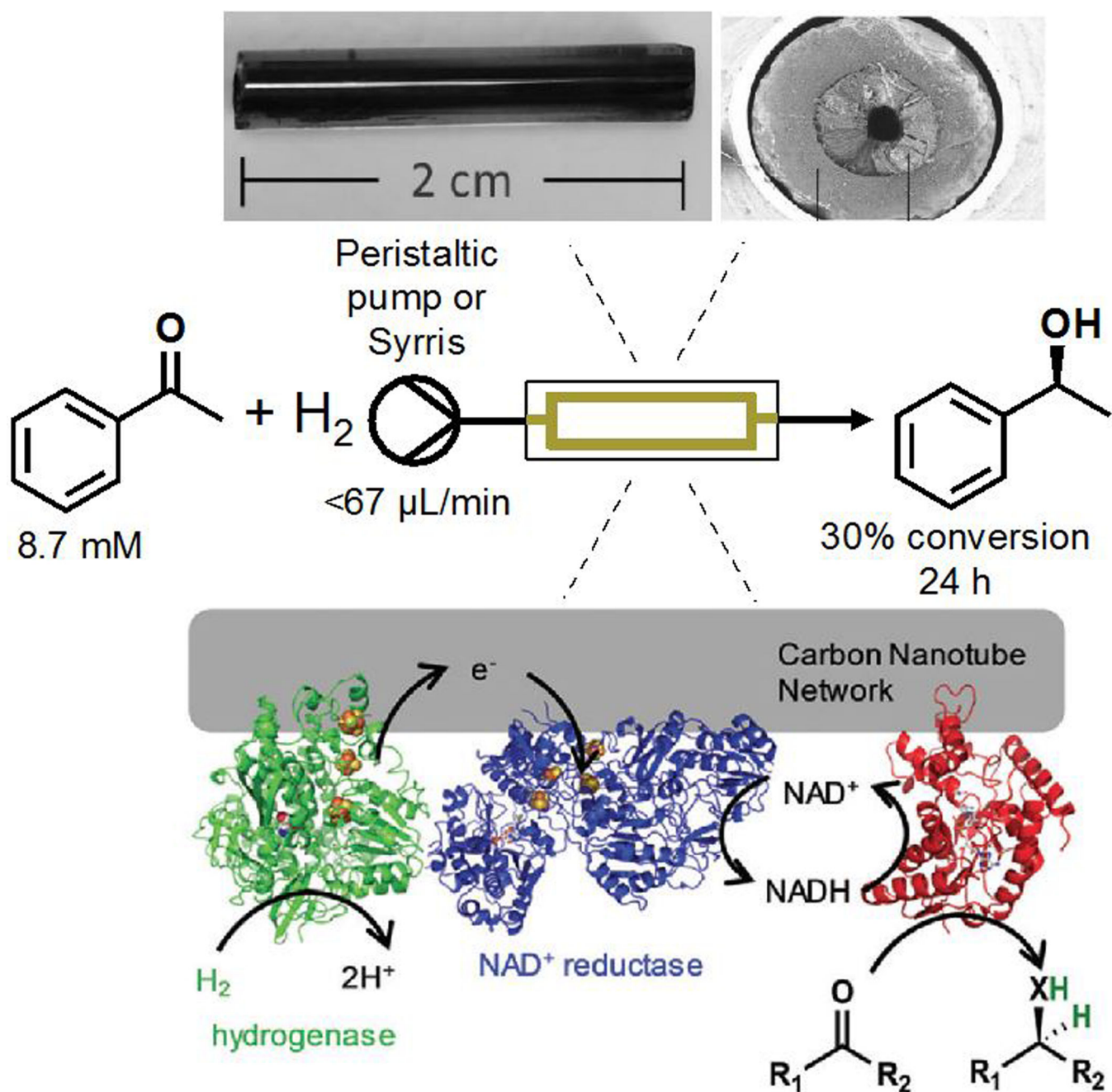
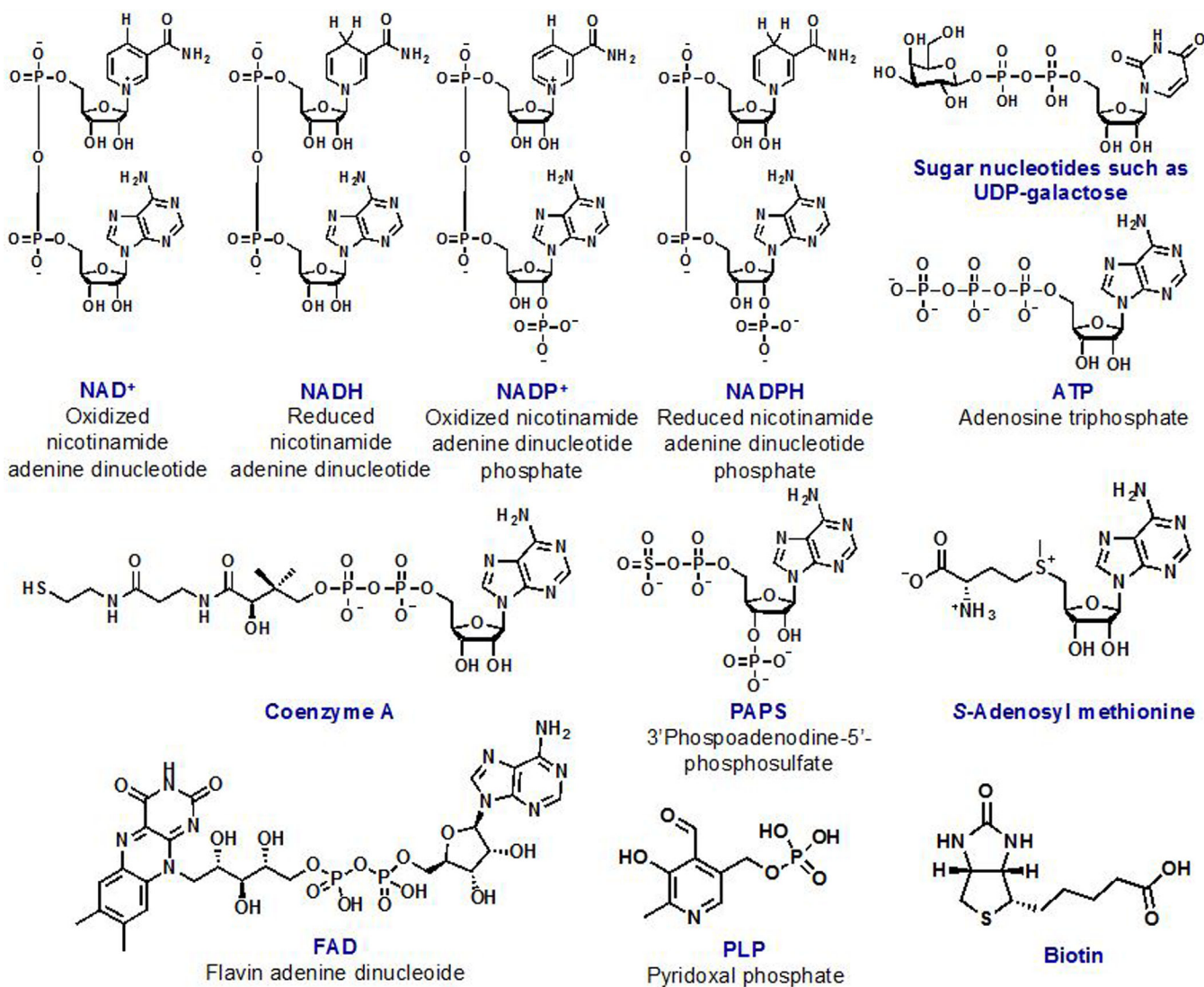


Figure 51. Continuous flow reduction of acetophenone using immobilized alcohol dehydrogenase. The photographs used in this figure were reproduced with permission from The Royal Society of Chemistry (2018).¹⁸⁸

**Figure 52.**

Co-factors for biosynthesis. The most common reaction for each co-factor is as follows: NAD⁺ and NADP⁺ = hydride acceptor, NADH and NADPH = hydride addition, ATP = phosphoryl transfer, Sugar nucleotides = glycosyl transfer, Coenzyme A = acyl transfer, PAPS = sulfuryl transfer, *S*-Adenosyl methionine = methyl transfer, Flavins = oxygenation, PLP = transamination and Biotin = carboxylation.

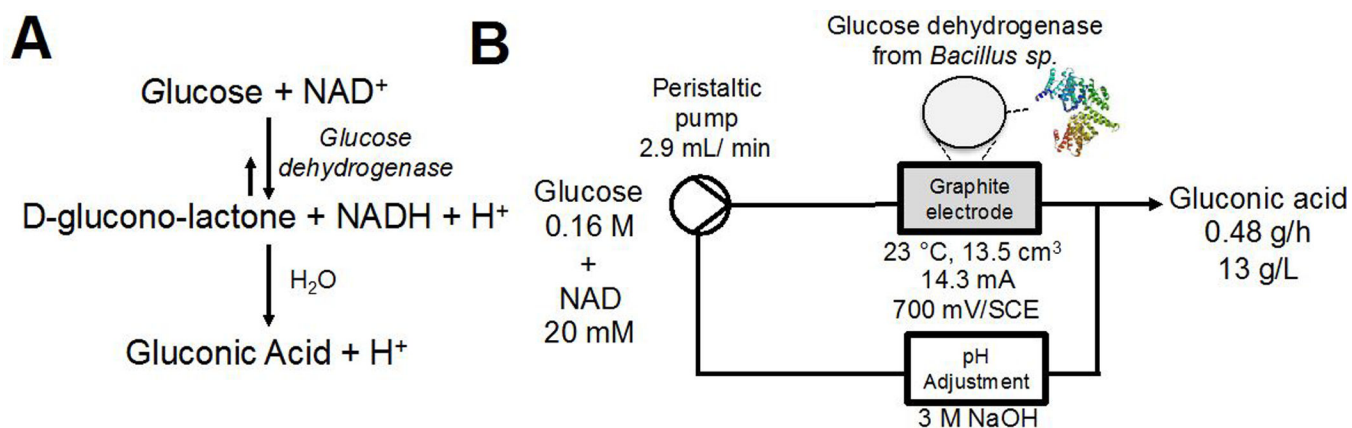


Figure 53.

Continuous electrochemical regeneration of NAD^+ by use of a graphite electrode. **A)** The reaction scheme showing the conversion of glucose to gluconic acid using glucose dehydrogenase. **B)** The continuous flow set-up used for the reaction and the electrochemical oxidation of NADH to NAD^+ .¹⁹⁷

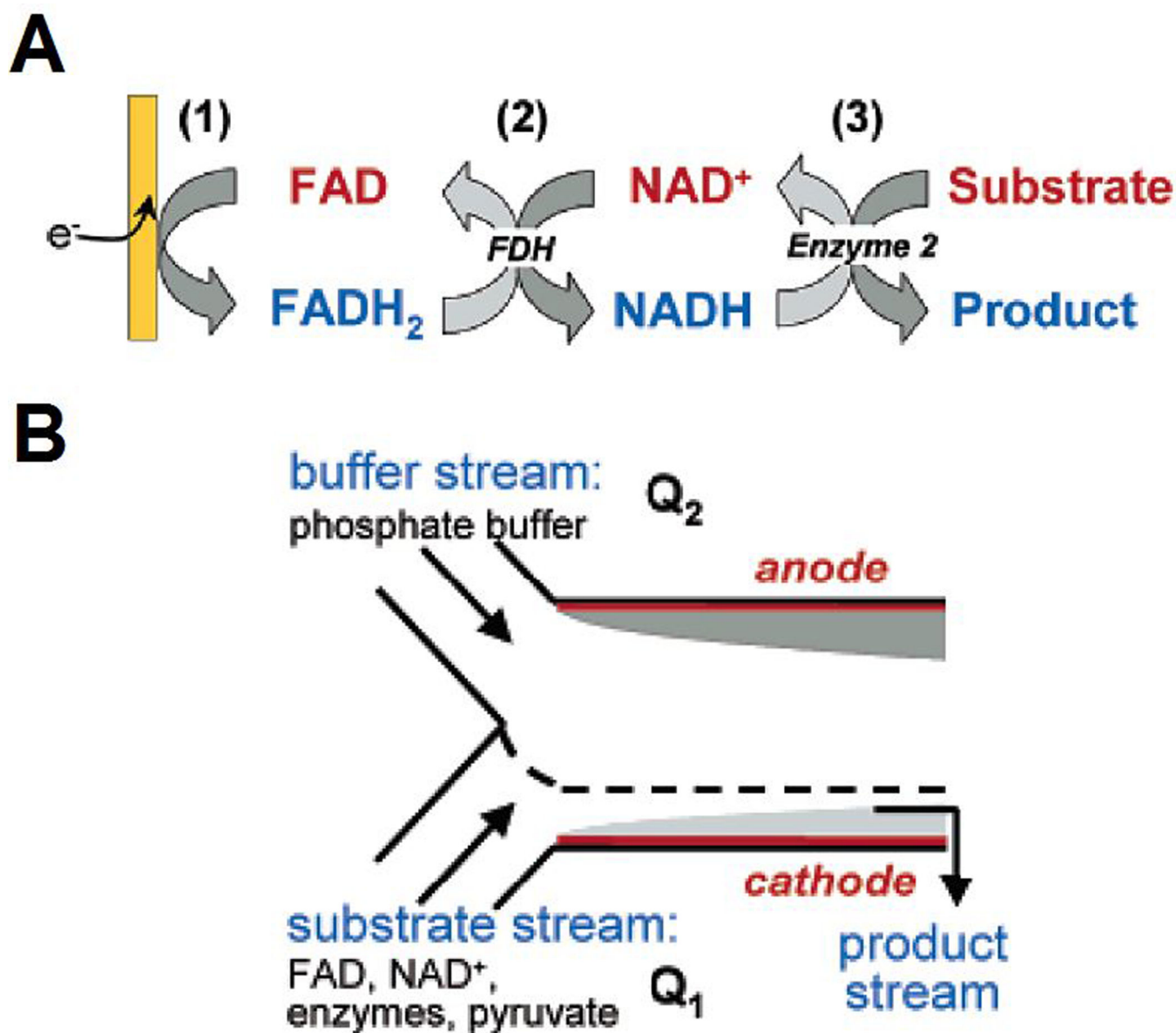


Figure 54.

Continuous electrochemical regeneration of NAD^+ using a Y-shaped system. **A)** The series of chemical reactions that take place in the system to convert NAD^+ back into NADH for another enzymatic reaction. **B)** The reactor system showing the chemical composition of each stream.¹⁹⁷ This figure was used with permission.¹⁹⁷ Copyright (2018) American Chemical Society.

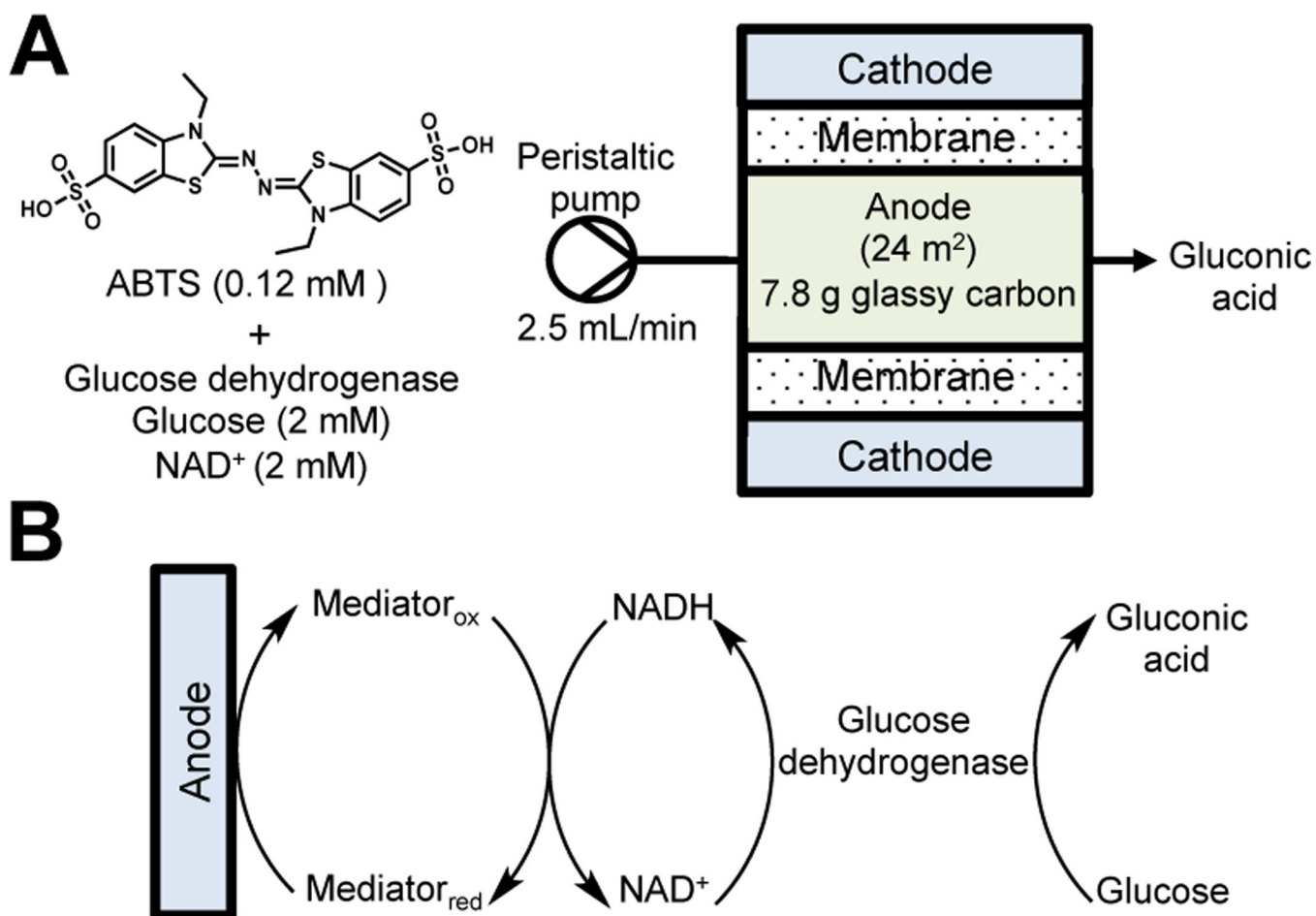


Figure 55. Continuous regeneration of NAD⁺ using a glassy carbon anode system. **A)** The continuous flow electrochemical set-up, the chemicals used for the regeneration and the biotransformation of glucose, and the molecular structure of ABTS. **B)** The chain of chemical reactions that take place to regenerate NAD⁺ for biocatalysis.¹⁹⁹

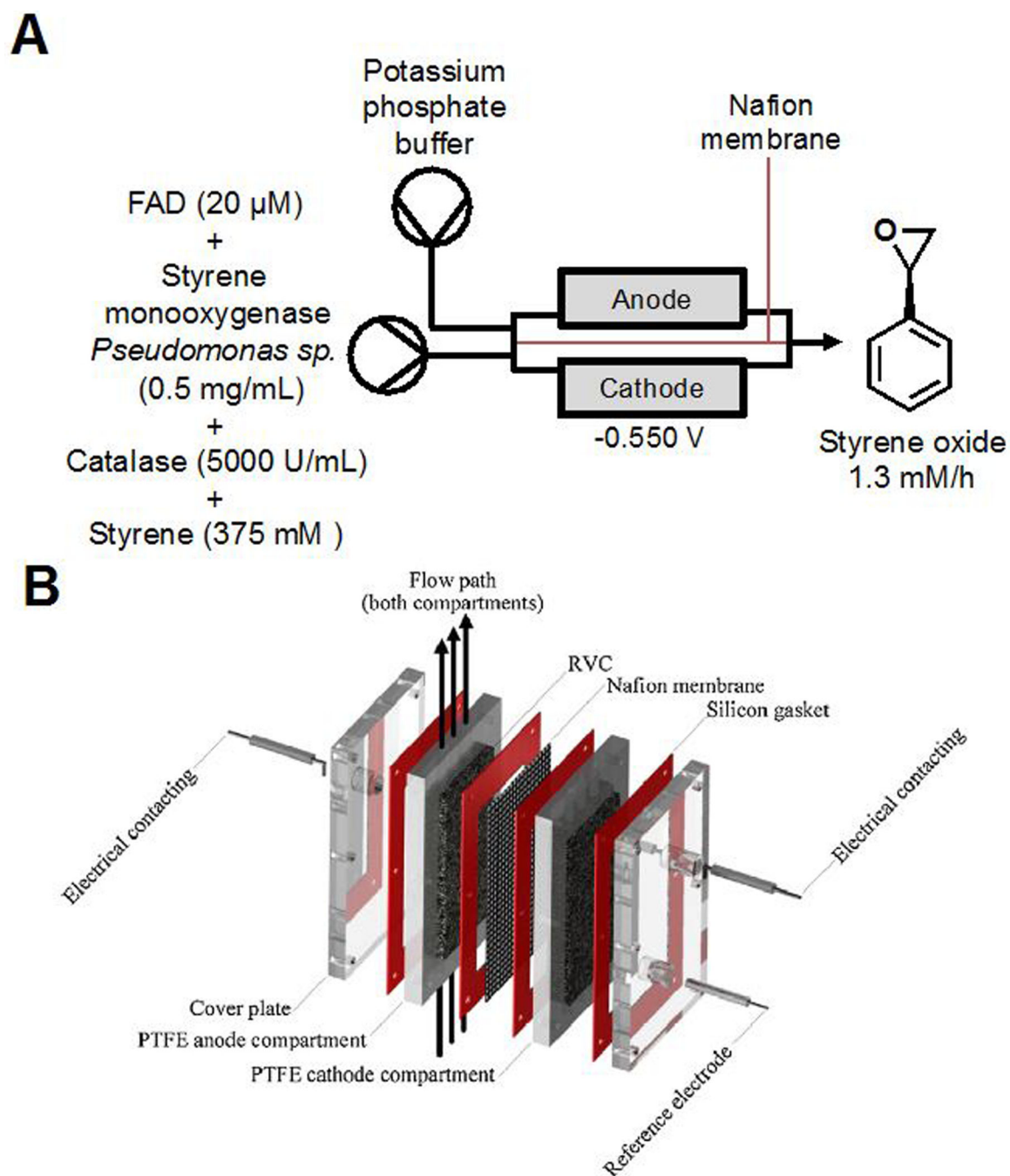


Figure 56.

The continuous reduction of FAD to facilitate styrene oxide production from styrene. **A)** The reactor set-up shows styrene oxide synthesis from styrene using the enzymes styrene monooxygenase and catalase, and co-factor FAD. **B)** A schematic of the electrochemical reactor.¹⁹⁷ The photographs used in this figure were reproduced with permission from Elsevier (2018).²⁰⁰

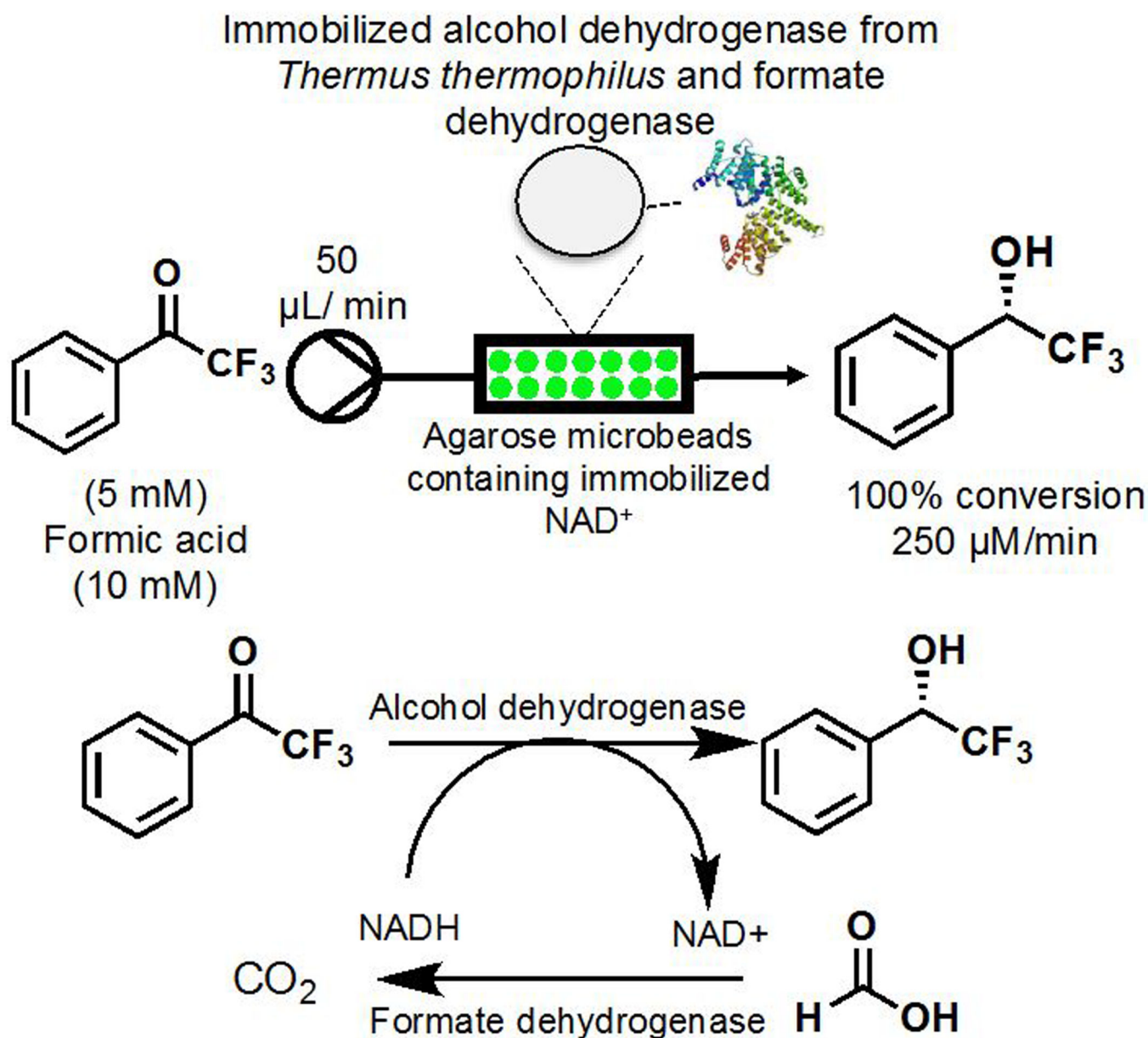


Figure 57. The continuous flow enantioselective reduction of an aryl ketone using co-immobilized alcohol dehydrogenase and formate dehydrogenase. Additionally, the co-factor NAD^+ is immobilized on agarose microbeads. The lower figure shows the chemical transformations that occur to make this a renewable system.²⁰⁸

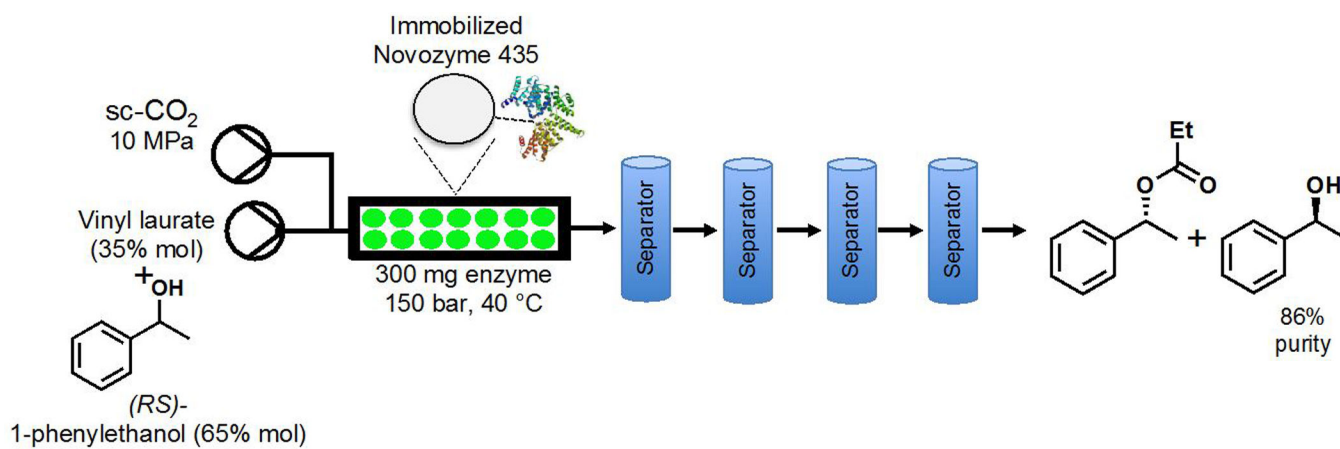


Figure 58.

Continuous resolution of (*S*)-phenylethanol using immobilized Novozyme 435 for (*R*)-selective esterification with vinyl laurate. This figure has been simplified to match the text, for the in depth schematic and information on the separators, see the original publication.²⁰⁹

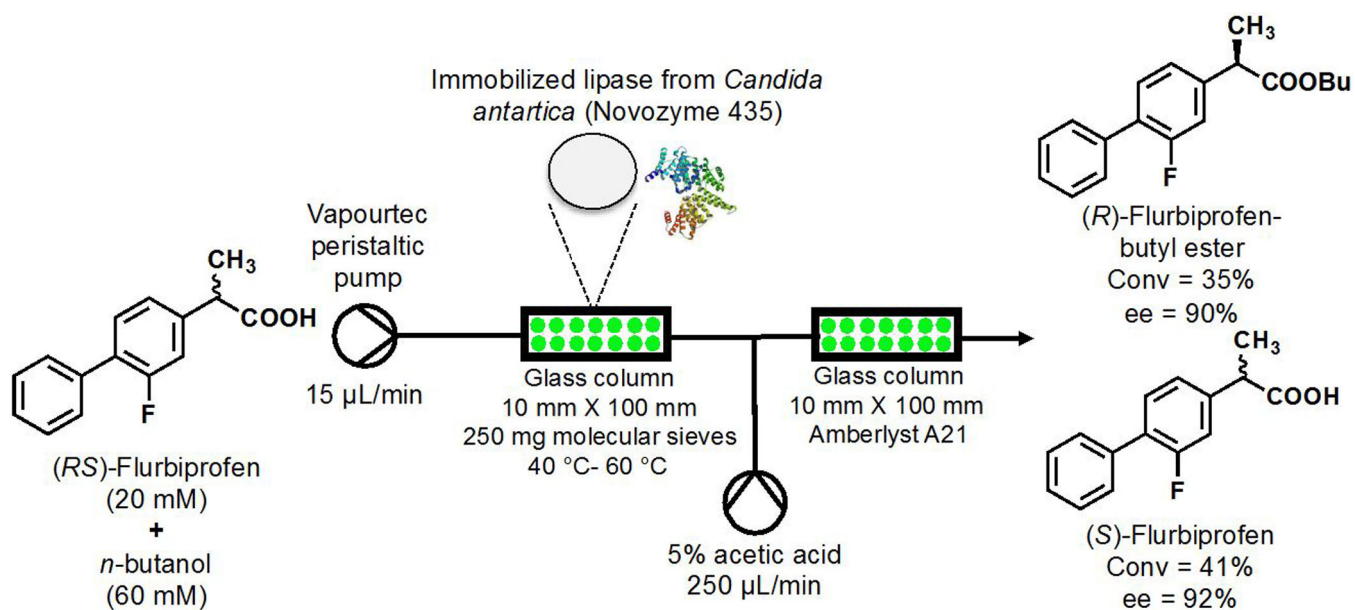


Figure 59.
 Continuous kinetic resolution of (*R,S*)-Flurbiprofen using an immobilized lipase and *n*-butanol.²¹⁰

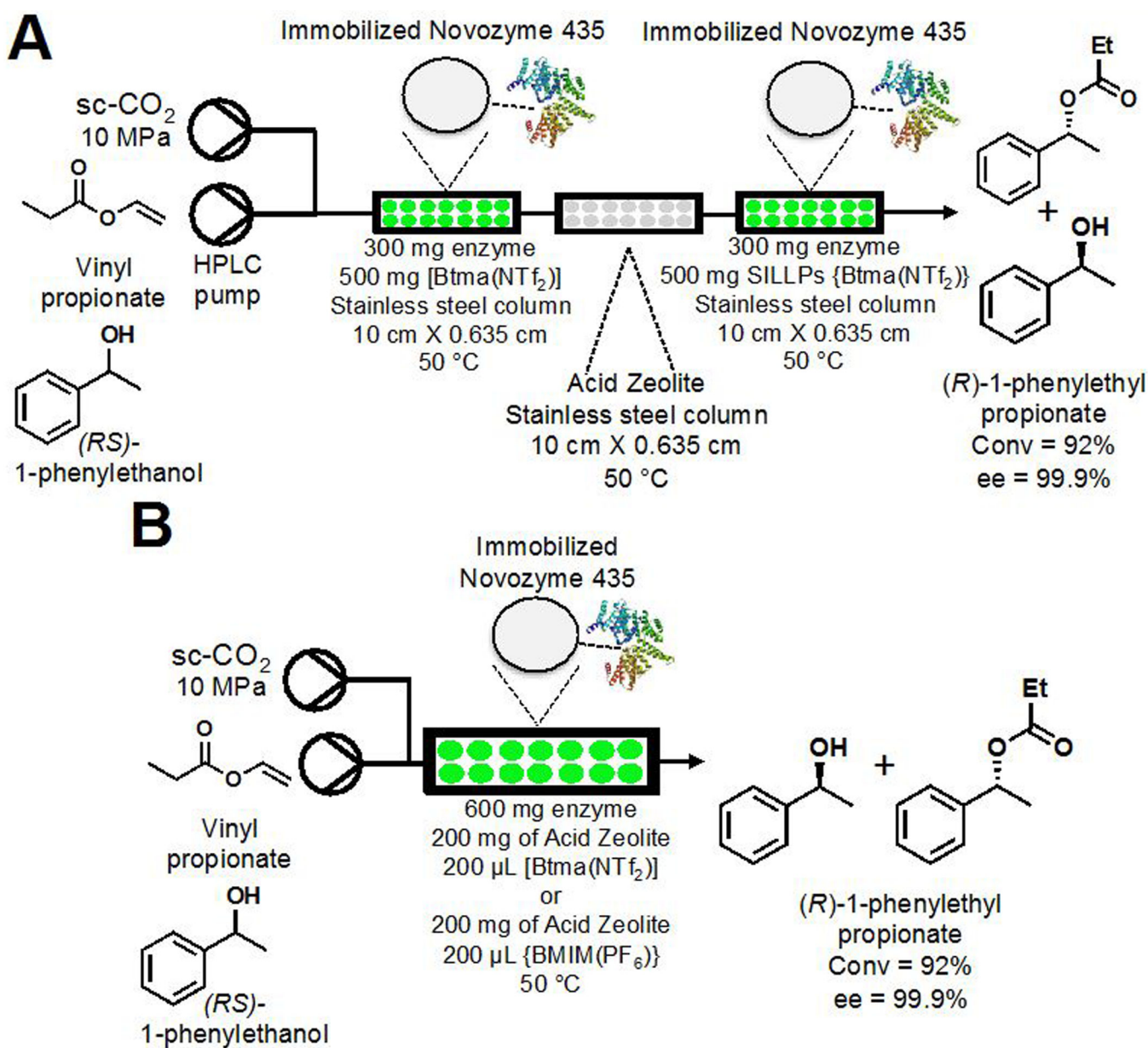


Figure 60. Continuous resolution of (*RS*)-phenylethanol using an immobilized lipase, vinyl propionate, and super critical CO₂.²¹³

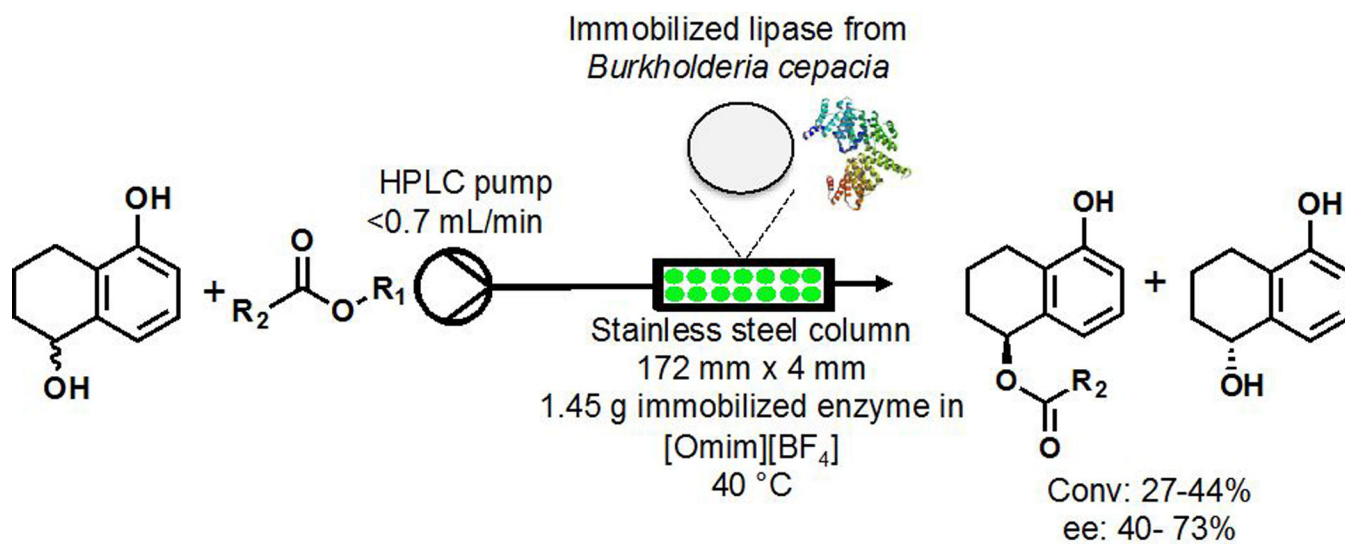


Figure 61. Continuous resolution of 1,5-dihydroxy-1,2,3,4-tetrahydronaphthalene using an immobilized lipase.²¹⁸

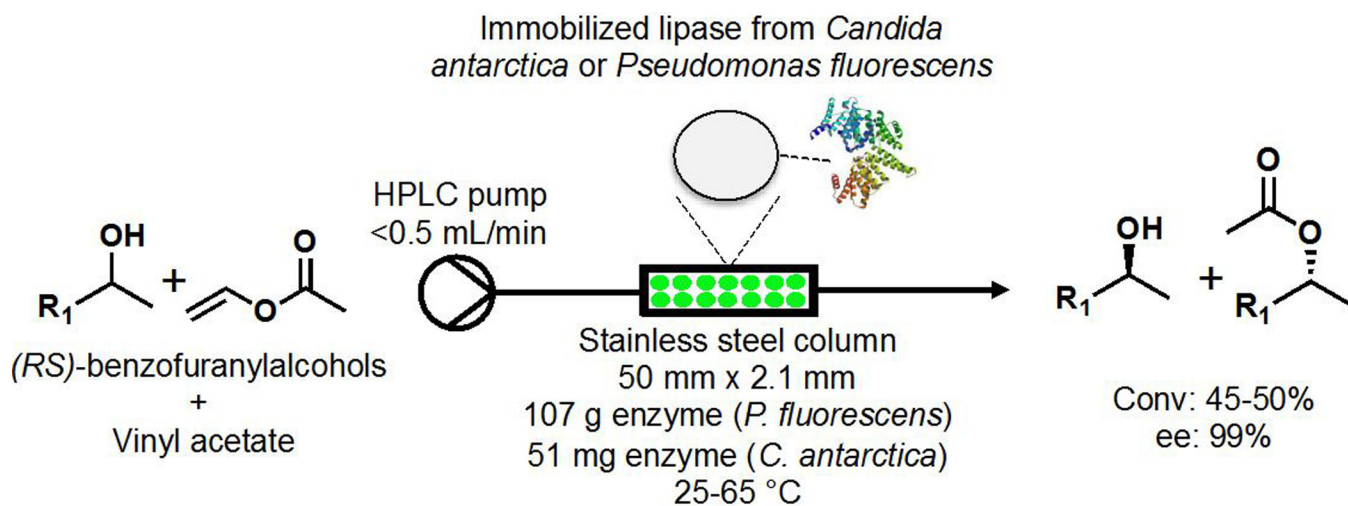


Figure 62. Continuous resolution using either an immobilized lipase from *Candida antarctica* or an immobilized lipase from *Pseudomonas fluorescens*.²¹⁹

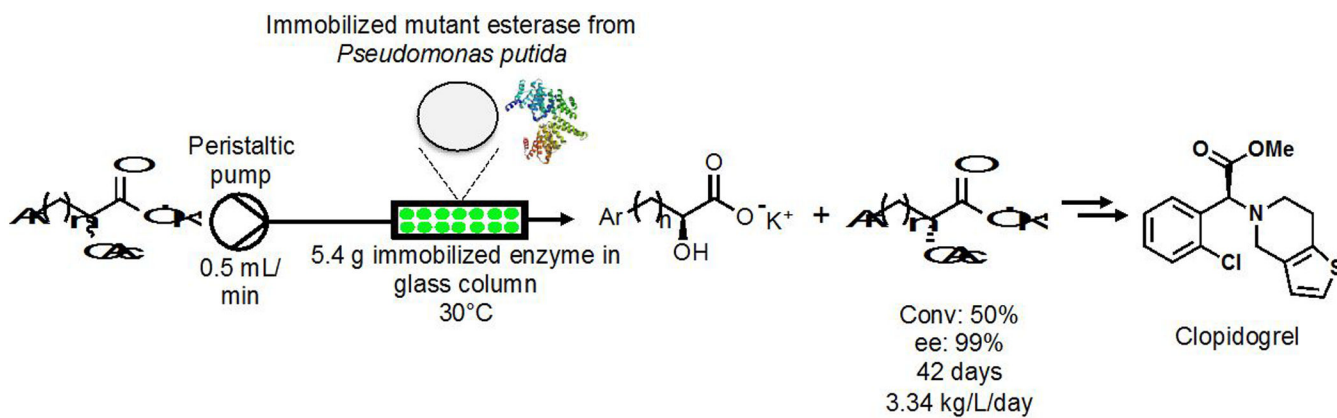


Figure 63. Continuous resolution of 2-acetoxy-2-(2-chlorophenyl)acetate using an immobilized mutant esterase from *Pseudomonas putida*.²²²

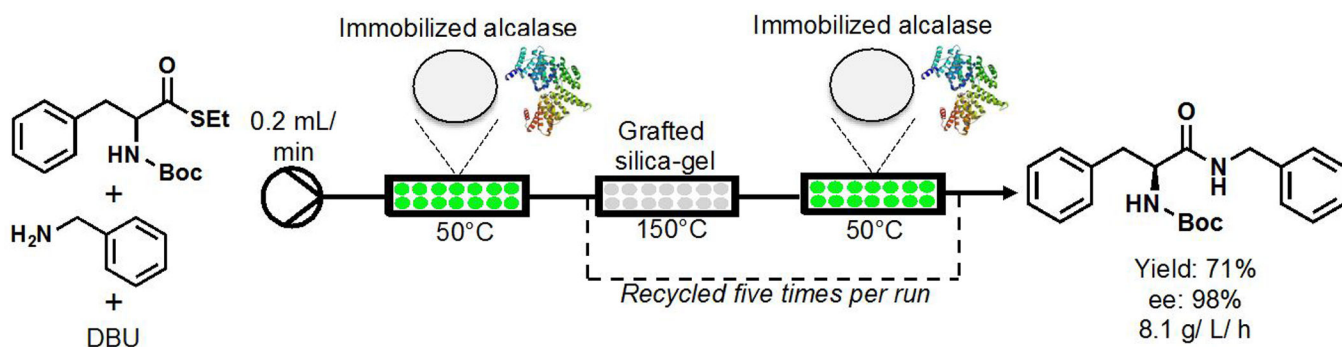


Figure 64. Continuous resolution of racemic N-Boc-phenylalanine ethyl thioester using cartridges filed with immobilized acylase and grafted silica gel.²²³

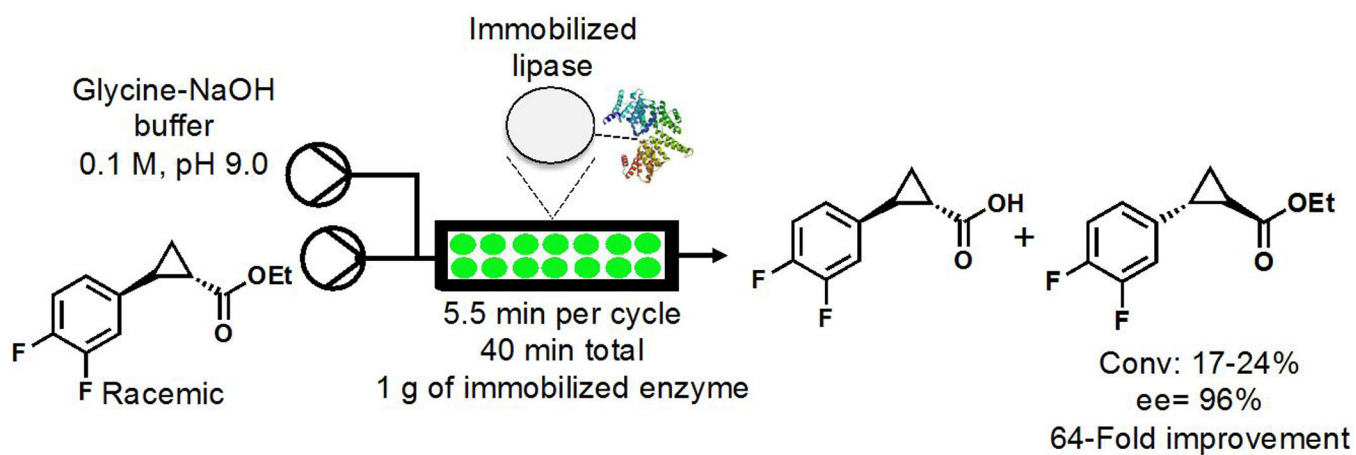


Figure 65.
Continuous flow lipase resolution of a cyclopropane carboxylate ester in a packed bed reactor for a total residence time of 40 min.²²⁴

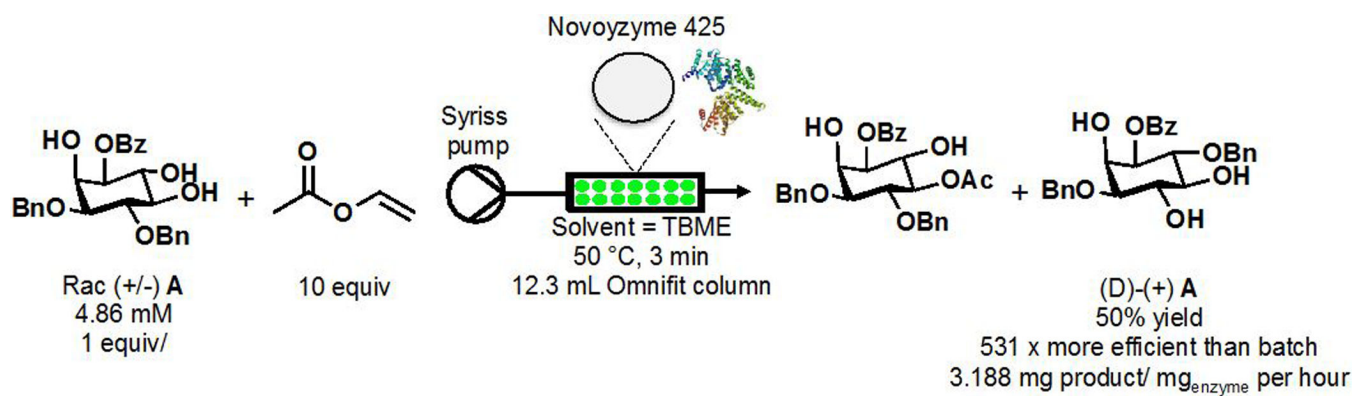


Figure 66. Continuous flow resolution of (\pm)-1,3,6-tri-O-benzyl-myoinositol with vinyl acetate and Novozyme 425.²²⁵